Caractérisation des surfaces de départ potentielles des avalanches dans les Alpes françaises et de leur évolution diachronique

Cécile Duvillier

THÈSE

Pour obtenir le grade de

DOCTEUR DE L'UNIVERSITÉ GRENOBLE ALPES

École doctorale : STEP - Sciences de la Terre de l'Environnement et des Planètes

Spécialité : Sciences de la Terre et de l'Environnement

UMR IGE

Caractérisation des surfaces de départ potentielles des avalanches dans les Alpes françaises et de leur évolution diachronique

Characterisation of snow avalanche potential release areas in the French Alps and their diachronic evolution

Présentée par :

Cécile DUVILLIER

Direction de thèse :

Nicolas ECKERT INGENIEUR HDR, ICPEF /INRAE	Directeur de thèse
Guillaume EVIN CHARGE DE RECHERCHE, INRAE	Co-encadrant de thèse

Rapporteurs :

Christophe CORONA
DIRECTEUR DE RECHERCHE, CNRS

Samuel MORIN
INGENIEUR HDR, ICPEF/CNRM

Thèse soutenue publiquement le **4 mai 2023**, devant le jury composé de :

Nicolas ECKERT INGENIEUR HDR, ICPEF, INRAE	Directeur de thèse
Christophe CORONA DIRECTEUR DE RECHERCHE, CNRS	Rapporteur
Vincent JOMELLI DIRECTEUR DE RECHERCHE, CNRS	Examinateur
Sandrine CAROLY PROFESSEUR DES UNIVERSITES, Université Grenoble Alpes	Président du jury
Samuel MORIN INGENIEUR HDR, ICPEF/CNRM	Rapporteur

Invité :

Guillaume Evin
CHARGE DE RECHERCHE, INRAE

Remerciements

Avant tout, je suis reconnaissante envers mes encadrants, Nicolas Eckert, Guillaume Evin, Michael Deschâtres, et les membres de mon comité de thèse Margherita Maggioni, Vincent Jomelli, Thierry Faug, pour leurs conseils tout au long de cette thèse.

Je tiens à remercier toutes les orthophonistes qui m'ont aidée dans mon combat acharné face au bégaiement. Sans elles, je n'aurai pas accompli tous les progrès de fluence actuels. Maintenant, je récolte le fruit de tous les efforts réalisés, et enfin je revis.

Je remercie mon directeur de master Claude Vella, pour son soutien dans mon projet de doctorat sur les avalanches, thématique originale pour une région où la neige est rare. Je remercie les personnes qui m'ont aidée et soutenue dans mon projet de doctorat, dont Cécile Grès une des orthophonistes qui m'a suivie et sa secrétaire Valérie, mes amis de master et de toujours Viviane, Brenda, Alexis, François, Isabelle, Bastien, Thibault…

Mon départ à Grenoble m'a permis de changer de vie et de région, de faire la connaissance de nouvelles personnes, et de découvrir le milieu montagnard qui m'est inséparable à présent. C'est dans ce milieu de je souhaite en apprendre davantage pour mieux le comprendre. Je remercie les personnes rencontrées au cours de mes sorties en montagne, que ce soit au cours d'une journée ou durant plusieurs jours, qui m'ont aidée et formée. Durant ma deuxième et ma troisième année de doctorat, je suis allée les midis à la salle d'escalade du campus. J'y ai rencontré des personnes formidables. Je remercie les deux adorables encadrants d'escalade Adrien et Sylvain, pour leur précieux conseils.

Au sein de l'INRAE, j'ai rencontré des personnes formidables avec lesquelles j'ai apprécié échanger. Je ne les oublierai pas.

Les membres du groupe d'orthophonie m'ont permis de m'ouvrir aux autres, et m'ont soutenue surtout dans la fin du doctorat. Leur aide m'aura été si précieuse, je leur en suis reconnaissante.

Je remercie mon frère pour son soutien dans les moments difficiles.

Je remercie toutes les personnes qui m'ont soutenue et qui ont contribué à ma réussite, et leur dédient ce travail.

Caractérisation des surfaces de départ potentielles des avalanches dans les Alpes françaises et de leur évolution diachronique

Les avalanches de neige entrainent des pertes humaines et des dommages matériels. Les avalanches historiques apportent des informations sur les caractéristiques des futures probables avalanches (localisation, type d'avalanche, dimension, etc.). A certains endroits, les données disponibles sont toutefois insuffisantes et, l'identification des zones de départ potentielles (PRAs) est alors d'une aide précieuse.

Dans cette thèse, une méthode d'identification des PRAs adaptée au contexte spécifique des Alpes Françaises a été développée. Elle se base sur des paramètres topographiques comme la pente, l'altitude, la distance à la crête, la présence ou non de forêt et la délimitation des bassins versants. Pour évaluer la méthode de détermination, nous confrontons les PRAs obtenues avec les emprises des avalanches observées qui sont répertoriées dans la CLPA, un cadastre d'emprises historiques richement documenté. Le cadre de validation proposé incluant différents scores établis sur la base de matrices de confusion constitue l'apport méthodologique générique de la thèse. Les scores obtenus confirment l'intérêt et la robustesse de la méthode développée, tout en soulignant les paramètres essentiels à une bonne détermination.

Le second axe de la thèse concerne l'analyse statistique des caractéristiques des PRAs à l'échelle de l'ensemble des Alpes Françaises et leur évolution sur des zones choisies en fonction des variations de la surface forestière au cours du temps. Nous détectons au total 101802 PRAs, formant une aire totale de 3799,2 km^2, ce qui représente 17,8% de l'ensemble de la surface des Alpes françaises. Nous regroupons les 23 massifs des Alpes Françaises en trois classes spatialement cohérentes en fonction des similitudes des caractéristiques topographiques de leurs PRAs. Nous montrons enfin que le développement de la couverture forestière en lien avec le recul de l'activité pastorale entre 1860 et 2013-2014, a significativement réduit le nombre de PRAs et, sans doute, l'activité avalancheuse. En effet, le nombre de PRAs est passé de 1793 en 1860, à 1578 en 2013 dans la haute vallée du Guil (massif du Queyras), et de 3043 en 1860 à 2971 en 2014 dans trois communes de Haute Maurienne.

Enfin quelques pistes pour des développements futurs sont discutés.

Characterisation of potential release areas of snow avalanches in the French Alps and their diachronic evolution

Snow avalanches cause casualties and material damage. Historical avalanches provide information on the characteristics of probable future avalanches (localisation, type of avalanche, size, etc.). In some areas, however, the available data is insufficient, and the identification of Potential Release Areas (PRAs) is therefore of great help.

In this thesis, a method for identifying PRAs adapted to the specific context of the French Alps is developed. It is based on topographic parameters such as slope, altitude, distance to the ridge, presence or absence of forest and delimitation of the catchment areas. In order to evaluate the determination method, we compare the PRAs obtained with observed avalanche extents, which are recorded in the CLPA, a rich cadastre of past events. The proposed validation framework that includes different scores established on the basis of confusion matrices constitutes the generic methodological contribution of the thesis. The scores obtained confirm the interest and robustness of the developed method, while highlighting the parameters which are essential for a good determination.

The second axis of the thesis concerns the statistical analysis of the characteristics of the PRAs at the scale of the whole French Alps and their evolution in selected areas according to the variations of forest cover over time. We detect a total of 101802 PRAs with a total area of 3799.2 km^2, which represents 17.8% of the area of the entire French Alps. We grouped the 23 massifs of the French Alps into three spatially coherent classes according to the similarity of the topographical characteristics of their PRAs. Finally, we show that the development of the forest cover in connection with the decrease of pastoral activities between 1860 and 2013-2014 reduced the number of PRAs, and, presumably, avalanche activity. In fact, the number of PRAs dropped from 1793 in 1860 to 1578 in 2013 in the Guil Valley (Queyras massif), and from 3043 in 1860 to 2971 in 2014 in three municipalities of Haute Maurienne. Finally, some avenues for future developments are discussed.

Table des matières

Chapitre 1 : Introduction

1 Contexte

Le risque lié aux avalanches

Les avalanches de neige entrainent des pertes humaines et des dommages matériels. Par exemple, l'avalanche de Montroc près de Chamonix, en 1999, a entraîné la mort de 12 personnes et la destruction de 14 chalets de montagne (Figure 1 ; Rapin et Ancey, 2000). Les deux avalanches de Saint-Calomban-des-Villards en 1943 et en 1978 ont entrainé la perte de 7 et 2 personnes, respectivement. En 2008, au Mont-Blanc, 16 alpinistes ont été emportés par une avalanche et seulement huit ont survécu (Naaim-Bouvet et Richard, 2015). Ainsi, l'estimation du risque d'avalanche reste toujours un problème à résoudre, pour la réduction des pertes humaines et des dommages matériels. Les skieurs, les responsables de la sécurité des pistes de ski, les autorités locales et autres gestionnaires sont confrontés au problème de l'estimation des risques d'avalanche. L'estimation du risque d'avalanche dépend des études existantes dans la région concernée et des données concernant les avalanches historiques.

Pour les zones habitées, le risque est la combinaison de l'aléa ou phénomène naturel (ici l'avalanche), associé à la vulnérabilité des enjeux (dommages humains et matériels). Pour adapter les constructions dans les territoires soumis à des risques naturels ou technologiques, les Plans de Prévention des Risques (PPR) ont été mis en place. Leurs objectifs consistent à délimiter les secteurs à risque, recueillir des informations sur les risques sur des territoires spécifiques, réglementer les projets de construction et de développement, définir les mesures concernant les bâtiments existants, définir les mesures de prévention, de protection et de sauvegarde, et orienter le développement vers les zones moins exposées aux risques. Dans un PPR, il y a les zones rouges caractérisées par une interdiction de construire, les zones bleues soumises à des prescriptions, et les zones blanches moins exposées aux risques. Le zonage est souvent effectué à partir des événements enregistrés, dans notre cas les données disponibles sur les avalanches observées dans le passé. Grâce au zonage, certaines zones à risques resteront inconstructibles, par exemple en aval de certains couloirs particulièrement avalancheux.

Intérêt de l'information historique et CLPA

Les avalanches historiques fournissent des données sur les dimensions et les types d'avalanches qui pourraient se produire à l'avenir (Maggioni et Gruber, 2003). Le manque de données sur les avalanches historiques a contribué au bilan catastrophique de avalanche de Val-d'Isère le 11 février 1970 qui a fait 39 morts (Figure *2*), et à celui de l'avalanche de Montroc en 1999 (Figure 1). Dans le cas de l'avalanche de Montroc en 1999, la catastrophe s'est produite dans la zone blanche du « Plan de prévention des risques » (PPR), c'est-à-dire considérée comme n'étant pas sujette aux avalanches, et qui couvrait des zones potentiellement atteignables par des avalanches, en raison d'un manque d'information sur les avalanches historiques (Ancey et al., 2000); (Glass et al., 2000). S'il y a un manque de données concernant les avalanches enregistrées, le risque ne sera pas pris en compte et ne pourra pas être cartographié. Il est possible de combler ce manque d'informations concernant les avalanches

enregistrées avec la détermination et la cartographie des zones de départ potentielles d'avalanche (*Potential Release Areas* en anglais, ou PRAs), qui constitue le cœur de cette thèse.

Figure 1 : Dégâts causés par l'avalanche de 1999, à Montroc. Source : (Rapin et Ancey, 2000).

Figure 2 : Dégâts causés par l'avalanche du 11 février 1970, à Val d'Isère. Source : le Dauphiné.

À la suite de l'avalanche de Val-d'Isère, le gouvernement français a exigé la création de la « Carte de Localisation des Phénomènes d'Avalanche » (CLPA). C'est une carte des avalanches observées dans le passé, où les avalanches sont représentées par les limites maximales atteintes. La CLPA est obtenue à l'aide de la photo-interprétation, de l'observation du terrain, des enregistrements, des témoignages de résidents et de professionnels de la montagne comme les guides de montagne, les services de secours, les professionnels des stations de ski (Bourova et al., 2016); (Naaim-Bouvet et Richard, 2015). La CLPA identifie les structures de protection, et est principalement produite à destination des professionnels et non pas des skieurs (Ancey, 1996).

En France, certains couloirs d'avalanche, principalement situés à proximité d'enjeux humains, sont surveillés par l'Office National des Forêts (ONF), et les données fournies alimentent les bases de données de l'Enquête Permanente sur les Avalanches (EPA) et L'Observation Permanente des Avalanches (OPA).

L'Enquête Permanente sur les Avalanches a commencé en Savoie en 1899.

Elle a pour objectif de fournir des informations sur toutes les avalanches moyennes à grandes qui se sont produites dans des couloirs d'avalanche spécifiques. Pour les couloirs accessibles, les données sont acquises en continu alors que dans les couloirs moins accessibles la collecte de données est limitée et incomplète. Les données fournies sont l'altitude de départ et d'arrivée, le dépôt de neige, les types d'avalanche et de neige, les conditions météorologiques précédant l'événement.

Par ailleurs, L'Observation Permanente des Avalanches a fonctionné de 1972 à 1985. Elle a permis de recueillir des observations précises sur des avalanches affectant des zones avec d'importants enjeux humains à protéger. Il s'agit de communes, de zones touristiques, et de futurs projets d'aménagement du territoire. En ce qui concerne les avalanches ayant entrainé des pertes humaines et des dégâts matériels, la base de données « événement » du service RTM (BD événement RTM) les répertorie également, avec plus ou moins de complétude (Kern et al., 2020).

Apport de la détermination automatique des zones de départ potentielles d'avalanche (PRAs)

Dans les régions montagneuses, les informations sur les PRAs sont rares car le territoire est immense et ces dernières ne sont souvent pas accessibles. Pour atténuer les risques d'avalanche à grande

échelle, y compris dans les secteurs où la documentation historique est partielle ou absente, la détermination automatique des PRAs constitue une information alternative (Figure 3). La PRA est la surface maximale pouvant se déclencher et être mobilisée en un seul départ d'avalanche. Dans chaque couloir d'avalanche, est identifiée au moins une PRA ou plusieurs. Dans la réalité, la plupart du temps, seule une partie de cette PRA est déclenchée car ces PRAs correspondent aux emprises maximales. Il peut y avoir plusieurs départs de PRAs simultanément dans un même couloir d'avalanche.
Par ailleurs, grâce aux PRAs, il est possible d'estimer le risque d'avalanche. En effet, en complément de la connaissance de la PRAs, s'il est possible de déterminer la profondeur de la fracture et le volume initial d'une avalanche (Maggioni et al., 2002), il est alors possible d'obtenir les emprises maximales des dépôts en utilisant un logiciel de simulation d'avalanche (Fischer et al., 2015), puis une évaluation du risque par combinaison avec la vulnérabilité d'enjeux réels ou hypothétiques. Une fois la zone de dépôt connue, il est également possible d'implanter des ouvrages de protection de bâtiments, ou au contraire de limiter de futures constructions dans ces zones à risque. De plus, l'étude des caractéristiques des zones de départ d'avalanches peut permettre de mieux comprendre la localisation des PRAs en fonction des paramètres topographiques, et quels paramètres en déterminent la localisation et la taille (Gleason, 1996).

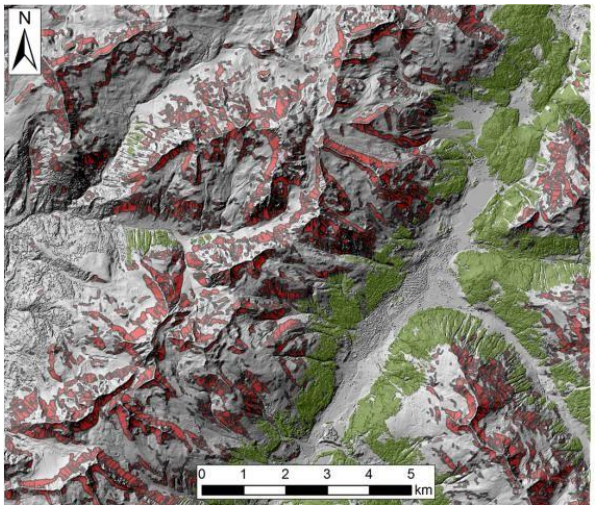

Figure 3 : Zones de départ potentielles d'avalanche (PRAs) dans la région du Davos en Suisse (rouge), en vert la forêt
Source : (Bühler et al., 2013).

A partir d'un MNT et d'une couche représentant la surface forestière, il est possible de déterminer la localisation et la surface des PRAs. De plus, l'automatisation de la méthode permet de l'appliquer sur de vastes secteurs comme des massifs, même à de fine résolution comme à 5m. Les cartes des PRAs sont largement utilisées pour l'évaluation de certains aléas naturels comme les laves torrentielles et les glissements de terrain, et, depuis moins longtemps, pour les avalanches. Pour obtenir une telle carte dite de susceptibilité pour les laves torrentielles dans les Alpes méridionales françaises, par exemple, les paramètres utilisés ont été les propriétés morphométriques du torrent qui déterminent l'initiation et la propagation de la lave torrentielle et la quantité de sédiments dans le bassin versant. En plus de la simple cartographie des zones potentiellement concernées, ces paramètres permettent d'estimer la probabilité d'occurrence des laves torrentielles (Bertrand et al., 2017).

2 Etat de l'art concernant l'activité avalancheuse et la détermination automatique des PRAs

Connaissances génériques concernant les avalanches, leur déclenchement et la topographie

Un couloir d'avalanche est constitué de trois parties, la zone de départ, la zone d'écoulement, et la zone de dépôt. La zone de départ est la zone où la neige s'accumule, et où l'avalanche est déclenchée. En aval, le chemin d'écoulement est souvent constitué d'un ravin dans lequel la neige coule sur le versant. Dans cette zone, la pente est souvent plus faible que dans la zone de départ. Enfin, en bas de la pente, la zone de dépôt est la zone où l'avalanche s'est arrêtée. Cette zone correspond souvent à la vallée (Ancey, 1996). Dans cette thèse, nous nous intéressons spécifiquement à la cartographie des zones de départ potentielles d'avalanches, désignés par PRAs dans la suite du texte.

Une avalanche peut être déclenchée spontanément sous des conditions météorologiques et de neige particulières, ou bien être déclenchée par le passage d'humains et d'animaux. Dans ce travail, nous nous concentrons principalement sur les départs d'avalanches spontanés pour lesquels les données historiques sont les plus complètes, et qui sont de loin les plus nombreux. Une avalanche se produit lorsque la force de résistance dans les couches de neige ne peut plus compenser la gravité. Cette rupture d'équilibre peut être due à une réduction des forces de résistance, ou à une augmentation de la force entraînant la neige vers le bas le long de la pente, ou les deux. Précisément, l'augmentation de la force gravitationnelle peut être causée par la combinaison de neige fraîche, le vent, la rupture de corniches, la traversée de skieurs ou d'animaux, ou l'explosion lors du déclenchement artificiel (Naaim-Bouvet et Richard, 2015).

Il existe communément 2 types de départs d'avalanche, les départs en plaque (Figure 4a) et les départs ponctuels (Figure 4b). Dans les départs ponctuels, la neige s'écoule dans la pente, la quantité de neige augmente au fur et à mesure de sa descente en entrainant la neige sur les côtés. Au final, le dépôt d'avalanche aura souvent une forme de poire. C'est le cas de certaines avalanches de neige fraiche, ou des avalanches humides de printemps.

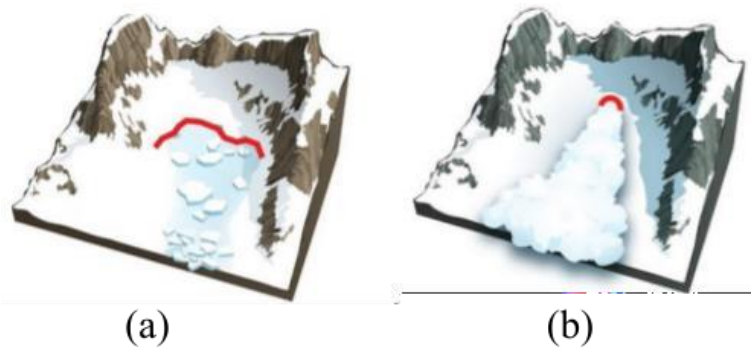

Figure 4 : (a) Départ d'avalanche en plaque, (b) départ d'avalanche ponctuel
Source : (Naaim-Bouvet et Richard, 2015)

Pour qu'une avalanche de plaque ait lieu, une couche de faible cohésion dans le manteau neigeux doit être recouverte par des couches avec une bonne cohésion. Une surcharge entraine la rupture de la couche de faible cohésion, qui se propage ensuite dans les autres couches du manteau neigeux. Au final, c'est tout un panneau de pente qui se décroche (Naaim-Bouvet et Richard, 2015).

Parmi ces deux types de départ d'avalanche, nous pouvons identifier 3 formes de relief spécifiques qui contrôlent le déclenchement: les plans horizontaux, les zones convexes comme les crêtes et les pics,

et les zones concaves comme les ravins et des trous qui retiennent la neige. La prise en compte de ces formes spécifiques constitue la base des méthodes de détermination automatique des PRAs.

Liens entre occurrence des avalanches et occupation des sols

La forêt protège les humains contre les avalanches, ou pourrait limiter les avalanches en ancrant le manteau neigeux. Précisément, à la cime des arbres, la neige est interceptée. Celle-ci est déplacée au sol sous forme d'eau de fonte et de paquets de neige, permettant l'ancrage de l'enneigement. De plus, les troncs d'arbres stabilisent l'accumulation de neige et le microclimat limite la formation de givre, qui pourrait devenir une couche fragile (Naaim-Bouvet et Richard, 2015). Ainsi, contrairement aux terres non boisées, dans les zones boisées, le manteau neigeux a un meilleur ancrage, et l'accumulation de neige est réduite. Une forêt dense recouvrant l'ensemble de la zone de départ représente une excellente protection contre les avalanches. Lorsque la forêt est clairsemée, une avalanche est possible et les effets protecteurs sont limités. En 1991, Gubler et Rychetnik ont étudié l'effet de la densité forestière sur la pente, et l'intensité de l'avalanche qui en résulte. En conclusion, plus la densité forestière est faible et la pente est raide, plus l'intensité de l'avalanche sera forte (Gubler et Rychetnik, 1991).

Par contre si un début d'avalanche se produit au-dessus d'une forêt, les troncs d'arbres apportés par l'avalanche (en plus des roches, de la neige) aggravent les effets destructeurs (Margreth, 2004).

Par ailleurs, l'effet protecteur de la forêt dépend des espèces présentes et de leur structure. Précisément, une forêt dense de conifères à aiguilles persistantes (sapins par exemple) permet de fixer et de piéger la couverture de neige d'où un risque faible de départ d'avalanches. Par opposition, une forêt avec des arbres à feuilles caduques (feuillus) ou des aiguilles qui tombent en hiver (mélèze) présente généralement un risque d'avalanche plus élevé car l'effet fixateur du manteau neigeux est limité. Une faible densité de végétation contribue à l'aération de la neige et génère de la neige sans cohésion près des arbustes (Ancey, 1996). Par ailleurs, l'herbe pâturée retient la neige, alors que l'herbe non pâturée se plie avec les premières chutes de neige et engendre des avalanches de fond (Bornard et Cozic, 1998).

On parle d'avalanche de fond quand le contact entre la neige et le sol (rocher, végétation, herbes) devient glissant. L'ensemble du manteau neigeux est alors entrainé puis glisse sur le sol mouillé. Par ailleurs, le reboisement des pentes avalancheuses est une solution pour limiter le déclenchement des avalanches. Un exemple illustratif concerne le site avalancheux du Chômais dans le massif du Beaufortin (Savoie), où la forêt recouvrant le versant avalancheux a été dévastée par des ouragans en 1928 et 1936. En conséquence, un départ d'avalanche a eu lieu en 1936 dans cette zone déboisée, et a détruit un chalet et bloqué une route. Pour empêcher que de nouvelles avalanches ne se reproduisent, le versant sera reboisé et des râteliers seront installés. Au final, il n'y a plus de départ d'avalanches, d'où l'utilité de la forêt pour limiter les départ d'avalanches (Berger, 1995).

Par ailleurs, pour mieux comprendre le rôle de la forêt sur les départs d'avalanches, un site expérimental d'une dizaine d'hectares a été créé au Stillberg près de Davos (Suisse) en 1975, à des altitudes entre 2000 et 2230m. Ce site a pour objectif de suivre l'évolution des espèces plantées : pins à crochets, arolles, mélèzes. Les conditions hivernales sont rudes, les températures sont basses, et l'accumulation de neige est importante. De plus, la période de végétation est courte, ce qui ralentit la croissance des végétaux. Enfin, les rafales de vent sont fortes, et les champignons menacent les pousses d'arbres. Parmi ces espèces, seuls les mélèzes ont su s'adapter au milieu tandis que les autres espèces ont été ravagées par des champignons. Un élément essentiel à la survie des espèces est la

disparition de la neige au printemps (Schnyder et Frey, 2005). Les forêts ont leur importance vis-à-vis des départs d'avalanches, c'est pourquoi il est nécessaire de contrôler leur état.
En France, une méthode de classification des forêts de protection a été créée, en fonction des aléas naturels (avalanches), de la vulnérabilité des enjeux menacés, de la structure et des paramètres dendrométriques des forêts. L'objectif est d'obtenir un zonage cartographique des zones où une intervention est nécessaire pour protéger les enjeux menacés et de la stabilité de la forêt. Pour obtenir ce zonage, différentes cartes ont été utilisées telles que la Carte de Localisation des Phénomènes d'Avalanches (CLPA), la carte de localisation probable des mouvements de sols, et la carte de localisation des parcelles forestières gérées par l'Office National des Forêts (ONF).
Si les forêts ont bien un rôle protecteur en limitant les départs d'avalanches, leur efficacité est toutefois limitée une fois l'avalanche déclenchée. C'est le cas du 9 janvier 2018, où un départ d'avalanche a eu lieu sous l'Aiguille du Gouter, puis a descendu le couloir du Bourgeat, les dépôts s'accumulant dans la vallée de Chamonix. En conséquence, la forêt située au-dessus de la vallée a subi des dégâts dû à l'aérosol, et certains arbres ont même été emportés, aggravant ainsi les dégâts matériels dans la vallée (Faug et al., 2018).

Evolution des pratiques de l'espace dans les vallées alpines au cours du temps, et conséquences pour l'occupation des sols et l'activité avalancheuse

L'activité humaine était autrefois axée sur l'agriculture (pastoralisme) et la foresterie. Depuis des siècles, les habitants utilisent la forêt pour se chauffer, pour chasser, et pour se protéger face aux risques naturels (Berger, 1995). Autrefois, la neige était considérée comme un fléau par les habitants. En effet, la neige enclave les vallées des autres communes, en recouvrant les habitations, les chemins, les pâtures, et les forêts.
Plus tard, les industries et les mines ont émergé avec la papeterie et la transformation de l'aluminium. Durant les années 1920 et 1930 commencent à se développer les stations de sports d'hiver, avec de grands travaux d'aménagement destinés au tourisme (remontées mécaniques, hébergements; Ancey, 1996). La commune de Gresse-en-Vercors en Isère, par exemple, deviendra une « ville station » (Brun-Cosme et Freydier, 2013). Tous ces aménagements du territoire ont conduit à la réduction de l'agriculture, et favorisé l'abandon des prairies ce qui a permis la croissance des forêts, entre 1860 et 2013-2014. Ces changements d'occupation du sol peuvent avoir des répercussions sur l'activité avalancheuse dû au dépeuplement et l'abandon des terres agricoles en montagne (Zgheib et al., 2020).
L'étude de (Mainieri et al. 2020) réalisée dans les Alpes françaises, et plus précisément dans le massif du Queyras, quantifie l'impact du changement d'occupation du sol sur l'activité avalancheuse. Pour ce faire, la dendrogéomorphologie est utilisée pour retracer l'historique des couloirs d'avalanches, entre 1750 et 2016. Concernant les couloirs d'avalanche avec une exposition sud, la fréquence des avalanches a augmenté dans les années 1970, car la forêt a été dévastée par une avalanche entre 1910 et 1920. Par opposition, les couloirs avec une exposition nord ont été reboisés à partir du milieu du 19ème siècle, suivi par les zones de départ d'avalanches reboisées elles aussi après la seconde guerre mondiale. Par conséquence, l'activité avalancheuse diminue depuis 1930. Par ailleurs, l'exode rural et la diminution du pastoralisme au cours du 19 ^{ème} et du 20ème siècle sont les facteurs qui ont le plus influencé l'activité avalancheuse, contrairement au réchauffement climatique qui dans ce cas précis a joué un rôle nettement moins important.
Les changements d'occupation du sol ont donc un impact important sur le risque d'avalanche, les deux évoluant conjointement au cours du temps. En effet, un travail a été réalisé dans les Alpes françaises, plus précisément dans le massif de la Haute-Maurienne, sur l'évolution du risque

d'avalanche de 1860 à 2013-2014 (Zgheib et al., 2020). Cette étude prend en compte les changements de couverture forestière, des études géohistoriques, et la modélisation qualitative du risque. Les grandes périodes concernant l'évolution de la sylviculture, l'élevage et le pastoralisme, et l'expansion urbaine, identifiées dans l'article de (Zgheib et al., 2020) sont les suivantes. La première période s'étend de 1860 à 1929. Les constructions sont groupées dans le centre du village, à proximité de l'église. Les habitants vivaient de l'agriculture et du pastoralisme. En 1860, la Haute-Maurienne était peu peuplée, les terres agricoles et les forêts étaient à l'abandon. Entre 1860 et 1929, la population décroit en raison de l'abandon des terres, des élevages (bovins, moutons), et des guerres. La baisse de l'élevage permet aux forêts de se restaurer avec la croissance des jeunes pousses d'arbres. La seconde période se situe entre 1929 et 1952, la population diminue avec la guerre, entrainant l'abandon des terres, des prairies et de l'élevage. Le cheptel de passage limite le développement de la forêt. La guerre aura comme effet de reconstruire et de développer la zone urbaine qui a été détruite. La troisième période se situe entre 1952 et 1979. Les prairies se sont développées permettant d'accroitre l'élevage, le pastoralisme, et la production de fromage. La population augmente, accompagnée de l'essor du tourisme lié au développement des stations de ski sur le territoire. En conséquence, la zone urbaine est en expansion. Ainsi, les nouveaux bâtiments construits se situent dans la partie supérieure des trois communes, à proximité des couloirs d'avalanches, et sont donc exposés au risque d'avalanche.
Comme ces deux études (Mainieri et al., 2020) ; (Zgheib et al., 2020) l'ont montré, l'activité humaine a bien un fort impact sur la forêt et donc sur l'activité avalancheuse. Il est donc incontournable de prendre en compte l'état de la forêt à différentes dates dans la méthode de détermination des PRAs pour y voir l'effet des activités humaines (agricoles, pastorales) et plus largement de l'évolution de l'occupation des sols sur l'activité avalancheuse.

Travaux sur la détermination des PRAs

La première méthode de détermination automatique des PRAs a été développée en 2002 par (Maggioni et al., 2002). Les caractéristiques utilisées comme des facteurs permettant l'identification des PRAs étaient la pente, le plan de courbure, l'exposition, la distance à la crête et l'aire minimale. Le MNT utilisé avait une résolution de 50m (Maggioni et al., 2002).
Un an plus tard, la même méthode a été appliquée pour calculer la distribution et la fréquence d'occurrence des avalanches dans ces zones, en fonction des paramètres topographiques (pente, exposition (Maggioni et Gruber, 2003). Cette méthode a été développée dans la même région avec une meilleure résolution de MNT de 5m, et en utilisant de nouveaux paramètres comme la présence de la forêt, la direction de l'écoulement au lieu de l'exposition et la rugosité. Les zones convexes comme les crêtes ont été enlevées en utilisant le plan de courbure afin d'exclure les avalanches déclenchées par la rupture des corniches. Pour tester l'algorithme de détermination des avalanches potentielles, les contours des avalanches de référence ont été découpés pour obtenir le tiers supérieur des polygones. L'algorithme permet de détecter de grandes avalanches de manière automatisée. Néanmoins, dans cette étude, une zone de départ se trouvant au-dessus de la forêt et de nombreuses petites avalanches près des zones boisées n'ont pas été détectées. De plus, certaines zones près des crêtes ont été « oubliées » parce que les crêtes ont été enlevées en utilisant la courbure et la rugosité (Bühler et al., 2013).
Dans les Pyrénées, une méthode de cartographie de la susceptibilité aux avalanches a été développée en utilisant un MNT d'une résolution de 5m, les paramètres de terrain et une analyse multicritère qui estime la vulnérabilité aux avalanches (faible, modérée, élevée, très élevée). Sont pris en compte

quatre paramètres de terrain dont la pente, la courbure, la rugosité du terrain et la présence de végétation, ainsi que l'altitude minimale de l'isotherme à zéro degré pour le mois d'hiver. Six types de sols (forêts, forêts ouvertes, broussailles, prairies, roches nues, zones urbanisées) ont été obtenus par photo-interprétation. L'altitude minimale de l'isotherme régional de 0° pendant l'hiver a été obtenue en analysant des conditions météorologiques de la région (Chueca et al., 2014).

En plus des autres paramètres topographiques, sont parfois utilisés une rugosité multi-échelle adaptée à la profondeur de neige, et un indice d'exposition au vent. Les trois paramètres considérés sont la pente, la rugosité et l'indice d'exposition au vent. L'indice d'exposition au vent permet de définir de nombreux scénarios de départ d'avalanches en fonction de la direction du vent ou d'une tempête (Veitinger et al., 2016). Dans cette étude, un MNT d'une résolution à 2m a été utilisé. Une logique floue a été appliquée pour lier et pondérer ces variables afin de trouver des scénarios de zones de départ d'avalanche en fonction du transport de la neige par le vent. Pour vérifier la validité de la méthode, les auteurs ont utilisé des données historiques. La méthode a été validée de deux manières différentes. La première validation a été effectuée sur une zone d'étude située dans la partie sud du village de Zuoz. Ce premier ensemble de données correspond à des zones touchées par les avalanches au moins une fois au cours de trente ans d'observation. Pour le deuxième ensemble de données (un sous-ensemble du premier), seules les parties supérieures de 80m de chaque polygone ont été sélectionnées. Pour tester la méthode de détermination, les zones ayant des pentes comprises entre 28 et 60° et une épaisseur de neige de 3 m ont été comparées aux zones de départ détectées, en utilisant les deux ensembles de données, des courbes ROC (Receiver Operating Characteristic), c'est-à-dire la courbe indiquant le taux de vrais positifs (fraction des positifs qui sont effectivement détectés) en fonction du taux de faux positifs (fraction des négatifs qui sont incorrectement détectés), et les aires sous la courbe ROC (AUC ; Veitinger et al., 2016).

Kumar et al. (2019) proposent une étude des PRAs dans l'Himalaya à l'aide d'un modèle probabiliste. La méthode de validation proposée consiste à utiliser un indice de densité relative des avalanches et une méthode ROC-AUC. Les paramètres suivants sont utilisés : la pente, l'exposition, la courbure, l'altitude et la végétation. La pente était limitée à l'intervalle [25°-45°], au lieu de [28°- 60°] en Suisse (Maggioni et al., 2002); (Bühler et al., 2013). En effet, selon Kumar et al. (2019), une pente au-dessus de 45° réduit l'activité avalancheuse parce que les pentes sont trop abruptes pour retenir la neige. Dans la zone d'étude choisie par les auteurs, la région de Lahaul dans l'ouest de l'Himalaya, 98 % des avalanches se produisent dans des altitudes comprises entre 3200 et 5800m. Les altitudes minimale et maximale de leur méthode de détermination sont adaptées à cette montagne : (altitude minimale fixée à 2800m et altitude maximale limitée à 5800m). En France l'altitude minimale utilisée dans la détermination des PRAs doit être inférieure car des avalanches apparaissent à des altitudes bien plus basses que 2800m.

Dans les zones d'étude, la présence de la forêt est généralement obtenue à partir de données satellitaires (par exemple provenant du programme d'observation Landsat) en utilisant un indice de végétation de différence normalisée (NVDI) (Bühler et al., 2013); (Kumar et al., 2019). Cet indice permet de séparer la végétation du reste du sol en utilisant la différence entre les bandes proches de l'infrarouge et du rouge, normalisée par la somme de cette bande (NVDI = NIR-R / NIR+R, où NIR sont les bandes proches de l'infrarouge, et R sont les bandes proches du rouge). L'échelle de mesure s'étend de -1 à 1, où 1 représente la forêt, 0 le manque de végétation, et où les valeurs négatives sont significatives des zones non différenciées (Silleos et al., 2006).

Enfin, une étude récente en Iran a déterminé les zones sensibles aux départs d'avalanches à l'aide de systèmes d'information géographique et de modèles statistiques (Yariyan et al., 2020).

Toutes ces études utilisent différents paramètres et seuils dans la détermination des PRAs, et sont appliqués à petite échelle en fonction des moyens et des données disponibles. Les méthodes de validation proposées dépendent surtout des données sur les avalanches passées enregistrées et sont très différentes d'un pays à l'autre. Il n'y pas encore de méthode de détermination des PRAs adaptées aux Alpes françaises. Cette thèse vise donc à proposer une méthode de détermination applicable de manière systématique sur toutes les Alpes française, et d'évaluer cette méthode à l'aide des informations disponibles sur les avalanches passées.

Caractérisation systématique du terrain avalancheux et des zones de départ des avalanchesvia des relations statistiques

A ce jour, seulement deux études statistiques concernent l'analyse des PRAs en fonction des paramètres topographiques (Gleason, 1996); (Vontobel et al., 2013). La première étude est réalisée en 1996, dans le Montana, plus précisément au Mont Lone. Cette étude a pour objectif de caractériser les paramètres topographiques propres aux PRAs. Cette étude traite des départs d'avalanche naturels et artificiels, distincts les uns des autres en raison de paramètres potentiellement spécifiques à chaque type de déclenchement. Les paramètres utilisés pour les départ d'avalanche naturels sont la pente, l'altitude, l'exposition, la rugosité de la surface, l'exposition au vent dominant, la géométrie de la zone de départ d'avalanche. Les paramètres utilisés pour les départs d'avalanche artificiels sont la pente, l'altitude, le nombre d'explosions, l'exposition au vent dominant, la forme de la zone de départ (profondeur/largeur), ainsi que la largeur et la profondeur de la zone de départ dans la direction transversale (Gleason, 1996). Une étude des caractéristiques des zones de départs artificiels, déclenchés par les skieurs, a été réalisée en Suisse en 2013 (Vontobel et al., 2013). Dans cette étude, 142 PRAs ont été cartographiées, et leurs caractéristiques géomorphologiques extraites d'un MNT (la pente, l'exposition, les crêtes, la rugosité, le profil de courbure.

Par ailleurs, l'étude statistique des caractéristiques des couloirs d'avalanche et l'étude des départs d'avalanche permettent de mieux comprendre l'activité avalancheuse, en particulier les paramètres topographiques du terrain qui génèrent les avalanches. De telles études sont bien plus nombreuses et conduites dans des buts variés : cartographie des extensions maximales possibles, relations entre caractéristiques des avalanches et conditions de déclenchement, etc. La première étude de ce type voit sans doute le jour en 1976, dans le comté de San Juan, au Colorado (Armstrong, 1976). Les paramètres étudiés dans les couloirs d'avalanches sont la température de l'air, l'accumulation de neige, la vitesse et la direction du vent, le taux de tassement de la neige, le taux et la quantité de précipitations, et le rayonnement total à la surface de la neige. Une fois les caractéristiques des avalanches trouvées, les causes de déclenchement des avalanches sont déterminées, puis un modèle permettant de prévoir les avalanches est créé (Armstrong, 1976).

Dans un but différent, dès 1980, les paramètres topographiques sont utilisés pour calculer la distance d'écoulement des avalanches (Lied et Bakkehoi, 1980). Pour cela, 423 couloirs d'avalanches ont été choisis en raison de la connaissance de leur emprise maximale par les habitants, et de l'accessibilité des dépôts sur le terrain. Les paramètres utilisés dans cette étude sont la topographie des zones de départ (cirques provenant de glaciers, dépressions, pentes convexes, surfaces sans courbure notamment les plateau), la pente de la zone de départ, la largeur de la zone de départ, la quantité de neige dans la zone de départ (zones de départ entourées de collines de faible pente permettant l'accumulation de neige, ou zones de départ à proximité des crêtes sans zones d'érosion permettant l'apport en neige), la pente moyenne, la largeur du couloir d'avalanche, le dénivelé total entre la rupture et le point le plus bas des dépôts de l'avalanche, le rayon de courbure maximale, et le profil

du terrain. En 1990, en plus des paramètres topographiques utilisés pour caractériser les couloirs d'avalanches, sont rajoutées avec le même objectif la lithologie et la structure géologique (Butler et Walsh, 1990). La zone d'étude se situe dans le parc national des Glaciers de l'EST du Montana. Depuis 1987 dans la zone d'étude, les avalanches sont répertoriées, enregistrées, et leurs emprises sont cartographiées. De plus, des données morphométriques ont été collectées dans chaque couloir d'avalanche pour faire cette étude. Les paramètres utilisés sont le contour des bassins versants, l'altitude, la pente, l'exposition, la lithologie des sédiments, les structures géologiques (failles), l'occupation du sol (roches, végétation : pin, épicéa), les sentiers et les routes.
Enfin, en 2020, une étude dans les Alpes françaises, plus précisément dans la commune de Bessans (massif de la Haute Maurienne), a pour objectif d'étudier les volumes des dépôts d'avalanche entre 1903 et 2017, et d'analyser l'influence des caractéristiques morphologiques des couloirs sur ces dépôts entre 2003 et 2017. Les couloirs d'avalanches proviennent de 3 sources de données qui sont, la Carte de Localisation des Phénomènes d'Avalanches (CLPA), l'Observation Permanente des Avalanches (OPA), et la base de données du service de Restauration des Terrains en Montagne (RTM) de l'Office National des Forêts (Kern et al., 2020). Pour chacun des couloirs d'avalanches étudiés, des variables morphologiques ont été calculés à partir d'un MNT d'une résolution de 1m. Dans cette étude, pour le calcul des variables, le talweg du couloir d'avalanche est distingué du couloir entier. Pour le talweg, on détermine la longueur, la pente minimale, maximale et moyenne. Pour le couloir entier, on détermine la superficie du couloir, la pente minimale, maximale et moyenne, et l'orientation moyenne du couloir qui est exprimée entre 0° et 360° par rapport à l'axe de la vallée (Kern et al., 2020).
Ainsi, parmi toutes ces études, et même si la thématique de la caractérisation systématique du terrain avalancheux se développe, seulement deux études concernent spécifiquement l'analyse des PRAs en fonction des paramètres topographiques (Gleason, 1996); (Vontobel et al., 2013). Ces travaux ne prennent pas en compte les changements dans le temps, comme c'est le cas avec la couverture forestière. En outre, à ce jour, il n'y aucune étude de ce type réalisée en France.

3 Problématique et objectifs de la thèse

Au vue de l'état de l'art, les thématiques d'étude que traitent cette thèse sont les suivantes : la détermination, la validation, et l'étude des PRAs, et leur évolution dans le temps en fonction de l'occupation du sol.

La détermination des PRAs

Le premier objectif concerne la délimitation des PRAs. En effet, dans les secteurs où la documentation sur les avalanches historiques est partielle ou absente, l'évaluation de l'aléa avalancheux sera difficile. Il est donc primordial de combler ce manque d'information avec une méthode de délimitation des zones de départ potentielles d'avalanche (PRAs) qui n'a pas encore été mise au point en France. En France, dans deux des 23 massifs qui constituent les Alpes, aucune information concernant les avalanches historiques n'est répertoriée dans la CLPA ou consultable sur le site avalanche.fr. D'où l'utilité de mettre au point une méthode de détermination des PRAs spécifique aux Alpes françaises.
Par ailleurs, la plupart des études sur l'identification des PRAs utilisent les mêmes paramètres topographiques, à savoir la pente ou l'exposition. Néanmoins, il existe de nombreux désaccords entre les chercheurs au sujet de certains paramètres et seuils utilisés. C'est le cas par exemple de la distance à la crête, ou de la courbure. Dans d'autres pays, les zones de départ sont détectées dans des zones peu étendues, comme dans la région du Davos en Suisse. Il est également important de souligner que les méthodes d'évaluation sont souvent rudimentaires ou peu explicites, car les données historiques

peuvent être manquantes. Dans la plupart des cas, les avalanches enregistrées comprennent l'ensemble de la zone traversée par l'avalanche, et non pas seulement la zone de départ qui nous intéresse. Il est donc important d'extraire uniquement les zones de départs dans les avalanches enregistrées, dans le but de les confronter avec les PRAs détectées. Une fois ces zones obtenues, nous nous en servirons dans la validation en tant que vérité terrain.
Ainsi, cette thèse vise à proposer en premier lieu une méthode de détermination des PRAs à partir de paramètres topographiques, en utilisant des seuils adaptés aux Alpes françaises, ainsi qu'une méthode de validation permettant de confronter et valider ces PRAs aux données de la CLPA.

L'étude des caractéristiques des PRAs

Les caractéristiques des PRAs comme la pente, l'altitude, l'exposition, la courbure, ou la distance aux crêtes n'ont pas fait l'objet d'analyses systématiques en France. Et même ailleurs, les rares études réalisées se déroulent à une petite échelle, dans des localisations précises. Pour l'instant, Il n'y a pas d'étude des caractéristiques des zones de départ réalisées à grande échelle. Cette thèse propose ainsi une description des caractéristiques des PRAs que nous avons obtenues à grande échelle, c'est-à-dire à l'échelle des Alpes françaises entières. Pour ce faire, nous utiliserons les paramètres topographiques calculés pour chacune des PRAs obtenues pour analyser la localisation des zones de départ d'avalanches en fonction des paramètres topographiques ainsi que leur évolution dans le temps.

Etude de l'évolution des PRAs dans le temps en fonction de la couverture forestière

Dans chacune des études précitées sur la détermination des PRAs, la surface forestière utilisée est considérée comme stationnaire, alors qu'elle évolue dans le temps. Par ailleurs, aucune étude n'a quantifié l'évolution des PRAs en fonction de l'occupation du sol, en particulier la forêt, que ce soit en France ou ailleurs dans le monde entier, alors que c'est un paramètre déterminant dans l'obtention des PRAs. Pour pallier à cette lacune, nous avons étudié l'évolution des PRAs en fonction de la couverture forestière au cours du temps. L'étude a été réalisée de 1860 jusqu'en 2013-2014, dans une zone où les données forestières sont bien documentées. Par ailleurs, le climat a aussi une importance sur les départs d'avalanche, mais nous nous concentrons dans cette thèse sur l'évolution de la forêt.

4 Grille de lecture de la thèse

Au final, cette thèse vise à combler les lacunes liées à chacune des trois thématiques évoquées précédemment, au sein de deux parties distinctes constituant des articles scientifiques autonomes.

La détermination automatique des PRAs et son évaluation en utilisant la CLPA sont traitées dans le premier article, qui est accepté dans la revue *Natural Hazards and Earth System Sciences* (NHESS). En plus de la mise au point de la méthode de détermination et de validation, une étude paramétrique a été réalisée sur différents massifs et zones d'études (massifs de la Maurienne, du Mont-Blanc, de la Chartreuse, zones d'étude à Chamonix et dans la Chartreuse) en faisant varier les paramètres et la résolution utilisés dans la méthode de détermination.

En ce qui concerne l'étude des caractéristiques des PRAs et leur évolution diachronique, les deux thématiques sont regroupées dans un unique article. Dans ce second article, les caractéristiques topographiques des PRAs sont étudiées à l'échelle des Alpes Françaises entières, puis des 23 massifs qui les constituent, et enfin à plus petite échelle dans le Queyras, plus précisément les communes d'Abriés, Ristolas, Aguilles, et dans la Haute-Maurienne avec les communes de Bessans, Bonneval-sur-Arc, Lans-le-Villard. A petite échelle, l'évolution des PRAs est étudiée de 1860 à 2013-2014, en fonction

de la couverture forestière fournie par (Zgheib et al., 2020). Ce second article sera soumis pour publication prochainement dans la revue *Cold Regions Science and Technology* (CRST).

Le dernier chapitre de cette thèse conclut sur le travail effectué et discute quelques perspectives pour le futur.

Chapitre 2 : Développement et validation d'une méthode d'identification des zones potentielles de départ d'avalanche, basée sur la délimitation des bassins versants.

This thesis chapter is now accepted as a research article in Natural Hazards and Earth System Sciences (NHESS).

Abstract. Snow avalanches are a prevalent threat in mountain territories. Large-scale mapping of avalanche prone terrain is a prerequisite for land-use planning where historical information about past events is insufficient. To this aim, the most common approach is the identification of Potential Release Areas (PRAs) followed by numerical avalanche simulations. Existing methods for identifying PRAs rely on terrain analysis. Despite their efficiency, they suffer from i) a lack of systematic evaluation on the basis of adapted metrics and past observations over large areas and ii) a limited ability to distinguish PRAs corresponding to individual avalanche paths. The latter may preclude performing numerical simulations corresponding to individual avalanche events, questioning the realism of resulting hazard assessments. In this paper, a method that well identifies individual snow avalanche PRAs based on terrain parameters and watershed delineation is developed, and confusion matrices and different scores are proposed to evaluate it. Comparison to an extensive cadastre of past avalanche limits from different massifs of the French Alps used as ground truth leads to true positive rates (recall) between 80-87% in PRA numbers, and between 92.4% and 94% in PRA areas, which shows the applicability of the method to the French Alps context. A parametric study is performed, highlighting the overall robustness of the approach and the most important steps/choices to maximize PRA determination, among which the important role of watershed delineation to identify the right number of individual PRAs. These results may contribute to better understanding avalanche hazard in the French Alps. Wider outcomes include an in-depth investigation of the issue of evaluating automated PRA determination methods and a large data set that could be used for additional developments, and to benchmark existing and/or new PRA determination methods.

1 Introduction

In mountain territories, snow avalanches are a prevalent threat, resulting in casualties and damages to buildings and critical infrastructures (Amman and Bebi, 2000; Braun et al., 2020). Identification of avalanche-prone terrain, hazard/risk mapping and construction of defence structure are, therefore, the most efficient ways to reduce death tolls and costs on the long range for settlements downslope (Arnalds et al., 2004; IRASMOS consortium, 2009; Eckert et al., 2012). To this aim, availability of historical information concerning avalanche location, frequency and magnitude is crucial (Giacona et al., 2017). For instance, spatial statistics can be used to interpolate the data available from a sample of paths (Lavigne et al., 2012; 2017) in order to assess avalanche hazard over large areas. However, even in the best-documented areas, historical information is far from exhaustive, and, in many mountain territories, it remains almost absent. The standard approach to delineate avalanche-prone terrain is then the automated identification of Potential Release Areas (PRAs) on the basis of terrain analysis followed by numerical (Naaim et al., 2004; Bartelt et al.. 2012) and/or statistical-numerical

avalanche simulations (Keylock et al., 1999; Eckert et al., 2010; Fischer et al., 2015). In these, PRA identification supplemented by snow cover information from neighbouring meteorological stations or reanalyses provide the input conditions for avalanche simulations, which defines hazard and risk levels downslope (Gruber and Bartelt, 2007; Barbolini et al., 2011; Bühler et al., 2018; Ortner et al., 2022). Wider benefits can also arise from the systematic determination of PRAs: better understanding of the avalanching process at large scale, identification of areas that need to be reforested to reduce hazard and risk, etc.

Snow avalanche PRA determination methods from terrain analysis belong to the class of susceptibility mapping methods, which are widely used for many mountain hazards (Bertrand et al., 2013; Eckert et al., 2018). Several automated snow avalanche PRA determination methods are now available in the literature, and, since first proposals (Maggioni et al., 2002; Maggioni and Gruber, 2003), different extensions have been implemented (e.g., Sykes et al., 2021). For example, while PRAs were historically assessed independently from snow and weather conditions, Chueca Cía et al. (2014) developed a multi-criteria analysis for snow avalanche susceptibility mapping that uses wind directions and snowdrift to identify PRAs in a dynamic way. Also, while most of existing approaches are deterministic (e.g., Bühler et al., 2013), Veitinger et al. (2016) apply fuzzy logic to relate past release areas to slope, roughness and a shelter wind index. Similarly, Kumar et al. (2019) detect PRAs in the Lahaul region of Western Himalaya using a probabilistic occurrence ratio and Yariyan et al. (2020) identify more broadly "avalanche sensitive areas" using different statistical models.

Most of existing PRA determination methods use forest cover and geomorphologic features such as slope, plan curvature, aspect, and distance to ridges as decisive factors. For instance, distance to ridges is generally retained as a useful quantity because it is a proxy for snowdrift, which is known to be an important triggering factor (e.g., Lehning et al., 2000). Also, forests limit avalanches release by anchoring snowpack and, more generally, lower avalanche hazard and risk downslope (Bebi et al., 2009; Zgheib et al., 2022; in press), so that presence of a dense forest is often considered as sufficient to exclude a given location from PRAs (e.g. Maggioni et al. 2002). Finally, PRA determination methods are primarily oriented towards large avalanches, which are of interest to assess long-term risk for people and settlements downslope, so that a minimal size is generally considered (e.g. Maggioni et al. 2002).

However, there are some disagreements between researchers about i) the exact choice and respective importance of the different factors to be used in PRA determination, and ii) the best parameter values/thresholds to be specified to reach maximal efficiency. For instance, in Maggioni et al. (2002), included factors are slope, aspect, curvature, forest presence, and distance to ridges, whereas Bühler et al. (2013) consider, in addition, information about roughness and flow direction. Also, it is generally admitted that, for slopes steeper than 60°, snow accumulation is low (e.g., Maggioni and Gruber, 2003). Yet, the range of slopes to be retained in automated PRA determination remains debated, as i) the true range of slopes over which avalanche release is actually possible remains uncertain (e.g., it varies with snow conditions, Schweizer et al., 2003; Naaim et al., 2013), and ii) it is not independent of the chosen Digital Elevation Model (DEM) resolution. Hence, the 28-60° range is selected in Veitinger et al. (2016) using a DEM with a 2m resolution, but 28-55° is preferred in Aydin and Eker (2017) using a DEM with a resolution of 10 m, and 25-40° is used in Kumar and al., (2019). Similarly, the range of elevations where PRAs are searched depends on the region of the world. Aydin and Eker (2017) consider the 1000-4000m a.s.l. range in Turkey, while Kumar et al. (2019) adapt this range to higher mountain environments with a minimal elevation fixed to 2800m a.s.l. Finally, dynamic PRA mapping methods consider snow and weather factors. As examples, Chueca Cía et al. (2014) make use of a

multi-scale roughness adjusted to snow depth and of a shelter wind index whereas other parameters describing the climatology (snowfall, temperature change, precipitation), lithology and land use are accounted for in Yariyan et al. (2020).

An important characteristics of most of existing PRA determination methods is their limited ability to distinguish PRAs corresponding to individual avalanche paths/events. Indeed, PRA determination methods mostly focus on terrain characteristics at the pixel scale. Hence, they do not easily segment large areas where factors are favourable to avalanche release (suitable slope, roughness, etc.) in different PRAs compatible with the physical processes involved in snow avalanching (Schweizer, 2003). This may lead to unrealistically wide PRAs that, in reality, correspond to different avalanche paths/events. This drawback is critical for using these PRAs for hazard assessment downslope, as it may preclude performing numerical simulations corresponding to realistic individual avalanche events. An exception is, however, the object-based approach of Bühler et al. (2018), where avalanche terrain is segmented into spatially coherent entities using an image classification step.

To evaluate the performance of PRA determination methods, most studies use recorded avalanches (Maggioni and Gruber, 2003; Bühler et al., 2013; Veitinger et al., 2016), with historical information provided either by local observers after each event or by interviewing local people. Evaluation is often qualitative, and compare the detected PRAs with avalanches boundaries obtained from residents (Aydin and Eker, 2017), from aerial or satellite photographs (Bühler et al., 2019) or from avalanche simulations (Nolting et al., 2018). Over the recent years, more quantitative evaluation methods have gained popularity in the snow avalanche field, notably to assess the efficiency of snow avalanche determination from satellite images (e.g., Karas et al., 2021), or of the prediction of snow avalanche occurrences on the basis of snow and weather conditions (Sielenou et al., 2021; Pérez-Guillén et al., 2021; Viallon-Galinier et al., 2022). These evaluation approaches use different metrics to quantify overall performance based on long historical records or large-scale field data taken as ground truth. Considered metrics include probabilistic occurrence ratios (summarized as confusion matrices) and receiver operating characteristic – area under curve (ROC-AUC criteria). To our knowledge, despite the strong development over the last years of different PRA determination methods, these quantitative evaluation methods have only seen limited use so far (Bühler et al., 2018) to evaluate their respective efficiency, advantages and limits in an objective way. This lack is partially attributable to the fact that information about avalanche release areas is even sparser than information about avalanches in general. Indeed, avalanche releases typically occur in remote uninhabited and/or difficult/dangerous-to-access areas, so that defining a reliable sample of “ground truth” PRA is extremely difficult, if not almost impossible.

On this basis, the main objective of the paper is to develop and evaluate an automated PRA determination method adapted to the context of the French Alps. The aim of our approach is to identify all locations where avalanches can occur. There is no notion of frequency, meaning that avalanche releases may occur very frequently in certain PRAs we detect, and extremely rarely in others. Also, our definition of an individual PRA is the maximal extent corresponding to the release of a single avalanche event. Hence, in practice, many avalanche releases may concern a (potentially small) fraction of a single PRA, especially for the largest PRAs we detect. To reach this goal, we build on already existing developments (notably by Maggioni, et al., 2003 and Bühler et al., 2013), so that our method uses topographical parameters (minimal elevation, range of slopes, maximum distance to ridges) and presence of forests as key factors. In addition to the careful selection of suitable values for these parameters and data sets, two research questions are specifically targeted: the determination of realistic individual PRAs using a watershed delineation algorithm and the evaluation of the method on

the basis of scores computed using two metrics, PRA numbers and areas. For the latter, an extensive cadastre of past avalanche limits from different massifs of the French Alps is used as a support to derive a ground truth validation sample, which is shown to be a non-trivial task. In what follows, Sect. 2. introduces datasets and study areas. Sect. 3 describes the proposed PRA determination method and evaluation framework. Sect. 4 details the results for study areas. Sect 5. discusses main findings and pro's and con's of the proposed approach. Sect. 6. concludes and points out outlooks for further applications and developments.

2 Data

Study areas

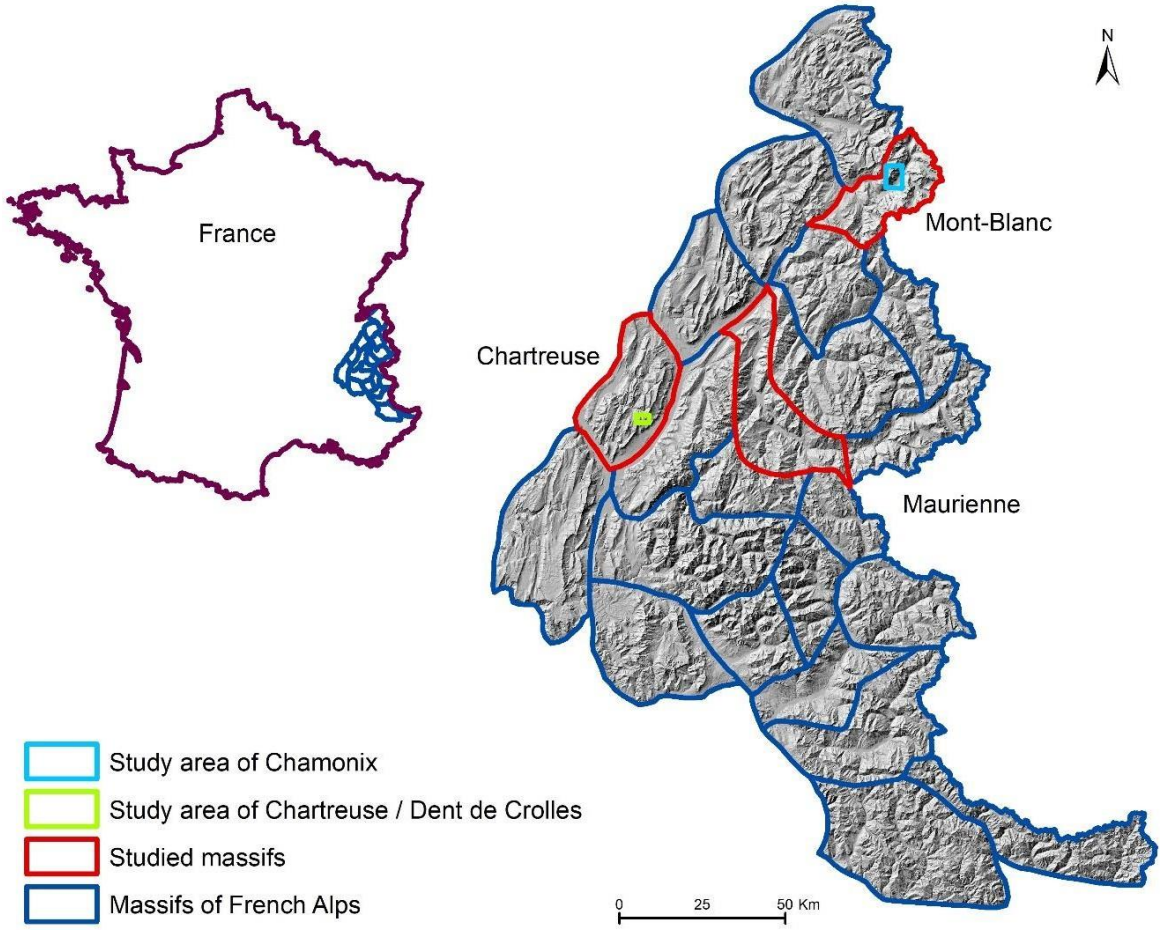

Figure 5 : Study areas: three entire massifs (within the 23 massifs of the French Alps) and two small highlighted areas, the one of Chamonix and the one of Chartreuse/Dent de Crolles. Digital Elevation Model ©IGN.

In this paper, we focus on the French Alps and its classical segmentation into 23 massifs for snow-climate reanalyses and operational snow avalanche forecasting (e.g., Durand et al.; 2009a; 2009b; Evin et al., 2021). Despite the high exposure to snow avalanche risk of this territory, no automated PRA determination method was systematically applied in it so far. For this study, three entire massifs with different characteristics are specifically considered to develop and evaluate the determination method: Mont-Blanc, Chartreuse, and Maurienne (Figure 5). In addition, a focus is made on two smaller test areas, so as to highlight some results and deepen the analyses at a fine spatial scale (Table 1).

The Mont-Blanc massif reaches an elevation of 4,809 m a.s.l. at the Mont-Blanc summit (top of Western Europe), and it is mainly composed of granite and gneiss. The valley of Chamonix is well known for mountaineering, but also to be extremely exposed to snow avalanches. A tragic example is the snow avalanches of Montroc (9 February 1999), which led to the loss of twelve residents and the devastation of fourteen chalets (Ancey et al., 2000). The massif of Chartreuse is a massif of the Prealps, mainly composed of limestone. This massif is less subject to snow avalanches because of its lower elevation (highest point is Chamechaude at 2,082 m a.s.l.), but destructive snow avalanches occurred in it in the past, such as in Saint-Hilaire-du-Touvet (Ancey et al.. 1999). The Maurienne massif has an intermediate elevation (highest peak reaches 3,160 m a.s.l.). Its economy is strongly oriented towards winter sports and several of its large ski areas are threatened by avalanches. The Chamonix area is a 34.3 km^2 area, which is part of the Mont Blanc massif and includes the municipality of Chamonix Mont Blanc. The Chartreuse / Dent de Crolles area is an even smaller area (7.6 km^2) located within the Chartreuse massif and with the Dent de Crolles (2,062 m a.s.l.) in its center (Figure S1 in the annexes).

	Chamonix area	Chartreuse / Dent de Crolles area	Chartreuse massif	Mont Blanc massif	Maurienne massif
Total area [km^2]	34.3	7.6	847	578	917.1
Total area covered by CLPA [km^2]	25.8	4.7	44	354.6	382.3
Fraction of area covered by CLPA	75.3%	61.7%	5.2%	61.3%	41.7%
Total area of PRAs within CLPA extents (validation sample) [km^2]	3.6	0.5	1.6	58.3	55.7
Total number of PRAs within CLPA extents (validation sample)	85	28	85	1522	1884
Total area of detected PRAs [km^2]	8.1	1.2	15.4	166.3	115.1
Total number of detected PRAs	210	58	721	3676	3638
Total area of detected PRAs within area covered by CLPA [km^2]	5.5	0.8	2.3	90.8	71.6
Total number of detected PRAs within areas covered by CLPA	107	39	108	2003	2575
Aerial fraction of detected PRAs within the area	23.7%	15.3%	1.8%	28.8%	12.5%
Aerial fraction of PRAs within the area covered by CLPA	21.2%	17.0%	5.3%	25.6%	18.7%
Aerial fraction of PRAs within CLPA extents with regards to total area of PRAs	67.2%	68.4%	15.3%	54.6%	62.3%
Fraction of PRAs numbers within CLPA extents with regards to total number of PRAs	40.5%	48.3%	11.8%	41.4%	51.8%

Table 1 : Characteristics of studied massifs and areas. For the PRA determination and the determination of the validation sample, all factors and the DEM resolution are set to their default values (Figure 7 and Figure 8), and forest cover data is from DB forest IGN.

DEM and forest cover

Topographic information used in the proposed PRA determination method is classically derived from a DEM. We primarily used the reference 25 m resolution DEM from the French National Geographical Institute (IGN) as a good compromise to i) detect the right number and areas of PRAs (even if the determination is then certainly less precise in terms of PRA boundaries that with finer resolutions, e.g. Bühler et al., 2013), and ii) being ultimately applicable over very large areas at reasonable computational costs. Sect. 4.2.3 investigates how using DEMs of finer resolutions (also provided by IGN) affects the results.

In addition to the DEM, our method considers forest cover as input data. For the French Alps, three nation-wide forest cover databases can potentially be used:

- The DB forest (database forest) provided by IGN (French National Geographical Institute) obtained from the interpretation of aerial infrared photographs. 32 classes of vegetation are available (notably, as function of tree species, ADEME and IGN, 2019). This data was created in 2013;
- Corine land cover is a database of land cover based on satellite imagery, which considers five classes of vegetation (artificial surfaces, agricultural areas, forests and semi natural areas, wetlands, and water bodies, Caetano et al., 2009). It is updated every 6 years, and the 2012 version was considered for the sake of comparison with the IGN data;
- Theia database is provided by the *Centre d'Expertise Scientifique* (CES), which extracts data about land use, soil humidity and snow cover from Sentinel 2A and 2B satellites (Baghdadi et al., 2021). The 2016 version was selected as the closest from 2013.

Our PRA determination method uses forest presence/absence only. We thus derived this information for the three databases in our study areas. None of them is free of errors. Specifically, visual comparison with aerial photographs shows that, logically, main issues occur when the forest density is low, which makes the limit between forests and non-forest areas difficult to set (Figure 6). However, several comparisons in different areas of the studied massifs suggested that the DB forest was, overall, the most accurate and it was thus primarily selected to be used in our PRA determination method. Sect. 4.2.1. assesses the sensitivity to this choice.

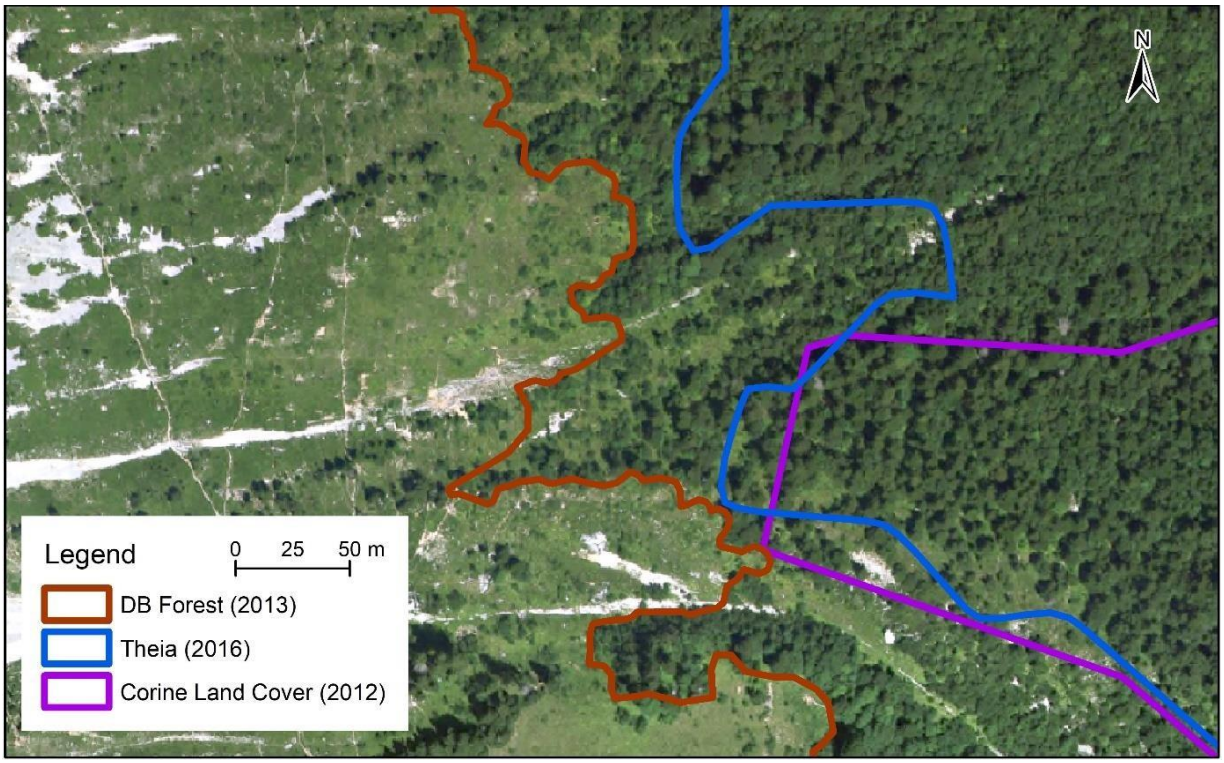

Figure 6 : Comparison of forest extents from Theia, Corine land cover, and DB Forest from IGN with aerial photographs (©IGN) taken in 2012 within the municipality of Le Sappey-en-Chartreuse, Chartreuse / Dent de Crolles study area.

Avalanche extents from the French avalanche cadastre (CLPA)

The lack of data concerning historical avalanches contributed to the Val-d'Isère disaster (11 February 1970), where an avalanche led to 39 casualties. Following this tragic event, the French government required the establishment of the CLPA cadastre. Its overall objective is to map the entire avalanche terrain, independently of any frequency consideration. It consists of a collection of maps indicating the maximum extents reached by avalanches in the past. CLPA is obtained using photo-interpretation, terrain observation, historical records, testimonies of residents and mountain professionals such as mountain guides, rescue services and ski resort professionals (Bourova et al., 2016; Naaim-Bouvet and Richard, 2015). CLPA also identifies protection structures (Figure S1 in the annexes). The target audience mostly includes mountain professionals (Ancey, 1996). CLPA now covers most of the French Alps, but some areas within the 23 massifs are still completely uncovered (e.g., less than 40% of the Mont Blanc Massif, but nearly 95% of the Chartreuse massif, Table 1). The whole information is freely available at http://www.avalanches.fr (Bonnefoy et al., 2010).

Due to its long history, its regular update by devoted technicians, the continuous financial support of the French ministry of the environment and the consideration in the determination of avalanche terrain of a large amount of different data sources, CLPA is very reliable, meaning that an avalanche extent which is within the CLPA is almost surely a true avalanche extent. By contrast, as all avalanche cadastres, CLPA is not entirely exhaustive. Very rare avalanches may not have occurred since the CLPA exists, and avalanches may have been missed in remote areas. In addition, forest stands that keep the footprints of past events in their landscape forms (e.g., Giacona et al., 2018) are absent in high elevation areas. As a consequence, in areas covered by CLPA, avalanche extents are more exhaustive near human settlements and assets, and less exhaustive in remote areas without stakes and which are difficult to access as well as in high elevation forest-free zones. This is for example the case for high mountain areas and/or remote valleys, as it is clearly visible in Figure S1 in the annexes. Within the

same line, CLPA extents are often less exhaustive close to release areas than in runout areas. Yet, CLPA is a very valuable source of information regarding locations where past avalanches occurred, and, among the rare existing cadastres at a spatial scale as large as the entire French Alps (Bourova et al., 2016).

3 Proposed PRA determination and evaluation method

The proposed determination of individual PRAs uses topographical information (distance to ridges, slopes, aspect and general curvature) calculated at the pixel scale from the DEM, forest cover extent and a watershed delineation algorithm. Thresholds and parameter values are chosen according to the literature, local peculiarities of the French Alps and a systematic parametric study (Sect. 4.2). Hence, with regards to most of existing methods, main difference is the watershed delineation step, whose underlying idea is similar to the one of the object-based approach of Bühler et al. (2018), namely identifying PRAs corresponding to realistic individual avalanche events. PRAs are detected without any consideration of release frequency, and identified PRAs correspond, for each avalanche path, to a maximal release area.

Calculations at the pixel scale

Determination of ridges

To compute the distance to ridges, we use the Geomorphon algorithm of the Grass GIS described in Jasiewicz and Stepinski (2013), which processes the DEM to classify landform elements (ridge, valley) depending on topography. Once ridges have been obtained, the smallest distance to ridges can be evaluated for each pixel of the DEM (it can be equal to 0 when a PRA is in contact with a ridge).

Slope, aspect and curvature

Slope is directly obtained as the first derivate of the DEM, and curvature as the second derivate (i.e. first derivate of the slope). Aspect is the maximum slope direction. Concerning curvature, three different quantities can be considered:

- Profile curvature is the curvature of the surface towards the steeper slope;
- Plan curvature is the curvature of the surface transverse to the slope direction;
- General curvature is the curvature of the surface itself. General curvature is positive in convex areas such as ridges, negative in concave areas such as valleys, and null if the plan is horizontal (Zevenbergen and Thorne, 1987). We focus on this last quantity considered as the most relevant for snow avalanching.

Slopes, aspects and general curvatures are obtained using the default option in SAGA GIS (Zevenbergen and Thorne, 1987).

Individualization of PRAs using watersheds

To obtain spatial entities which correspond to individual avalanche paths/events, a delineation method is applied as follows (Figure S2 in the annexes). First, slopes are calculated for a central pixel and its eight neighbours following Kinner (2003). We then compute the flow direction (Stojkovic et al., 2012). Downward or negative slopes indicate the direction where water flows and provide the flow direction and flow accumulation. The number of accumulated pixels is then obtained for each pixel of the DEM as the sum of all pixels upstream, i.e. which converge in this direction. Flow accumulation is always non-zero except for pixels located on extremities. Individualized watersheds are obtained from flow accumulation values by identifying the most important flows and by attributing each pixel to one of

these flows as detailed in Djokic and Ye (2000). Computations are made with the watershed algorithm of the ARCGIS environment.

The different steps of the proposed PRA determination method

Our determination method is composed of 12 steps (Figure 7). It is based on a DEM with a resolution of 25 m and forest cover extents from IGN DB forest. Following most of existing approaches, it is a binary deterministic classification approach based i) on topographical parameters that do not change with time, and ii) on the presence/absence of forests.

In details, first, we create a layer of points corresponding to filtered pixels of the DEM and for which we evaluate slope, curvature, elevation, aspect, distance to the nearest ridge as stated above, as well as the name of the corresponding massif, latitude, and longitude. To this aim, pixels below the altitude of 1400 m are excluded, as lower elevations receive too little snow in the French Alps under current climate conditions (Durand et al., 2009b) and climate projections clearly indicate a further decrease of snow accumulations in the future for these low elevations (Castebrunet et al., 2014; Verfaillie et al., 2018). Besides, following Maggioni and Gruber (2003), only pixels with a slope between 28° and 60° are kept. Also, only pixels situated at less than 600 m from the closest ridge are further considered. Figure S3 in the annexes shows the pdf of the distance to the closest ridge for the study area close to Chamonix, which quickly decreases with distance and is close to zero above 600 m. Hence, even if this latter filter makes sense due to the impact of snowdrift on avalanche release, it generally affects limited areas. Finally, we remove areas covered by a dense forest according to the DB forest of IGN and the pixels kept are converted to a layer of points. The following processing step consists in applying the delineation algorithm to individualize each PRA (Sect. 3.1.3) and only polygons with a minimal planar area of ten pixels (i.e., 6250 m^2) are conserved. The resulting polygons are converted to a vector layer. For each polygon corresponding to a PRA, different PRA-scale attributes are stored: distance to the closest ridge, name of the corresponding massif, slope, aspect, elevation, curvature, latitude, longitude, and planar area.

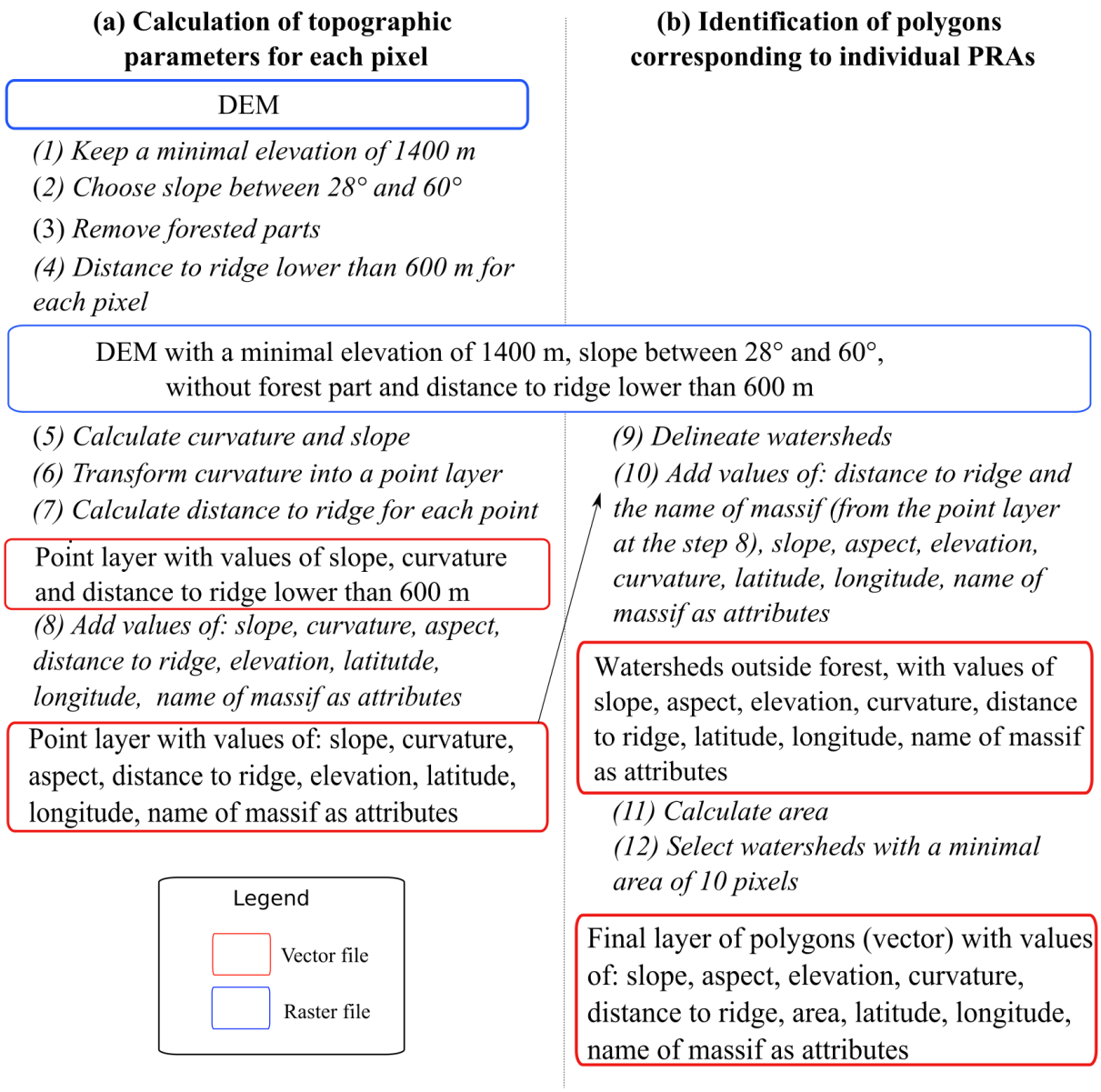

Figure 7 : The 12 steps of the proposed PRA determination method. Calculations at (a) the pixel scale, (b) at the scale of identified polygons.

Processing of the CLPA for PRA evaluation

Thanks to the 50-year history of CLPA, the mapped avalanche extents it contains are getting closer and closer to the true maximal extent of avalanche terrain. The CLPA cadastre is therefore a good candidate to be used as ground truth to validate our PRA determination method. However, a direct comparison is meaningless. Indeed, i) there is simply no CLPA at all in some areas of the French Alps (Table 1), ii) path boundaries in CLPAs are not systematically mapped, especially in release areas (Figure S1 of the annexes), iii) the CLPA documents the entire maximum extents of observed past avalanches (Figure S1 of the annexes), whereas our PRA determination approach only focuses on release areas. Hence, i) our evaluation focuses on the fractions of massifs / study-areas covered by CLPA, and ii) in these, CLPA avalanche extents are processed as follows in order to generate a validation sample that can be compared with our PRAs. First, all boundaries of the CLPA polygons are merged together, leading a single polygon layer representing the maximal extent of past avalanches according to available records, testimonies and photo-interpretation insights. Second, the same criteria of slope, minimal elevation,

distance to ridge, and presence of forest as for the PRA determination are used to filter this polygon. Finally, individual PRAs are identified with the watershed delineation algorithm, and those with a minimal area of 6250 m^2 are kept (Figure 8). We use the concept of “validation sample” as it is taken as the “ground truth”. However, given that this sample and the overall comparison scheme are not free of discussible limitations (Sect. 5.3), we prefer speaking of an evaluation rather than of a validation approach. Sect. 5.3 discusses its pro’s and con’s.

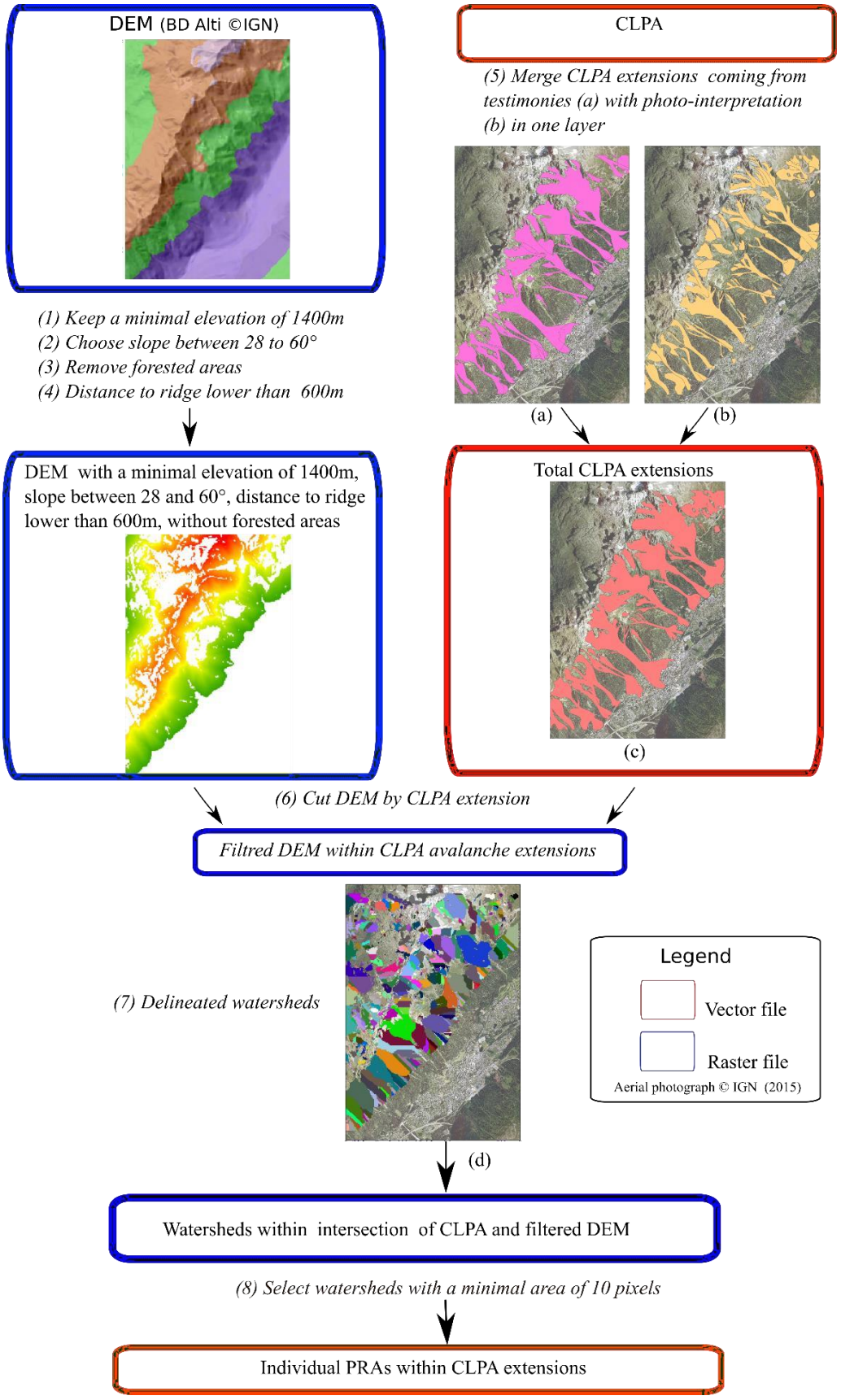

Figure 8 : The French avalanche cadaster (CLPA) and the processing steps used to identify individual PRAs within CLPA avalanche extents ("avalanche extensions") as a validation sample for the proposed PRAs determination method. (a) CLPA avalanche extents coming from testimonies, (b) CLPA avalanche extents coming from photo-interpretation, (c) Union of CLPA avalanche extents, (d) Delineation of individual PRAs within CLPA avalanche extents. Aerial photograph ©IGN 2015.

Confusion matrices and evaluation scores

Confusion matrices (Table 2) can be obtained from the comparison between the detected PRAs and the processed CLPA extents (Sect. 3.3), the latter being considered as a reference dataset (ground truth). A confusion matrix includes four numbers (or rates, i.e. standardized numbers): true positives (TP), true negatives (TN), false positives (FP), and false negatives (FN). A true positive means that the prediction and the reference values match, i.e. detected PRAs match processed CLPA extents. A false positive means that a PRA is detected outside the processed CLPA extents. True negatives correspond to areas which are neither detected by our PRA determination method nor included in processed CLPA extents, and false negatives to processed CLPA extents that are not detected by our method.

		Detected PRAs (Figure 7)	
		Yes	No
Processed CLPA extents (Figure 8)	Yes	True positive (TP)	False negative (FN)
	No	False positive (FP)	True negative (TN)

Table 2 : Principle of a confusion matrix and application to our PRA determination method.

Accuracy and error rates that summarize the confusion matrix are classically computed as follows:

$$Accuracy\ rate = \frac{True\ positive + True\ negative}{True\ positive + True\ negative + False\ positive + False\ negative} \quad (1)$$

$$\text{Error rate} = \frac{False\ positive + False\ negative}{True\ positive + True\ negative + False\ positive + False\ negative} \quad (2)$$

As the CLPA processing method (Figure 8) applies the same filters than our PRA determination method and because the comparison is restricted to the area covered by CLPA extents (Sect. 3.3), by construction, only true positives can be confidently assessed. Our evaluation therefore focuses on the true positive rate (TPR) also know as recall or sensitivity of the method:

$$TPR\left(recall\right) = \frac{TP}{TP + FN} \quad (3)$$

Finally, to evaluate the ability of our method to detect i) the right number of PRAs and ii) their correct extents, the confusion matrix is computed both in terms of areas (comparison of the areas of the polygons) and numbers (comparison of the number of polygons). In terms of numbers, a detected PRA and a validation polygon match as soon as their intersection is non-zero. The confusion matrix in area is computed by evaluating intersected areas.

Robustness of the determination and evaluation method

In order to tune the different factors involved in the PRA determination method, and, more generally, to assess the robustness of our PRA determination and evaluation approach, our scores (Eqs. 1-3) were computed for a large number of input factors and data sets. In details, we first quantified to which extent the marginal effect of the different factors and data sources involved in our determination method gradually increase evaluation scores. We then more deeply analysed the sensitivity to the most critical factors using a parametric study. In addition, we assessed the impact of the DEM resolution, not only on scores but also on the determination of the validation sample and the subsequent changes in PRA determination. Small study areas were used to understand and showcase

detailed results, but the efficiency of the method was primarily analysed in terms of massif-scale scores, which provide a much more systematic assessment free of local effects.

4. Results

Results for study areas and massifs

We first illustrate the results of the PRA determination method with the default factor values and data sets (Figure 7 and Figure 8) in the study area of Chamonix (Figure 9). Avalanche extents from the CLPA, when processed according to Sect. 3.3, lead a validation sample of 85 individual PRAs in this area (PRAs/CLPA, Table 1). For the same area, the automated determination method leads 107 PRAs within the area covered by CLPA, and 103 PRAs outside (PRAs/AUTO outside the area covered by CLPA). The latter are mainly in remote areas not covered by CLPA, the city of Chamonix being surrounded by high mountains, which are difficult to access and document. Among the 107 PRAs detected within the area covered by CLPA, 90 intersect the processed CLPA extents (PRAs/AUTO inside the areas covered by CLPA and matching PRA/CLPAs). By contrast, 17 PRAs detected within the area covered by CLPA do not intersect the processed CLPA extents at all (PRAs/AUTO inside the areas covered by CLPA and not matching PRA/CLPAs).

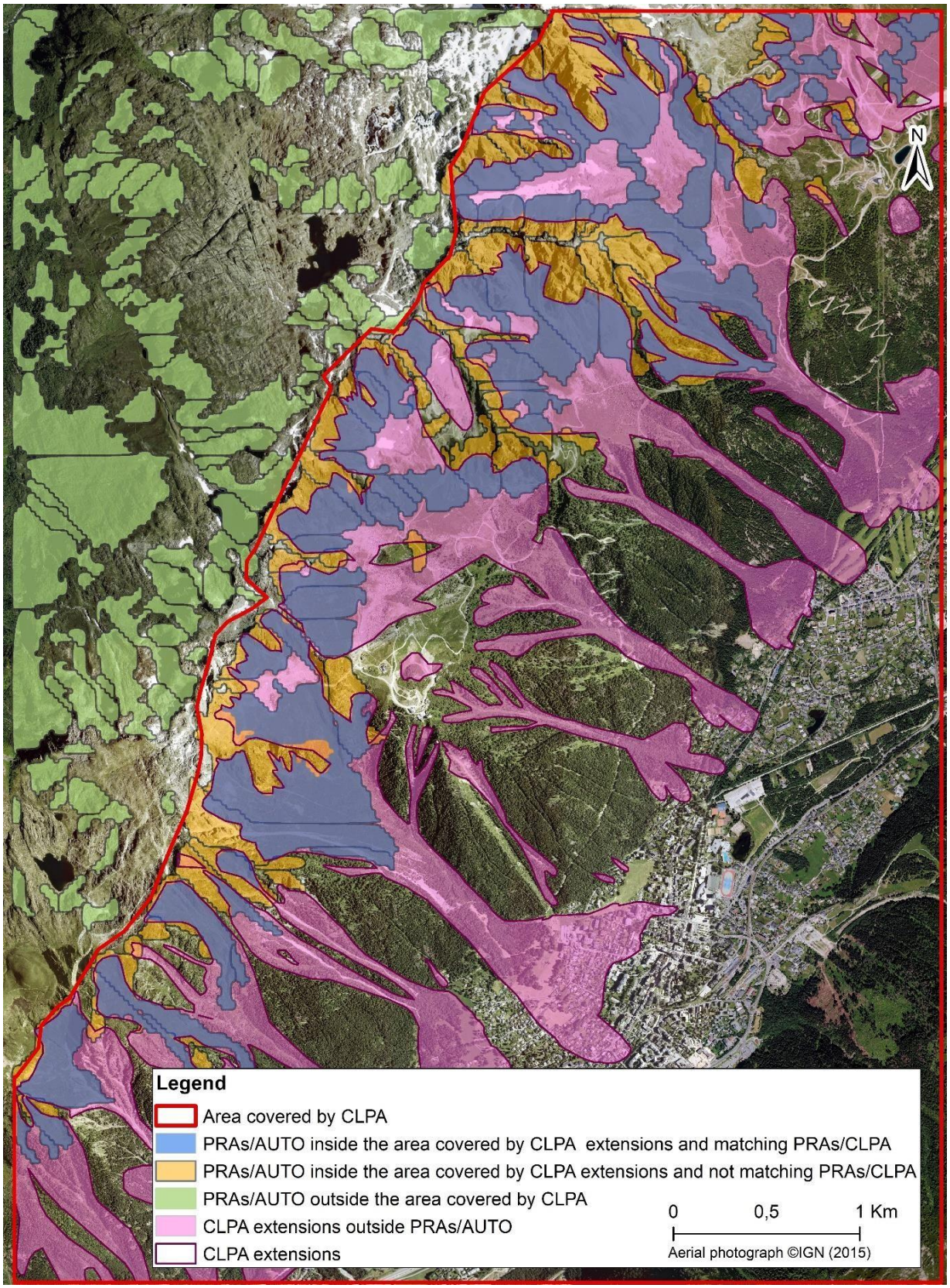

Figure 9 : Result of the proposed PRA determination method for the study area of Chamonix. Agreement and mismatches with the avalanche extents from the French avalanche cadastre ("CLPA extensions") are highlighted. For the PRA determination and the determination of the validation sample, all factors and the DEM resolution are set to their default values (Figure 7 and Figure 8), and forest cover data is from DB forest IGN.

The two confusions matrices are computed for the areas covered by CLPA only. They evaluate the performances of the determination method in terms of number and surface of detected PRAs. In numbers, the 90 detected PRAs that intersect the processed CLPA extents represent 84.1% of the total number of detected PRAs within the areas covered by CLPA (true positive rate, Eq. 3). The false positive rate (15.9%) complements the true positive rate, and 100% of PRAs within CLPA extents are detected according to our evaluation approach, by constraint (Table 3). This leads an accuracy rate of 92.1% and an error rate of 7.9% in numbers (Eqs. 1-2). In term of areas, the total area covered by the detected PRAs in the areas covered by CLPA is 5.48 km2 (Table 1), and, among them, 5.29 km^2 intersect CLPA extents (true positive rate of 96.5 %). This leads an accuracy rate of 98.3 %, and consequently an error rate of 1.7% in terms of areas.

Confusion matrix in areas [km^2] (%)		Confusion matrix in numbers (%)	
5.29 km^2 (96.5%)	0 (0%)	90 (84.1%)	0(0%)
0.19 km^2 (3.5%)	3.56 km^2 (100%)	17 (15.9%)	85 (100%)

Table 3 : Confusion matrix (Table 2) in areas (%) and numbers (%) for the study area of Chamonix. For the PRA determination and the determination of the validation sample, all factors and the DEM resolution are set to their default values (Figure 7 and Figure 8), and forest cover data is from DB forest IGN.

We now switch to massif-scale results and focus on true positive rates that, given our evaluation scheme, summarize all relevant information concerning the efficiency of the PRA determination. For the Chartreuse massif, the PRA determination method with the default factor values and data sets lead 721 individual PRAs, for a total area of 15.4 km^2, which represents 1.8% of the surface of the massif. Logically, detected PRAs are concentrated close to the main ridges, where the only areas in the Chartreuse massif that are both high and steep enough and forest free are located (Figure 10). The area covered by CLPA is located on the east flank of the massif along a main ridge and close to the large Gresivaudan valley, which is densely urbanized. Visually, the matching between the PRAs within processed CLPA extents and the automatically detected PRAs appears satisfactory. True positive rates reach 87% in numbers and 92.4% in areas. Due to the small fraction of the massif covered by the CLPA, the total area of detected PRAs within the area covered by CLPA is 2.3 km^2 only, which corresponds to 108 individual PRAs. These are 11.8% and 15.3% of detected PRA numbers and areas in the massif, respectively. Finally, as the CLPA focuses of the part of the massif where avalanche activity is more likely, the aerial fraction of detected PRAs is higher within the area covered by CLPA (5.3%) than at the massif scale (Table 1).

Figure 11 and Figure 12 display massif-scale results for the Mont-Blanc and Maurienne massifs. Both massifs are more prone to avalanche activity that the Chartreuse massif due to their topography and elevation. As a consequence, total numbers and areas of detected PRAs are much higher than in the Chartreuse massif. Notably, the aerial fraction of detected PRAs is 12.5% in the Maurienne massif and peaks at 28.8% in the high elevation Mont Blanc massif (Table 1). Also, both the Mont Blanc and Maurienne massifs are much more largely covered by CLPA than the Chartreuse massif, so that around half of the PRA numbers and areas detected in these massifs are within CLPA extents (Table 1). Hence, in both massifs, evaluation scores are computed over large validation samples.

Table 4 sums up obtained true positive rates for all massifs and study areas. They are always high, especially in areas (92.4-94% for the tree massifs). The lowest true positive rate is in numbers for the massif of Mont-Blanc (80%). It can probably be explained by the fact that avalanche activity is, on average, more exhaustively documented close to release areas within the extents of CLPAs in the massifs of Chartreuse and Maurienne, making the validation sample more comprehensive in these massifs. The reason is that, in the Mont-Blanc massif, many avalanche release areas included within

the area covered by CLPA (South-East of Figure 11) are located at high elevations and in remote zones, and very far from any forest stand. Hence, related avalanche activity was missed during the establishment of CLPAs, as no insights from past snow avalanches could be retrieved, either from testimonies or from photo-interpretation (visual determination of avalanche corridors in forested slopes), which led to missing PRAs in the validation sample. By comparison, in Maurienne and Chartreuse, PRAs in areas covered by CLPA are, on average, located closer to valleys and forest stands, making arguably CLPAs, and, hence, validation samples more accurate.

		Chamonix area	Chartreuse / Dent de Crolles area	Chartreuse Massif	Mont-Blanc Massif	Maurienne Massif
True positive rate (recall), Eq. 3	In numbers (%)	84.1	87.2	87	80	82.8
	In areas (%)	96.5	80.4	92.4	93.6	94

Table 4 *:* Summary of true positive rates calculated in numbers and areas for the different areas and massifs. For the PRA determination and the determination of the validation sample, all factors and the DEM resolution are set to their default values (Figure 7 and Figure 8), and forest cover data is from DB forest IGN.

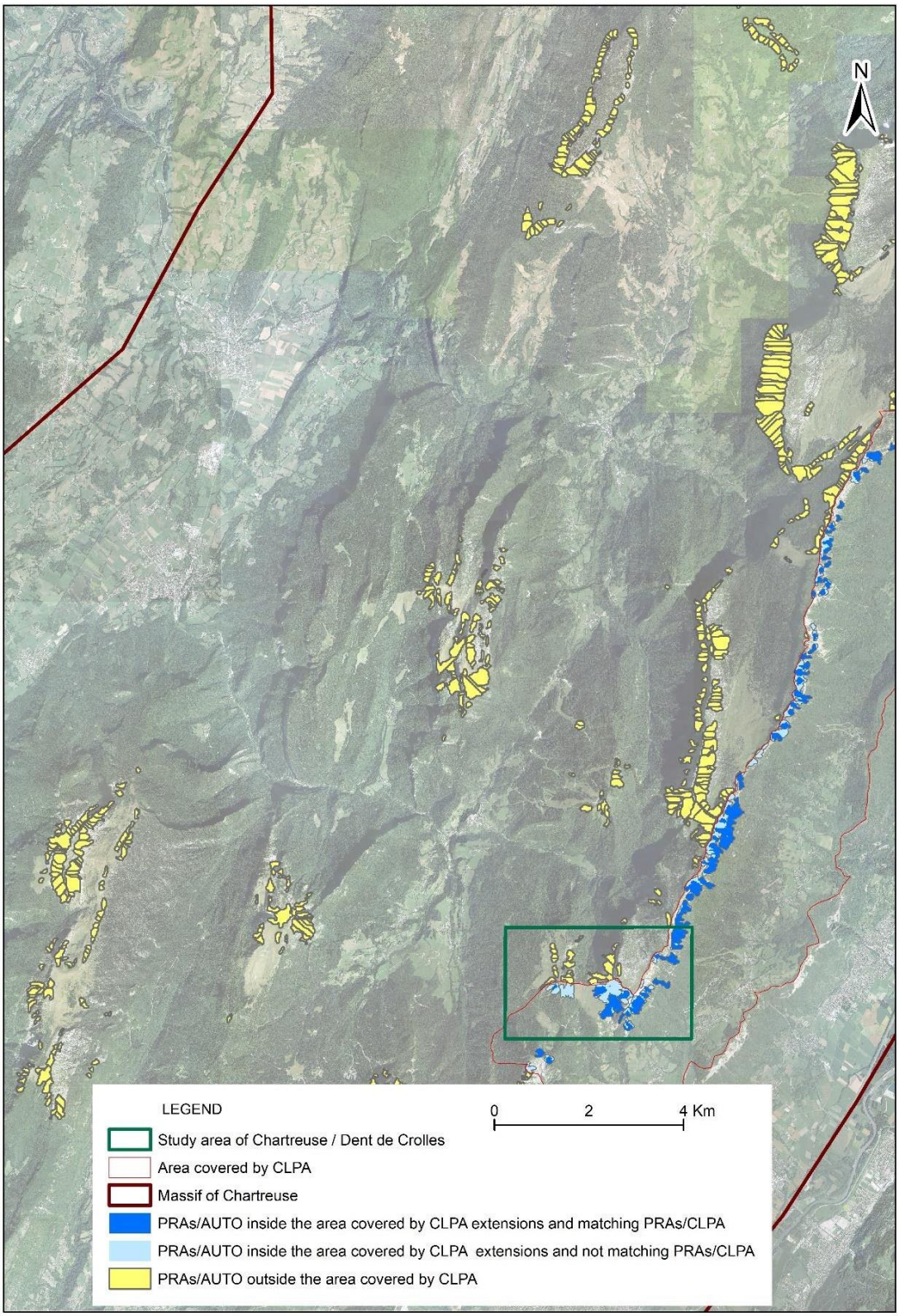

Figure 10 : Result of the proposed PRA determination method for the entire Chartreuse massif. For the PRA determination and the determination of the validation sample, all factors and the DEM resolution are set to their default values (Figure 7 and Figure 8), and forest cover data is from DB forest IGN. “CLPA extensions” refer to avalanche extents from the French avalanche cadastre. Aerial photograph ©IGN 2012.

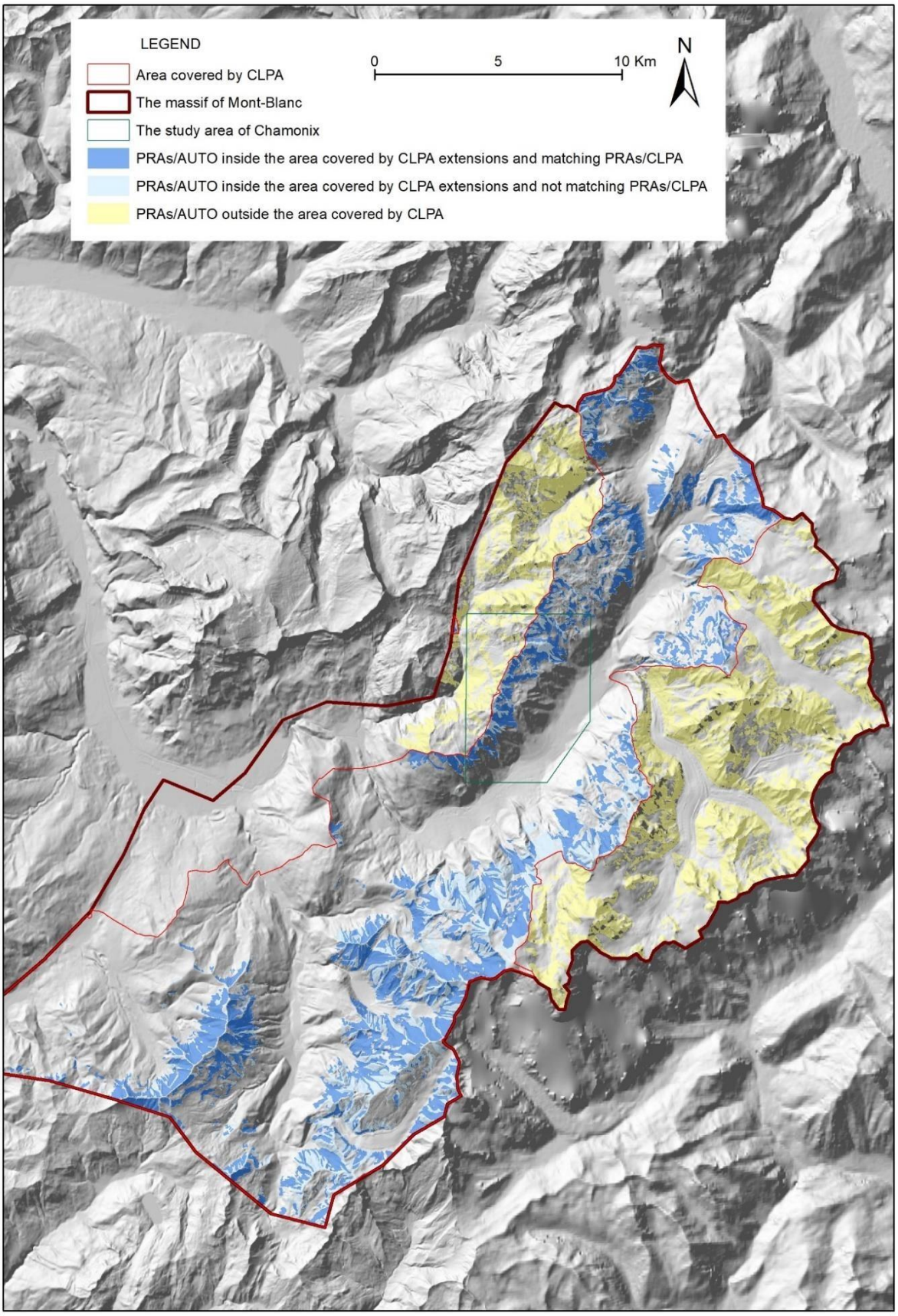

Figure 11 : Result of the proposed PRA determination method for the entire Mont Blanc massif. Digital Elevation Model ©IGN. For the PRA determination and the determination of the validation sample, all factors and the DEM resolution are set to their default values (Figure 7 and Figure 8), and forest cover data is from DB forest IGN. “CLPA extensions” refer to avalanche extents from the French avalanche cadastre.

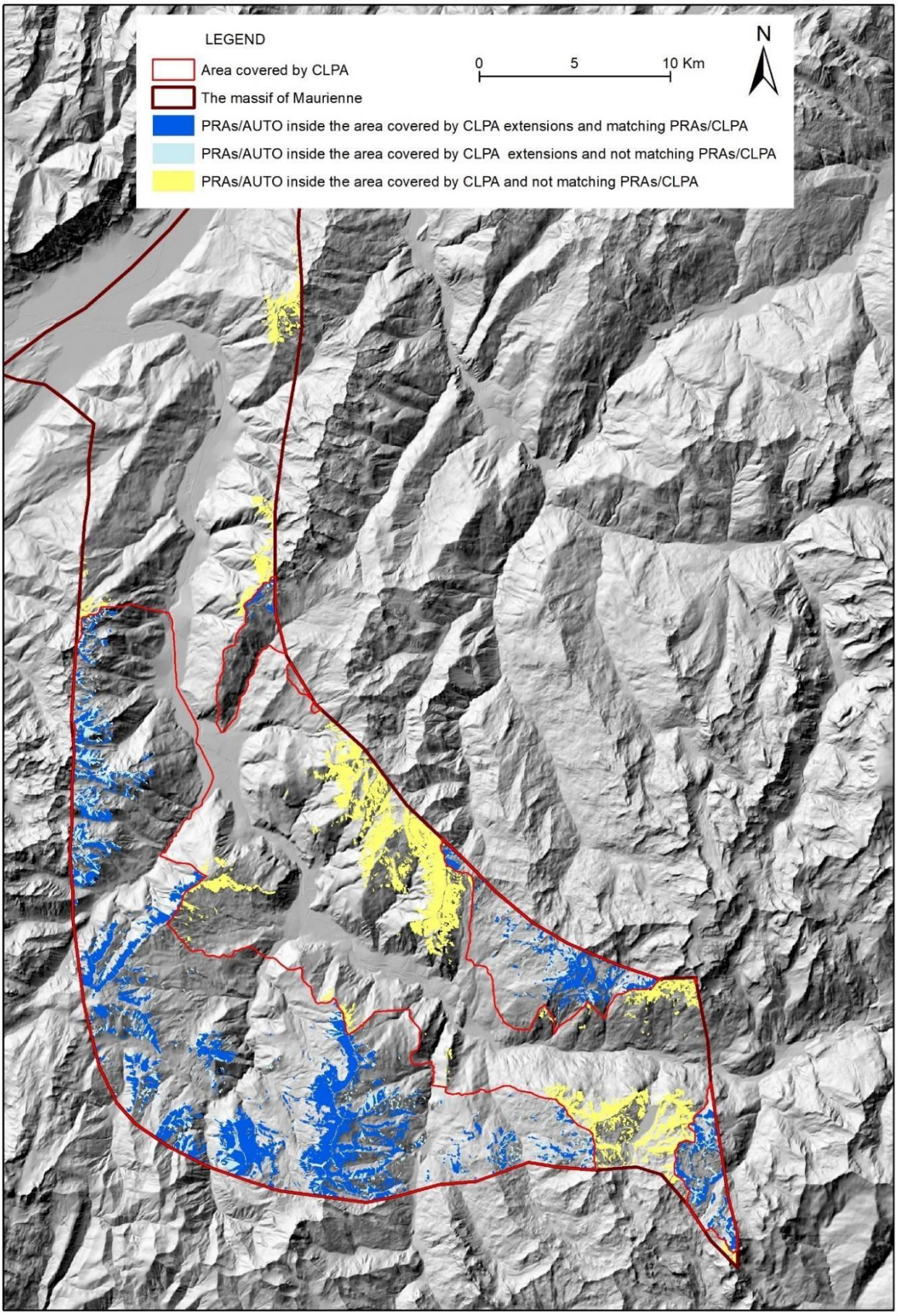

Figure 12 : Result of the proposed PRA determination method for the entire Maurienne massif. Digital Elevation Model ©IGN. For the PRA determination and the determination of the validation sample, all factors and the DEM resolution are set to their default values (Figure 7 and Figure 8), and forest cover data is from DB forest IGN. “CLPA extensions” refer to avalanche extents from the French avalanche cadastre.

Robustness of the determination method

Marginal effect of the different factors and data sets

Table 5 shows the marginal effect on detected PRA numbers and areas and true positive rates of the different factors and data sources for the Mont Blanc massif. Corresponding results for the Chartreuse and Maurienne massif are provided in Tables S1-S2 of the annexes. At this stage, the same validation sample obtained with the default setting is always considered. Main result is that, in terms of PRA numbers, the default choices lead always the best true positive rates in the three massifs. The results are almost similar for PRA areas, except that very slight increases in true positive rates are obtained for the Maurienne massif i) without the watershed delineation step (+2.4%) and ii) with forest cover extents form Corine Land Cover instead of DB forest from IGN (+0.2%). This overall result supports in a pragmatic way the usefulness of the different steps of the method, and the choices made, even if the effect of one specific filter or data set choice can be relatively minor (e.g. true positive rates are often quite similar with/without certain filters or with two competing data sources).

In more details, regarding the four different topographic filters (minimal elevation, slope range, minimal area size and maximal distance to ridge,) in all three massifs, the minimal area size has a strong impact on true positive rates, notably in terms of PRA numbers. Its influence on PRA areas is much lower, because this filter removes many small PRAs, modifying the overall PRA extent only slightly. Also, for the three massifs, the minimal elevation threshold has a limited impact, both on PRA numbers and areas, with decreases in true positive rates never exceeding 5.4%. Yet, without it, a few PRAs are detected at low elevations, notably in rather unrealistic locations (if avalanches were actually released at these locations, testimonies would definitely have been available and included in CLPAs). The two other filters have an effect which is more variable from one massif to another. The effect of the maximum distance to ridges is substantial in the Maurienne massif (with a 21.8-23.4% decrease in the true positive rate when it is not used) but moderate in the Mont Blanc massif and null in the Chartreuse massif, as in the latter massif distance to the closest ridge is usually below the default 600 threshold. Lastly, the effect of the slope range filter is particular strong on PRA numbers in Maurienne (with a 36.8% decrease in the true positive rate when it is not used), whereas it has limited effect on PRA determination in the two other massifs. The reason is probably that, in both the Mont Blanc and Chartreuse massifs, avalanche terrain is very steep, so that the filter is not very restrictive.

Comparison of the performances with/without the application of the watershed delineation algorithm shows that this step may affect the efficiency of PRA determination in a crucial way. The gain in true positive rates is very strong in the Mont Blanc massif (up to almost 76%, Table 5), more moderate in the Chartreuse massif (4.4-5.2% in numbers and areas, respectively) and contrasted in the Maurienne massif, where this step largely improves the true positive rate in PRA numbers (by 28.6%) but slightly decreases (by 2.8%) the true positive rate in PRA areas. The reason is that keeping PRAs of at least 6250m^2 (10 pixels) only removes very small areas when the watershed delineation is used that are kept when it is not. Yet, this effect is of limited impact, and more than largely compensated by the large increase in the true positive rate regarding PRA numbers / individualisation.

Finally, we compared to the default results the results obtained, i) with the two other nation-wide forest databases introduced in Sect. 2.2, or ii) without any forest cover filter. When forested areas are not removed at all, a much higher number of PRAs covering large areas is detected. This leads decreases in true positive rates exceeding 20% in the Mont Blanc and Maurienne massifs. This decrease in the true positive rate reaches 33% in numbers in the Chartreuse massif, which is logical, as it is the

massif where the forest is the most widespread among the massifs we study. This result shows the interest of the forest filter to exclude correctly many areas where avalanche release are virtually impossible. Comparing the different forest databases to each other's shows that the best true positive rates are obtained with the DB forest from IGN, but with drops in true positive rates not exceeding 20% both in numbers and areas when any of the two other candidates is used. A detailed analysis in the study area of Chamonix (Figure 9) confirms that, i) for some low elevation areas, Corine land cover and Theia both indicate dense forests that actually do not exist according to the aerial photograph, ii) forested areas provided by Theia are, at some locations, too segmented with regards to reality. These artefacts may explain the slightly better results obtained with the DB forest from IGN. Indeed, with the latter, detected PRAs in the area mostly only correspond to high elevations that are forest-free according to aerial photographs. Only one PRA remains detected at a low elevation near the tower of a chairlift. This corresponds to an area where a large hiking trail eroded by walkers prevents the forest development, making an avalanche release actually possible, as slope is favorable.

			With default values	Without minimal elevation filter	Without slope filter	Without distance to ridge filter	Without minimal area filter	Without watershed delineation	Without forest filter	With Corine Land Cover forest	With Theia forest
Validation sample	Total area of PRAs within CLPA (validation sample) [km^2]		58.3	58.3	58.3	58.3	58.3	58.3	58.3	58.3	58.3
	Total number of PRAs within CLPA extents (validation sample)		1522	1522	1522	1522	1522	1522	1522	1522	1522
Detected PRAs	Total area of detected PRAs [km^2]		90.8	98.1	97.9	102.3	102.8	96.6	135.1	109.0	104.1
	Difference in area with regards to default values [km^2]		/	7.33	7.15	11.55	11.98	5.80	44.31	18.21	13.34
	Difference in area with regards to default values (%)		/	8.1%	7.9%	12.7%	13.2%	6.4%	48.8%	20.1%	14.7%
	Total number of detected PRAs		2003	2085	2074	2173	4315	262	2803	2170	2218
	Difference in numbers with regards to default values		/	82	71	170	2312	-1741	800	167	215
	Difference in numbers with regards to default values (%)		/	4.1%	3.5%	8.5%	115.4%	-86.9%	39.9%	8.3%	10.7%
	Total area of detected PRAs within CLPA extents [km^2]		84.9	86.6	86.6	89.3	87.1	17.2	102.3	93.1	89.8
	Total number of detected PRAs within CLPA extents		1601	1622	1623	1626	2061	111	1597	1528	1607
Evaluation	True positive rate (recall), Eq. 3	In numbers (%)	80	77.8	78.2	74.8	47.8	42.2	57	66.6	71.8
		In areas (%)	93.6	88.2	88.4	87.2	84.8	17.8	75.8	83.8	86
	Difference in recall with regards to default values	In numbers (%)	/	-2.2	-1.8	-5.2	-32.2	-37.8	-23	-13.4	-8.2
		In areas (%)	/	-5.4	-5.2	-6.4	-8.8	-75.8	-17.8	-9.8	-7.6

Table 5 : Marginal effect on true positive rates of the different factors and data sources, Mont Blanc Massif. Total area of detected PRAs and total number of detected PRAs are those of the part of the massif covered by CLPA (Table 1). For the PRA determination, in each column, only the considered factor is removed/varies according to the column label. All other factors and the DEM resolution are set to their default values (Figure 7). For the determination of the validation sample, all factors and DEM resolution are set to their default values (Figure 8), and forest cover data is from DB forest IGN.

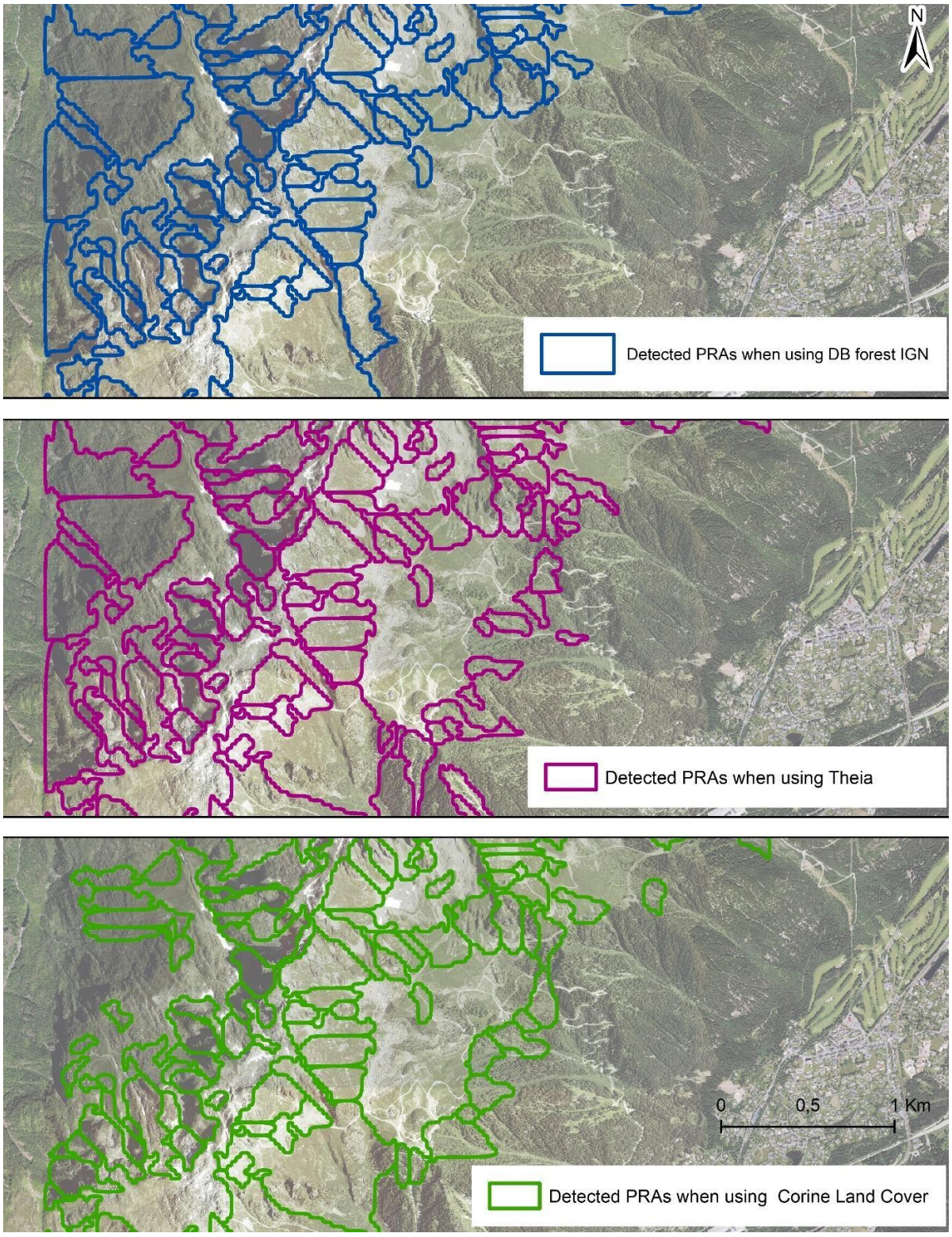

Figure 13 : Effect of forest data source on detected PRAs, study area of Chamonix. For the PRA determination, forest data source varies, and all other factors and the DEM resolution are set to their default values (Figure 7). Aerial photograph ©IGN 2015. For the determination of the validation sample, all factors and DEM resolution are set to their default values (Figure 8), and forest cover data is from DB forest IGN.

In-depth parametric study of the influence of the different topographic filters

We additionally conducted a more systematic search, varying the different topographic filters in the PRA determination over a range of values plausible according to the literature and local peculiarities of the French Alps (elevation range and corresponding snow cover characteristics), again keeping always the same validation sample. Results at the scale of the Mont Blanc massif show that, overall, true positive rates decrease with distance to the default values (Table 6). True positive rates seem nevertheless rather stable over considered ranges of parameters/thresholds, with slope range being the most influential parameter over the tested range (up to a 18% decrease in the true positive rate for numbers).

Regarding differences in the detected PRA numbers and areas, they can be larger, especially with slope range for PRA areas, and with slope range and minimal area size for PRA numbers. For instance, slope ranges more restrictive than our default choice lead to decreases in detected PRAs up to 43% in areas and up to ~25% in numbers for the Mont Blanc Massif. By contrast, the minimal area size strongly affects PRA numbers, but PRA areas much less, because increasing the minimal area size gradually discards the small PRAs below the considered threshold (Table 6). Detailed analyses of specific areas such as the Chartreuse / Dent de Crolles area confirm that a too large minimal area size (Figure 10), a too high minimal elevation (Figure S4 of the annexes) or a too restricted slope range (Figure S5 of the annexes) misses release areas that an expert analysis would definitely consider as suitable locations for avalanche releases. This is the case, e.g., of the “small” PRAs detected in Figure 14 a with the default minimal area size, but missed in Figure 14c with a two times larger minimal area size.

		With default values	Minimal area (m^2)			Minimal elevation (m)			Slope range (°)				Maximal distance to ridge (m)			
			3125	9375	12500	1200	1600	1800	[26-60]	[30-60]	[32-60]	[34-60]	400	500	700	800
Total area of detected PRAs [km^2]		90.8	93.8	88.2	85.2	90.7	88.9	88.7	90.8	64.5	58.9	51.8	81.0	88.5	94.3	95.0
Difference in area with regards to default values [km^2]		/	3.0	-2.6	-5.6	-0.1	-1.9	-2.1	0.0	-26.3	-31.9	-39.0	-9.8	-2.3	3.5	4.2
Difference in area with regards to default values (%)		/	3.3%	-2.8%	-6.2%	-0.1%	-2.1%	-2.4%	0.0%	-28.9%	-35.1%	-43.0%	-10.8%	-2.6%	3.9%	4.6%
Total number of detected PRAs		2003	2632	1654	1369	2000	1979	1941	2002	1598	1582	1505	1877	2008	2088	2104
Difference in numbers with regards to default values		/	629	-349	-634	-3	-24	-62	-1	-405	-421	-498	-126	5	85	101
Difference in numbers with regards to default values (%)		/	31.4 %	-17.4%	-31.7%	-0.1%	-1.2%	-3.1%	0.0%	-20.2%	-21.0%	-24.9%	-6.3%	0.2%	4.2%	5.0%
Total area of detected PRAs within CLPA extents [km2]		84.9	85.7	83.3	81.2	84.7	83.1	76.6	84.8	61.9	56.3	49.6	75.3	82.3	87.5	87.5
Total number of detected PRAs within CLPA extents		1601	1768	1391	1201	1590	1589	1520	1597	1409	1406	1349	1468	1576	1622	1621
True positive rate (recall), Eq. 3	In numbers (%)	80	67.1	79.8	78.5	79.2	78.5	68.8	79.7	73.8	68.4	61.9	70.5	76.2	67.2	76.9
	In areas (%)	93.6	91.4	93.6	93.4	93.3	93.0	82.6	93.3	92.0	89.5	85.1	90.0	92.3	85.2	92.1
Difference in recall with regards to default values	In numbers (%)	/	-12.9	-0.2	-1.5	-0.8	-1.5	-11.2	-0.3	-6.2	-11.6	-18.1	-9.5	-3.8	-12.8	-3.1
	In areas (%)	/	-2.2	0.0	-0.2	-0.3	-0.6	-11.0	-0.3	-1.6	-4.1	-8.5	-3.6	-1.3	-8.4	-1.5

Table 6 : Parametric study: effect of minimal area size, minimal elevation, slope range and maximal distance to ridge on PRA determination, Mont Blanc Massif. Total area of detected PRAs and total number of detected PRAs are those of the part of the massif covered by CLPA (Table 1). For the PRA determination, in each column, only the considered factor varies. All other factors and the DEM resolution are set to their default values (Figure 7), and forest cover data is from DB forest IGN. For the determination of the validation sample, all factors and DEM resolution are set to their default values (Figure 8), and forest cover data is from DB forest IGN.

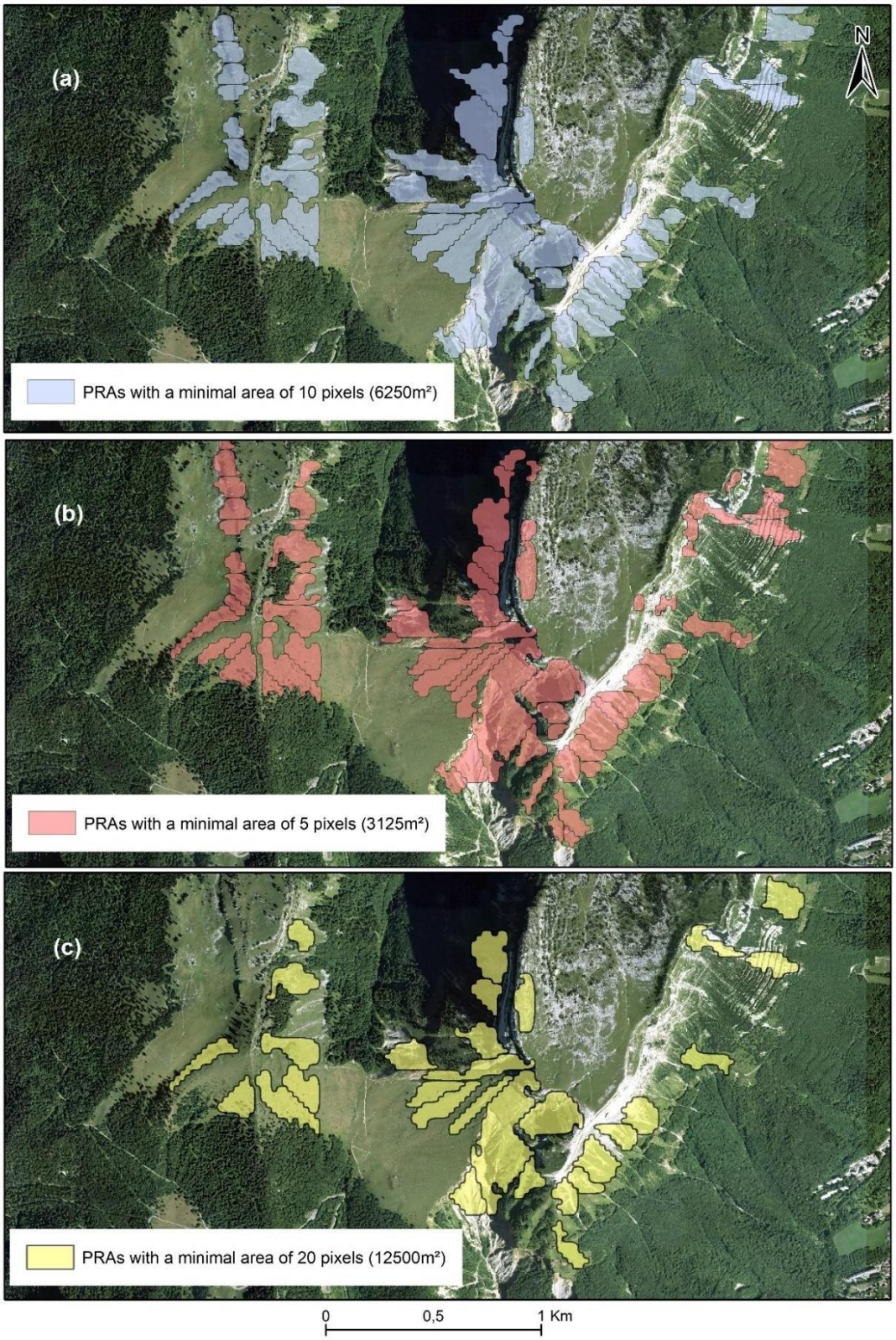

Figure 14 : Effect on PRA determination of the minimal area size, Chartreuse/Dent de Crolles study area: a) with a 6250 m^2 minimal area size, b) with a 3125 m^2 minimal area size, c) with a 12500 m^2 minimal area size. For the PRA determination, minimal area size varies, all other factors and the DEM resolution are set to their default values (Figure 7) and forest cover data is from DB forest IGN. Aerial photograph ©IGN 2012. For the determination of the validation sample, all factors and the DEM resolution are set to their default values (Figure 8) and forest cover data is from DB forest IGN.

Impact of DEM resolution

The robustness of our results to the DEM resolution was studied over the Mont Blanc massif (Table 7). With finer resolution DEMs, the number of detected PRAs significantly increases (by up to 56.3%), but the overall PRA area decreases (by ~21%). This is attributable to the fact that, with finer resolution DEMs, sharper PRA boundaries arguably more consistent with terrain characterises are evidenced (Figure 15 and Figure 16). Yet, surprisingly enough, performing the PRA determination with finer resolution DEMs does not improve true positive rates when the default validation sample is considered (i.e. the one determined using Figure 8 's scheme with the 25 resolution DEM), leading small 3-6% decreases for PRA numbers and areas. This holds true even if the finer resolution DEM is used also for the determination of the validation sample from CLPA avalanche extents (Table 7).

			DEM resolution 25 m / default values	DEM Resolution 10 m	Resolution 10m, adjusted validation sample	DEM Resolution 5m	Resolution 5m, adjusted validation sample
Validation sample	Total area of PRAs within CLPA (validation sample) [km^2]		58.3	58.3	53.5	58.3	45.9
	Difference in area in validation sample with regards to default values [km2]		/	/	-4.8	/	-12.4
	Difference in area in validation sample with regards to default values (%)		/	/	-8.3%	/	-21.2%
	Total number of PRAs within CLPA extents (validation sample)		1522	1522	2061	1522	2181
	Difference in numbers in validation sample with regards to default values		/	/	539	/	659
	Difference in numbers in validation sample with regards to default values (%)		/	/	35.4%	/	43.3%
Detected PRAs	Total area of detected PRAs [km^2]		90.8	84	88.9	71.8	71.7
	Difference in area with regards to default values [km^2]		/	-6.8	-1.9	-19.0	-19.1
	Difference in area with regards to default values (%)		/	-7.5%	-2%	-20.9%	-21%
	Total Number of detected PRAs		2003	2989	3081	3131	3130
	Difference in numbers with regards to default values		/	986	1078	1128	1127
	Difference in numbers with regards to default values (%)		/	49.2%	53.8%	56.3%	56.3%
Evaluation	Total area of detected PRAs within CLPA extents [km^2]		84.9	76.8	76.6	66.8	64.1
	Total number of detected PRAs within CLPA extents		1601	2420	2339	2694	2457
	True positive rate (recall), Eq. 3	In numbers (%)	80	75.8	76	74	78.6
		In areas (%)	93.6	90.2	86.2	89.8	89.4
	Difference in recall with regards to default values	In numbers (%)	/	-4.2	-4	-6	-1.4
		In areas (%)	/	-3.4	-7.4	-3.8	-4.2

Table 7: Effect of DEM resolution on PRA determination, Mont Blanc Massif. With both the 10 and 5m resolution DEMs, two cases are considered: either the default validation sample determined with the 25m resolution DEM is kept, or a new validation sample is determined following Figure 8. For both the PRAS determination and determination of the validation sample, all other factors are set to their default values (Figure 7 and Figure 8) and forest cover data is from DB forest IGN.

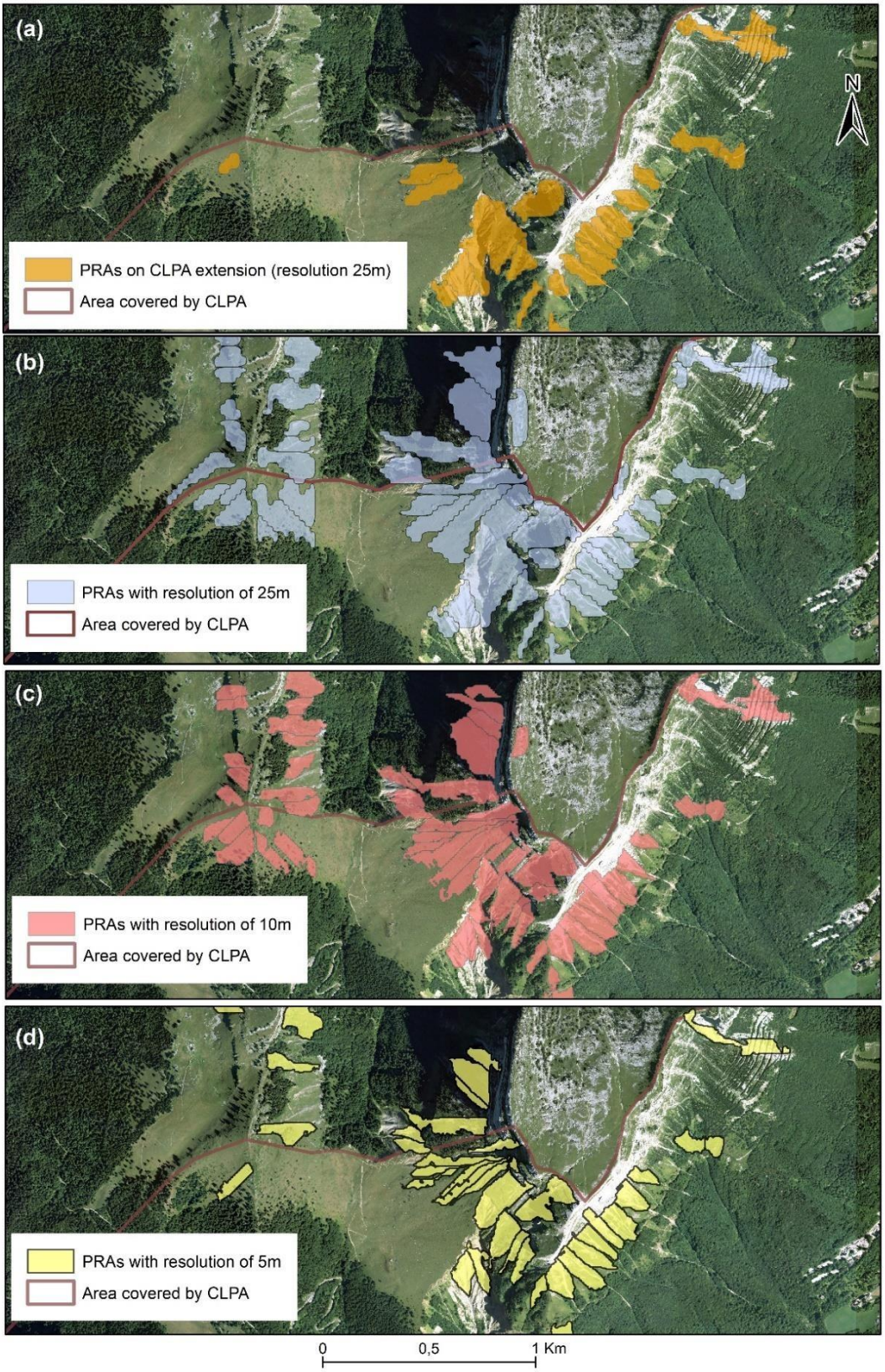

Figure 15 : Effect of DEM resolution on PRA determination, Chartreuse/Dent de Crolles study area. Aerial photograph ©IGN 2012. a) For the determination of the validation sample, all factors and the DEM resolution are set to their default values (Figure 8) and forest cover data is from DB forest IGN; the absence of CLPA in the upper left corner is clearly visible. b-d) For the PRA determination, DEM resolution varies, other factors are set to their default values (Figure 7) and forest cover data is from DB forest IGN. In a), CLPA extensions" refer to avalanche extents from the French avalanche cadastre.

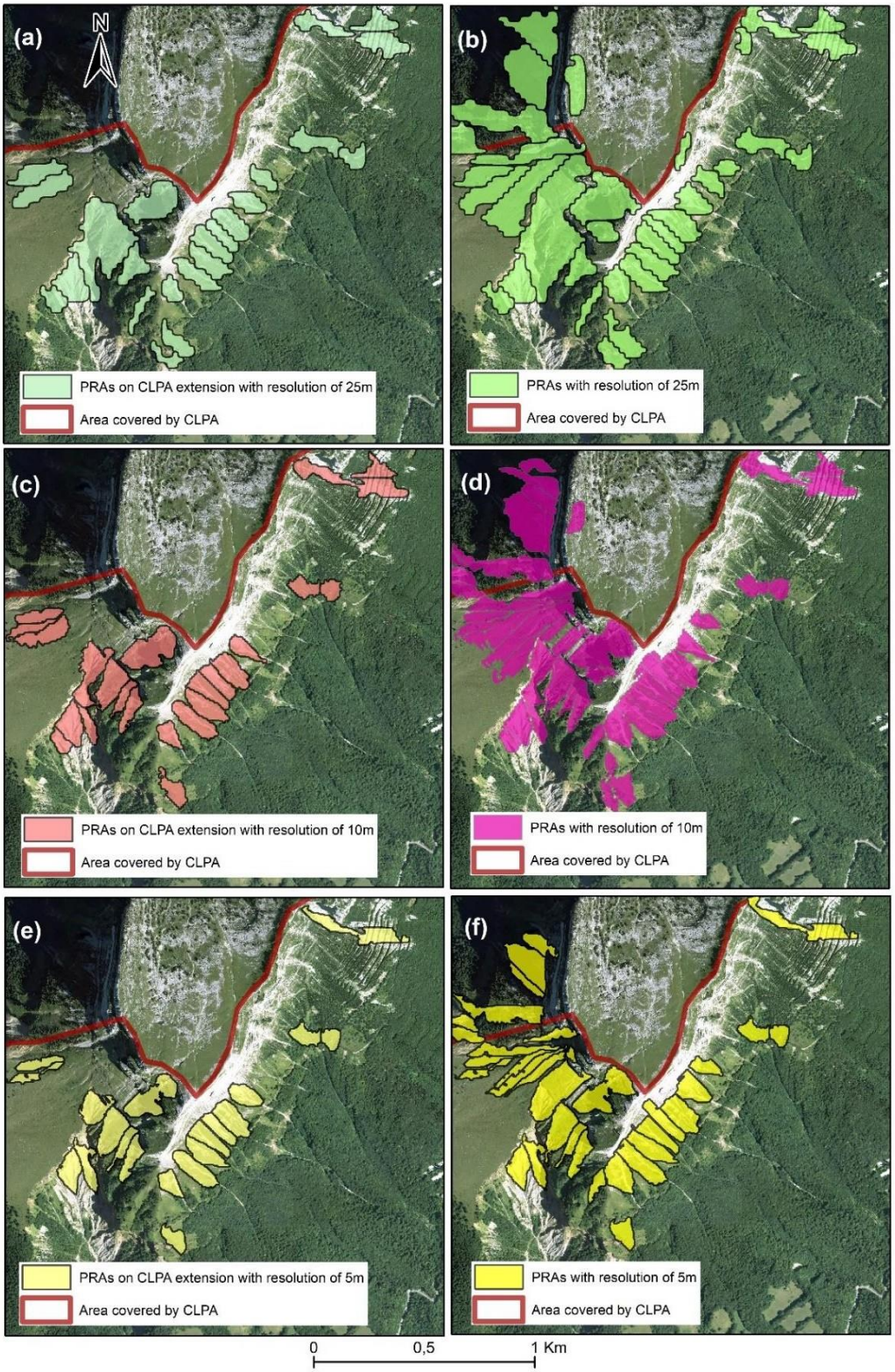

Figure 16 : Combined effect of DEM resolution on the selection of the validation sample (left) and PRA determination (right), Chartreuse/Dent de Crolles study area. For the PRA determination and the determination of the validation sample, DEM resolution varies, all other factors are set to their default values (Figure 7 and Figure 8), and forest cover data is from DB forest IGN. Aerial photograph ©IGN 2012. Left, the absence of CLPA in the upper left corner is clearly visible, and CLPA extensions" refer to avalanche extents from the French avalanche cadastre.

5 Discussion

Main outcomes of the work

This study proposes a procedure for the automated determination of PRAs without any consideration of release frequency and applies it to three entire massifs of the French Alps, Chartreuse, Maurienne, and Mont-Blanc, demonstrating its applicability to large areas (Table 1). The approach classically uses topographical filters as follows: a minimal elevation of 1400 m, slopes between 28° and 60°, a distance to the closest ridge limited to 600 m, and a minimal area of 6250m^2 for the resulting PRAs. It also excludes forested areas, and uses a watershed delineation algorithm, which provides spatial entities comparable to individual avalanche paths. Retained DEM resolution is 25m and forest cover data is the one of DB forest from IGN.

Massif-scale true positive rates obtained ranged between 80-87% in PRA numbers, and between 92.4% and 94% in PRA areas (Table 4). Also the parametric study highlighted a rather high robustness of these scores to many choices, e.g. moderate decreases in true positive rates when the best values were replaced by other realistic values. As the chosen three massifs rather well represent the diversity of altitudinal and lithological contexts of the French Alps, these results suggest that the developed method could be systematically used for the entire French Alps, a large territory where no automated PRA determination has been systematically implemented so far. This will allow in the future the determination of PRAs within the 23 massifs even in areas which are still not covered by CLPA. Yet, we want to remember that we evaluated “true positives” only. Also we acknowledge that our evaluation approach, and notably the definition of the validation sample, favours the comparison with our detected PRAs (Sect. 5.3). As a consequence, our evaluation scores should not be directly compared with scores obtains with other approaches on other data sets, but only taken as an indication that our approach performs rather well in the French context, which was further confirmed by visual inspections in small areas.

Selected factors and data sets and comparison to existing methods

Default settings of the developed PRA determination method were determined/confirmed on the basis of an evaluation approach (see below), and a large parametric study (Table 5-7and Tables S1-S2 of the annexes). Note that what we did is neither an extensive grid search testing all possible combinations, which would have been extremely numerically consuming over entire massifs, nor a proper sensitivity analysis in the strict sense of the term, which would have required more sophisticated techniques introduced in the snow avalanche field only recently, and so far not for PRA determination (e.g. Heredia et al., RESS 2021; 2022). Yet, a large effort was conducted over large fractions of entire massifs, combining different complementary analyses: removing each filter one by one, replacing one data source by another, etc. Besides, raw massif-scale evaluation scores were supplemented by detailed visual investigations in smaller study areas (Figure 13 to Figure 16) and Figures S4-S5 of the annexes). Obtained results allowed quantifying the robustness of the PRA determination method and, to a certain extent, identify optimal choices (or, at least, sets of suitable values / data), based on changes in evaluation scores with competing solutions. Most of our choices are largely in accordance with those of several past studies (e.g., Maggioni et al, 2002), except the retained resolution of the DEM that we found less important to reach high efficiency in PRA determination than in other studies (Bühler et al., 2013).

In details, a minimal elevation of 1400 m for snow avalanche release seems appropriate in the French Alps considering the limited amounts of snow precipitation expected in current and future conditions

below this elevation. Yet, this threshold is dependent to the local climate and should be adapted for other regions. Our other choices regarding slope and distance to ridge are i) largely in accordance with the state of the art (Maggioni and Gruber, 2003; Bühler et al., 2013), and ii) compatible with broader knowledge regarding snow avalanche formation (Schweizer et al., 2004). Regarding the DEM, a 25 m resolution appeared as a good compromise between high efficiency in the determination and the computational burden, even if, arguably, it leads less realistic PRA boundaries than finer DEM resolutions.

Even if its effect was found to vary from one massif to another, our watershed delineation step, in essence rather similar to the OBIA approach of Bühler et al. (2018), was found to greatly improve true positive rates, especially in terms of PRAs numbers. As PRA determination is mostly oriented towards avalanche simulations to evaluate hazard and risk downslope, this gain is crucial, and much more important that the slight loss in true positive rates in PRA area obtained for one of the three studied massifs. Indeed, the segmentation avoids unrealistically wide PRAs that correspond to different avalanche paths/events, which may allow performing simulations corresponding to realistic individual avalanche events.

Our parametric study showed higher true positive rates both in numbers and areas when forested terrain was excluded than when this filter was not considered. As forest cover is known to be effective to prevent avalanche release, this result is logical. We tested the three main forest data sources available at the scale of the entire French Alps. None of them is perfect, and information that is more accurate may be available in other areas/countries. However, visual analyses in different areas showed that at least the DB forest we retained is acceptable (Figure 6). In addition, the systematic analysis performed over the three entire considered massifs showed that it leads the highest true positive rates both in numbers and areas with regard to the other available forest data sources. We yet acknowledge than even better forest data could lead to results that are even more reliable. Also, a less stringent PRA / No PRA rule as function of forest presence/absence (e.g. a higher release susceptibility with decreasing forest density) would be an interesting option for further developments.

Finally, even if we are able to compare the steps and choices involved in our approach with those involved in other PRA determination methods existing in the literature, we did not a direct comparison to existing algorithms. For this we would need i) to run all existing algorithms which for now are not available to the community as open access codes, and ii) to test them on different datasets with different characteristics (resolution, climatic and topographic context, etc.). i) is because the description provided in the scientific literature is not always sufficient to recode the algorithms, and, even when it is, following published guidelines/equations does not guarantee that what has been done can be reproduced exactly, due to, e.g., differences introduced by different numerical implementation schemes. ii) is because different algorithms may perform better in different contexts, so that, possibly, there is no universal “best algorithm” for PRA determination.

Evaluation of detected PRAs based on the CLPA / avalanche cadastres

In order to evaluate the proposed method, we compared detected PRAs to the CLPA after isolating individual release areas within CLPA extents. However, evaluating a PRA determination method and even determining a suitable validation sample is by essence difficult, which contributes to explain why i) such validation data sets are rare and generally small, and ii) even proper evaluation exercises are seldom in the literature (e.g., Bühler et al., 2018). What follows discusses the pro’s and con’s of the approach we chose and provides insights from the work done that may help designing more efficient evaluation techniques for PRA determination methods.

Despite drawbacks inherent to any avalanche cadastre (uncertainty regarding some extents, or even missing avalanche extents), the CLPA is a remarkable source of information regarding past avalanches (Bourova et al., 2016) due to its old history, its rigorous protocol and because it includes various complementary sources of information (testimonies, landscape footprints, etc.). In addition, its principle makes it suitable to evaluate a method that aims at automatically identify the maximal avalanche prone terrain. Notably, as CLPA extents are concatenations of all observed avalanche extents on a given avalanche path, CLPA is more likely to provide an accurate estimate of the entire "ground truth" than any observation of single avalanche events. Yet, identifying a validation sample for a PRA determination method from CLPA extents is not that easy. First, within a given massif, some areas are covered by CLPA and some of them are not (Table 1, Figure 15 and Figure 16), and the fraction of the territory covered by CLPA varies from one massif to another. As a consequence, evaluation scores can be computed only over areas which are covered by CLPA, namely much larger areas in Mont Blanc and Maurienne Massifs than in the Chartreuse massif (Table 1). Second, in areas covered by CLPA, it is known that CLPA is very complete and precise on lower slopes and in forested terrain and more likely to i) miss avalanche prone terrain (and release areas) and ii) map boundary of avalanche extents less precisely far from inhabitants and forests, notably in high elevation areas. In such latter cases, "false positives" in our evaluation scheme may be true PRAs that are simply missing in the CLPA. This may explain, e.g., why true positive rates slightly higher in numbers where obtained in Chartreuse than in the two other studied massifs (Table 4). Lastly, CLPA does not distinguish release areas from flow paths and runout zones, which implies that a pre-processing is required to isolate individual release areas within CLPA extents that can be compared with our detected PRAs. To this aim, we used the same filters than for the PRA determination. This makes that the identified PRAs and our validation data are no longer independent.

The way we define our validation sample may therefore be criticized. However, obtaining a fully independent exhaustive sample of "ground truth" PRA may simply be impossible. A first reason is that even "live", what can be observed is the full extent of an avalanche, and separating its release area from the flow path may be very difficult, so that the delimitation of any release area may always involve some uncertainty. Second, assuming that one is able to precisely map a release area, there is little chance that it corresponds to the entire PRA for the considered path. Third, even in the best avalanche cadastre, some avalanche extents corresponding to the rarest events that can be released under very specific conditions only may be missing. As a consequence:

even with the best validation sample at hand, one will never be sure that i) all potential PRAs have been identified, ii) the maximal potential extent that can be released under the most extreme conditions has been identified for all paths. This is why only "true positives" PRAs can be trustfully validated, as it is never sure that a complete PRA or a part of a PRA automatically identified but not present in the validation sample is not simply erroneously missing in the validation sample;

the definition of any PRA validation sample will always involve some partially subjective decisions. Our choice was to use filters explicitly in a transparent manner. This has the drawback of allowing the evaluation of true positives only. We already argued that i) focusing on true positives in PRA evaluation is sensible, ii) the raw values of our scores should be considered with care. However, it should be noted additionally that, even if focusing the PRA search and evaluation on terrain which is presumably favourable to avalanches may indeed favour high scores (and notably increase the number of false positives), it is an interesting option to maximise the efficiency of the determination. It is indeed now a rather standard approach in machine learning (e.g., Giffard Roisin et al., 2020) that is increasingly used in susceptibility mapping approaches outside the snow avalanche field in order to focus the determination on most suitable areas and thus increase the determination power.

Finally, confusion matrices and performance criteria were seldom used so far to evaluate PRA determination methods (to our knowledge, only in Bühler et al, 2018), and with one single metric, which may not be enough to fully judge the efficiency of a PRA determination method, as, e.g. the right number of PRAs can be identified but with wrong extents, and vice-versa. As a first step towards improved evaluation schemes for PRA determination methods, we proposed to evaluate efficiency with true positive rates (recall) computed both for PRA numbers and areas, which may cover the two most critical dimensions of the problem. Yet, in the future, additional metrics should probably be considered, notably metrics that combine both information (e.g., with "success" for different thresholds defined as minimal matching areas), and/or metrics related to various characteristics of the detected PRAs (shape, elevation, etc.). This may help assessing even more precisely the strengths and weaknesses of our (or another) PRA determination method. In addition, we performed the evaluation of our determination method over unusually large areas covering significant proportions of three entire massifs with diverse characteristics. A similar approach could be further used for comparing several PRA determination methods (Sect. 6) and/or in other mountain environments with validation data having strengths and weaknesses different from those of the CLPA. This would help understanding to which extent the high scores we obtain i) are strongly influenced by our evaluation framework, ii) can be reproduced in other contexts, iii) how the most critical parameter need to be changed to fit various conditions (e.g. lower minimal elevation in colder climate).

6 Conclusion and outlooks

To map and mitigate avalanche risk at large scales, the automated determination of PRAs is a powerful solution, notably to provide inputs for avalanche simulation softwares (e.g., Gruber and Bartelt, 2007). In this study, a PRA determination method adapted to the characteristics of the French Alps was developed and tuned on the basis of the CLPA, a valuable large-scale data source regarding past avalanches. In addition to the potential benefit for better understanding and assessing avalanche hazard in the French Alps and in mountain environments with similar characteristics (see below), outcomes of the work include i) the determination of individual PRAs using a watershed delineation algorithm, ii) an approach to define a validation sample from a cadaster of avalanche extents, iii) an evaluation procedure based on two metrics, PRA numbers and area, and iv) a better definition of evaluation scores that should be interpreted in the context of PRA identification. These methodological developments should help progressing towards more efficient approaches for PRA determination and evaluation.

Future works may expand the effort to the 23 massifs of the French Alps and provide a statistical assessment of the detected PRAs. The latter could also be, combined with available extreme snowfall/snow depth estimates (Gaume et al., 2013; Le Roux et al., 2021), for a large-scale mapping of avalanche hazard and risk in the French Alps using simulation tools, as already done in other countries (e.g. Bühler et al., 2018; 2022). To this aim, the most direct use of our PRAs would be to consider all of them and, for each of them, their entire area, as well as "maximal" snow depths and "minimal" friction parameters for avalanche simulation. This may lead to the delineation of the entire avalanche prone terrain. To go further and evaluate hazard and risk levels downslope, additional assumptions/choices would be required regarding the magnitude and frequency of potentially triggered avalanches. This may include several scenarios and/or the entire probability distribution for i) the frequency of trigger in each PRA, ii) the fraction of each PRA which is released, iii) the snow depth, iv) friction parameters, etc. Ultimately, results could be compared to existing hazard assessment based on interpolation of existing avalanche runout data (Lavigne et al., 2015).

A second potential outlook would be to apply the method as it is in other close territories such as the Pyrenees (Oller et al., 2021) or the Vosges Mountains (Giacona et al., 2017). Yet, this would imply further tuning of some parameters of the method such as minimal elevation and distance to ridge, to adapt these to local peculiarities. More ambitious outlooks relate to improvements of the PRA determination method: i) make it dynamic to assess PRAs conditional to snow and weather conditions (e.g., Chueca Cía et al., 2014), ii) switch from deterministic to probabilistic determination rules (e.g., Kumar et al., 2019) to, e.g., include in it the uncertainty about the best parameter values to be used, and/or iii) use CLPA extents not only as an evaluation support but as a training sample. Finally, a comparison of PRA determination methods would certainly be beneficial for the community and should be envisioned in the future. To this aim, we hope that our data, now freely available (Data availability Sect.), will foster further benchmarks between already existing or new PRA determination algorithms in order to draw firmer conclusions regarding the respective efficiency of the different proposals in different contexts.

Chapitre 3 : Zones de départ potentielles d'avalanche dans les Alpes françaises : caractéristiques statistiques actuelles et évolution sur un siècle et demi avec les changements d'occupation du sol.

This content of this thesis chapter will be submitted as a research article to Cold Regions Science and Technology soon.

Abstract

Potential release areas (PRAs) of snow avalanches, obtained from the analysis of terrain characteristics, provide valuable information for avalanche risk assessment. Some studies have described the statistical characteristics of these PRAs and/or of entire avalanche paths, but, so far, for small areas / sample sizes, and under current conditions only. In this article, we propose a study of the statistical characteristics of PRAs i) over the whole French Alps and their 23 massifs under current conditions, and ii) in two smaller study areas (the Guil valley in the Queyras massif, and three municipalities in the Haute-Maurienne massif) as a function of the evolution of forest cover over almost a one and a half century.

The PRAs are obtained using a method developed specifically for the French Alps. Accuracy scores obtained by comparison to the CLPA taken as ground truth were shown to vary with massifs characteristics, but are shown to be high enough in all massifs for the approach to be used to better understand the properties of avalanche terrain. We detected a total of 101,802 PRAs with a total area of 3799.2 km^2, which represents 17.8% of the entire French Alps. We also propose a clustering of the 23 massifs in three spatially coherent groups according to the similarities of the topographic characteristics of their PRAs. Eventually we show that in the Guil valley and for the three municipalities in the Haute-Maurienne massif, due to the reduction in pastoralism and changes in agricultural practices which favored the colonization of PRAs by trees and shrubs, the number and total area of PRAs, significantly decreased.

1 Introduction

Avalanches can lead to casualties and important material damages. Therefore, avalanche risk assessment and mitigation remains an important issue in mountainous areas. In these, information on avalanche release areas is often scarce, the territory being vast and sometimes difficult to access. While observations of past avalanches provide data on the size and types of avalanches that may occur in the future, this source of information is generally not exhaustive in time or in space, with notably large areas that remain almost undocumented. In order to reduce the risk due to avalanches at large scale, even in areas where there is little or no historical documentation, the automatic determination of Potential Release Areas (PRAs) is an interesting option. PRAs data provides essential information for avalanche risk assessment. For example, PRAs can provide estimates of potential fracture depths and avalanche volumes (Maggioni and coll., 2002), which could be used in a decision-making framework. PRAs can also be exploited to identify deforested or avalanche-eroded areas that need to be reforested, in combination with an avalanche simulation software (Fischer and al. 2015). Among the existing PRA detection methods, the one proposed by Duvillier and al. (2023) allows the detection of

PRAs over the entire French Alps by applying the following filters: a minimum elevation of 1400 m, slope between 28° and 60°, absence of forest and a minimum distance to the closest ridge of 600 m. In order to individualize the PRAs, a watershed delineation algorithm is applied to the resulting areas. Only PRAs with a minimum area of 10 pixels (6250 m^2) are retained.

The study of the statistical characteristics of the PRAs can provide a better understanding of the location of the PRAs according to topographic parameters, and of parameters that determine their location and size. However, to date, only two statistical studies have focused on this type of description (Gleason, 1996; Vontobel and al., 2013). The first study was carried out in 1996, in Montana, more precisely at Mount Lone. This study deals with natural and artificial avalanche triggers, which are distinct from each other because of the potentially specific conditions of each type of trigger. The parameters used to obtain PRA for natural avalanches are slope, elevation, exposure, surface roughness, exposure to prevailing winds, and geometry of the avalanche starting zone. Concerning PRAs for artificial avalanches, the parameters were slightly different: slope, elevation, number of explosions needed to trigger the avalanche, exposure to the prevailing wind, shape of the starting zones (depth/width), and width and depth of the starting zones in the transverse direction. Similarly, Vontobel and al. (2013) study the characteristics of artificial starting zones triggered by skiers in Switzerland. In this study, 142 PRAs were mapped, and their geomorphological characteristics (slope, exposure, ridges, roughness and curvature profile) were extracted from a Digital Elevation Model (DEM).

In addition, the statistical study of the characteristics of avalanche paths and especially of their starting zones allows a better understanding of avalanche activity. Such studies are much more numerous and were conducted for a variety of purposes: mapping of maximum possible extensions, relationships between avalanche characteristics and triggering conditions, etc. The first study of this type was probably conducted in 1976 in San Juan County, Colorado (Armstrong, 1976). The parameters studied in the avalanche paths were air temperature, snow accumulation, wind speed and direction, snow packing rate, precipitation rate and amount, and total radiation on the snow surface. This study provided the characteristics of the avalanches to be expected, the causes of avalanche triggering, and some hints for avalanche forecasting (Armstrong, 1976).

For a different purpose, as early as in 1980, topographic parameters were used to calculate the flow distance of avalanches (Lied and Bakkehoi, 1980). To this aim, 423 avalanche paths were selected on the basis of the inhabitants' knowledge of their maximum extent and the accessibility of the deposits on the ground. In 1990, in addition to the topographical parameters used to characterize avalanche paths, the lithology and geological structure were added with the same objective (Butler and Walsh, 1990) for a study area located in Eastern Glacier National Park in Montana. Since 1987, avalanches in this study area have been recorded and mapped and morphometric data were collected in each avalanche path. Finally, Kern and al. (2020) study the volumes of avalanche deposits between 1903 and 2017 in Bessans (Haute-Maurienne massif), and analyze the influence of the morphological characteristics of corridors on these deposits between 2003 and 2017. In this study, the avalanche paths are derived from three data sources: the Carte de Localisation des Phénomènes d'Avalanches (CLPA), the Observation Permanente des Avalanches (OPA), the Enquête Permanente sur les Avalanches (EPA), and the database of the “Restauration des Terrains en Montagne” (RTM) from the “Office National des Forêts” (ONF).

From a different perspective, over the last decades / centuries, changes in mountain societies linked to the development of winter sports, and the modification of agricultural practices which allowed the growth of forests and the reforestation of avalanche paths had strong consequences on avalanche activity (Zgheib and al., 2020; Mainieri and al., 2020). It is, therefore, necessary to take into account the evolution of the forest cover, in the study of the characteristics of the PRAs, at different dates, to see the effect of forest cover changes on avalanche activity.

Hence, among all existing statistical studies on topographical characteristics of snow avalanche terrain, only two of them specifically concern the analysis of PRAs according to topographical parameters (Gleason, 1996 ; Vontobel and al., 2013). In addition, they concern small areas / sample sizes, and were conducted under "current conditions" only. To date, there is no large-scale study of the characteristics of PRAs, describing their evolution over time. To fill these gaps, this article proposes a statistical exploitation of the PRAs obtained at the scale of the French Alps using the method proposed in Duvillier et al. (2023), in order to provide a comprehensive description of the PRAs in the French Alps, and, for specific areas, of their evolution in time as a function of land cover changes (in our case the forest cover).

2 Data and methods

Study areas

The Alps stretch from Nice to Vienna and are shared by six countries: France, Germany, Italy, Switzerland, Austria, and Slovenia. The French Alps are divided into 23 massifs. Among these massifs, we carry out the diachronic study in the Haute-Maurienne and Queyras massifs (Figure 17). Specific targeted municipalities were chosen because of the available forest cover data. Three municipalities were targeted in the Haute-Maurienne massif: Bonneval-sur-Arc, Bessans, Lanslevillard, and two municipalities in the Queyras massif: Aiguilles and Abriès-Ristolas.

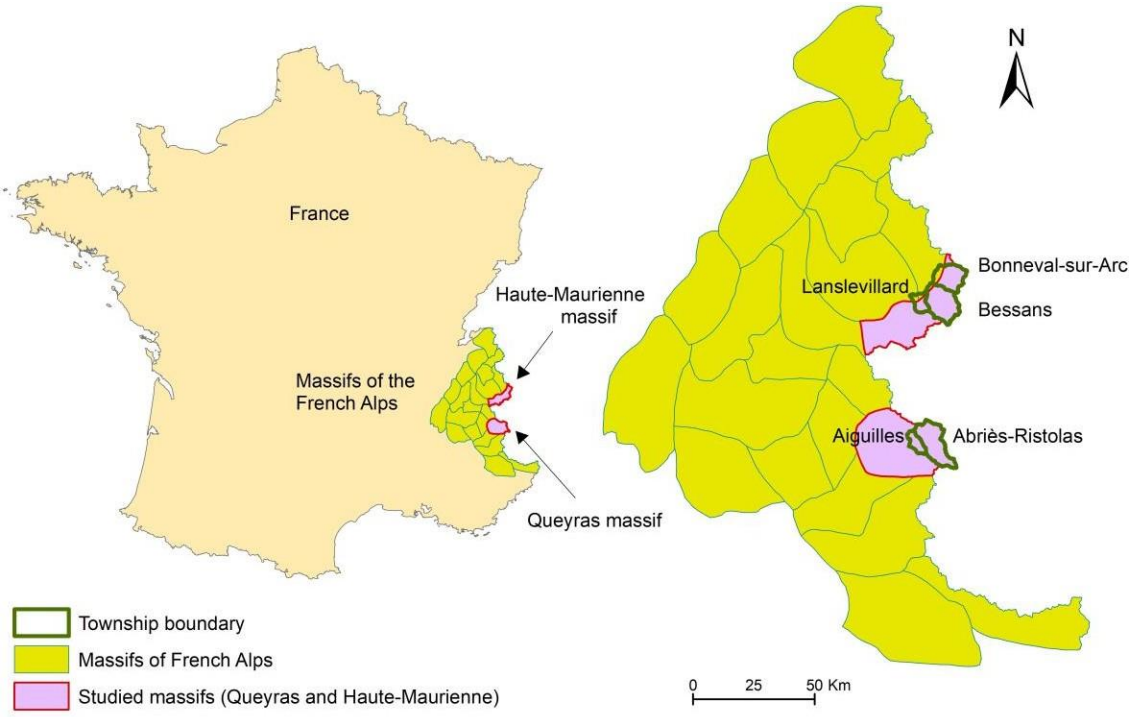

Figure 17 : The 23 massifs of the French Alps and massifs (Haute-Maurienne, Queyras), and townships (Bessans, Bonneval-sur-Arc, Lanslevillard, Aiguilles, Abriès-Ristolas) specifically targeted in the diachronic study.

From the DEM used (see below) the distribution of elevations and slopes of the French Alps can be inferred (Table 8).

% pixels from the French Alps	Elevation	Slope
25 (1st quartile)	1075.6 m	14.9°
50 (2nd quartile)	1576.7 m	24.9°
75 (3rd quartile)	2156.7 m	33.7°

Table 8 : Elevation and slope of pixels in the French Alps, for the three quartiles.

	Area of the French Alps : 21 339.2 km^2	
	Forested area	Total area covered by study area of the CLPA
Surface (km^2)	9526.4 km^2	4881.8 km^2
Percentage (%)	**44.6%**	**22.9%**

Table 9 *:* Documented forest and avalanche areas about the French Alps.

In France, CLPA provides extensive information about past avalanches, including maps of their maximum extent (Bonnefoy and al., 2010). These extents cover 22.9% of the area of the 23 massifs of the French Alps (Table 9).

Available data

In this study, we use a DEM of the French Alps at a resolution of 25 m from the IGN (Institut National de Information Géographique et Forestière) database. This DEM is used to provide the distribution of elevations and slopes at the scale of the 23 massifs. This DEM is further used to obtain PRAs according to the method described in Duvillier et al. (2023). For each pixel included in these PRAs, we retrieve the following characteristics: slope, elevation, curvature, distance to the closest ridge, exposure, and name of the corresponding massif.

Concerning forested areas, the IGN forest database is the reference for the year 2000 and provides information about different species (deciduous, fir, poplar, etc.), moorland, and herbaceous plants. In addition, for the diachronic study, land cover data before 2000 was obtained following the method described in Zgheib and al. (2020). Land cover information comes from handmade historical maps available in 1860 and 1952, digitalized and divided into eight classes including forest, grassland, agricultural land, glaciers, urban areas, roads, water bodies, and rocks, and sands. Aerial photographs obtained in 1952 allow the analysis of historical land use changes and are more accurate than handmade topographic maps. They provide seven different classes of land cover: forest cover, grassland, roads, snow, water bodies, rocks, and urban area.

Finally, a lithology was associated to each massif according to two categories based on the hardness and erodibility of its constitutive rock. The hardness of a rock is a quantity representing the resistance of a rock, Here, we use the Mohs scale (Harman and Rule, 2006) which ranges from 1 (soft rocks such as talc) to 10 (hardest possible rock, i.e. diamond). In this study, we consider a first category corresponding to erodible rocks with a low hardness such as limestone with a hardness of 3, or marl. The second category concerns rocks with a higher hardness and less prone to erosion, such as gneiss with a hardness between 6 and 7, and granite with a hardness of 7. The massifs made of erodible rocks are: Aravis, Bauges, Chablais, Chartreuse, Dévoluy, Embrunais-Parpaillon, Haut-Var Haut-Verdon, Pelvoux, Queyras, Thabor, Ubaye, Vercors and the massifs made of rocks with lower erodibility are Belledonne, Beaufortin, Champsaur, Grandes Rousses, Haute-Maurienne, Haute-Tarentaise, Maurienne, Mercantour, Mont-Blanc, Oisans, Vanoise.

3 Determination of PRAs

Method for determining PRAs

In this study, we apply the method described in Duvillier and al. (2023) to obtain the PRAs over the whole French Alps The first step of the method consists in obtaining a layer of points corresponding to the pixels of the DEM and for which we assign values for slope, curvature, elevation, orientation, distance to the nearest ridge, name of the corresponding massif, latitude and longitude. Firstly, pixels below 1400 m are filtered out, as low elevation areas receive little snow in the French Alps (Castebrunet and al., 2014). Climate projections also clearly indicate a decrease in future snowfall for these lower elevations (Verfaillie and al., 2018). Secondly, only areas with a slope between 28° and 60° are selected, snow deposits being generally very small for areas with larger slopes (Maggioni and Gruber, 2003). Areas with a forest presence are filtered out, as forests limit the probability of avalanches occurring, by anchoring the snowpack and limiting snow accumulation. A maximum distance to the ridge of 600 m is also applied, and the ridges are removed because of wind effects near the ridges contributes to the loading of the snow and forms cornices conducive to the start of slab avalanches. Pixels with a slope between 28° and 60°, a minimum elevation of 1400 m, a distance to the nearest ridge limited to 600 m, and outside the forest are selected and converted into a point layer. The second step is to apply a watershed algorithm to individualise each PRA. The resulting polygons are converted into a vector layer. For each polygon corresponding to a PRA, different attributes can be provided: distance to the nearest ridge, name of the corresponding massif, slope, elevation, orientation, curvature, latitude, longitude. We calculate the global area for each zone, and only polygons with a minimum area of ten pixels are kept (i.e. 6250 m^2). Indeed, very small PRAs are considered less prone to avalanches due to the moderate amount of snow that can accumulate on these surfaces. Figure 18 summarizes the main steps of the method.

Three classes of curvature are also defined for each pixel: concave, convex, and no curvature (i.e. horizontal planes), the curvature being obtained with the Geomorphon algorithm associated with the Grass GIS software (see Jasiewicz and Stepinski, 2013, for further details). Convex pixels are grouped in a single layer: ridges, peaks, and rocky spurs. Concave pixels correspond to hollows, valleys, and downslopes.

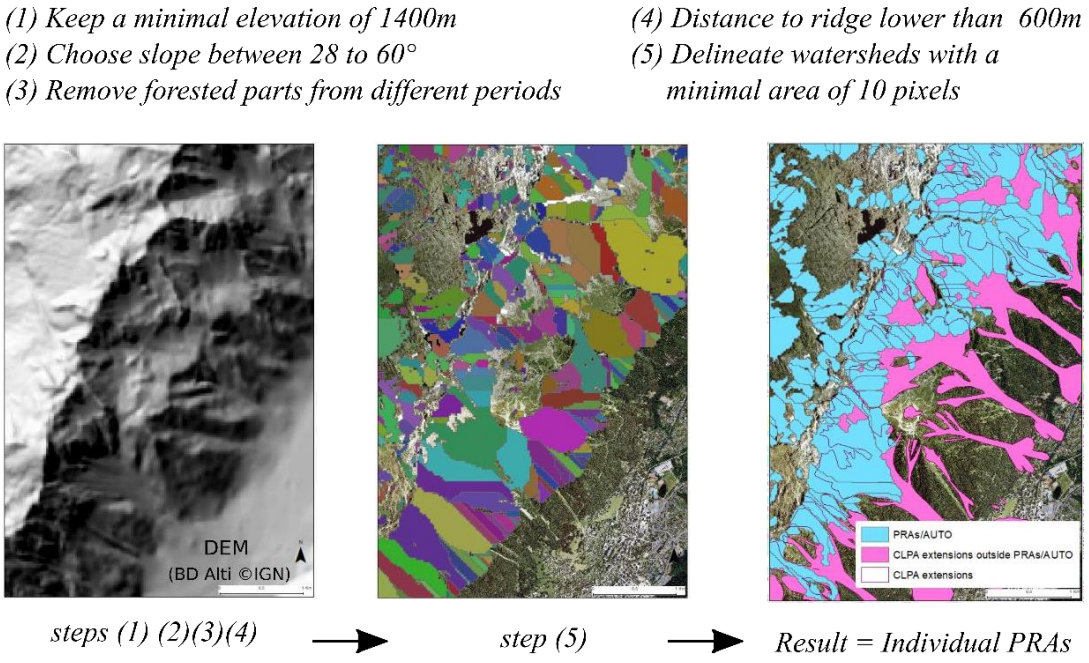

Figure 18 : Main steps of the PRAs detection method.

Evaluation of the PRA detection method all over the French Alps

To evaluate the PRA detection method, we exploit the information provided by the CLPA. However, CLPA is not exhaustive and covers limited parts of each massif, the percentage of surface covered varying from 0% (Bauges, Vercors) to 59.2% (Haute-Maurienne), see Table 10. As a consequence, the evaluation of the PRA detection method can only concern the PRAs included in the area covered by the CLPA. In addition, as the CLPA records the maximum extension reached by past avalanches and not only release areas, the same filters used to obtain the PRAs (minimum elevation, slope, distance to the ridge, presence of forest, watersheds with a minimum area of 10 pixels) are applied to the CLPA avalanche extensions. In the end, we obtain individualized PRAs within CLPA extents (see right plot in Figure 18). From the PRAs obtained over the whole French Alps and the PRAs detected in the CLPA areas, considered as a reference data set, we can calculate a confusion matrix in number and in area. The performances are quantified using a confusion matrix which is composed of four numbers: true positives (TP), true negatives (TN), false positives (FP), and false negatives (FN). A true positive means that the prediction and baseline values match, i.e. the detected PRAs correspond to the CLPA extensions. A false positive means that a PRA is detected outside the CLPA extensions. True negatives correspond to areas that are neither detected by our determination method nor included in the CLPA extensions. False negatives correspond to CLPA extents that are not detected by our method. By construction, the TN rate is equal to 100% and the FN rate is equal to 0% because the CLPA post-processing and the PRAs detection apply the same filter. Also the comparison is restricted to the area covered by the CLPA extensions.

Accuracy and error rates that synthetize the confusion matrix are classically computed as follows:

$$\text{Accuracy rate} = \frac{\text{True positive}+\text{True negative}}{\text{True positive}+\text{True negative}+\text{False positive}+\text{False negative}}, \quad (1)$$

$$\text{Error rate} = \frac{\text{False positive}+\text{False negative}}{\text{True positive}+\text{True negative}+\text{False positive}+\text{False negative}}. \quad (2)$$

We applied the determination method on the 23 massifs of the French Alps using the forested areas in 2017 as indicated in the IGN database, and compared it with the CLPA. The confusion scores in number and area are provided in Table 10.

Massifs	Accuracy rate (%)		Forested area (%)	Surface covered by the CLPA (%)
	In number	In area		
Aravis	92.2	97.9	55.4	17.5
Bauges	NA	NA	55.9	NA
Belledonne	89.0	95.8	51.8	17.8
Beaufortin	92.1	95.8	43.6	19.6
Chablais	92.5	96.2	51.8	21.6
Champsaur	94.4	98.3	31.7	25.3
Chartreuse	93.5	96.2	60.9	1.5
Dévoluy	91.8	97.6	49	4.2
Embrunais-Parpaillon	95.6	98.8	56.3	13,1
Grandes Rousses	81.8	86.8	12.1	51.1
Haute-Maurienne	93.4	97.6	19.1	36.1
Haute- Tarentaise	93.7	97.7	14.8	59.2
Haut-Var Verdon	94.4	97.7	54.7	14.5
Maurienne	92.1	97.1	51.5	24.1
Mercantour	92.1	96.5	54.1	35.6
Mont-Blanc	89.8	96.7	28	36.2
Oisans	90.1	95.7	35.9	33
Pelvoux	92.9	98,3	27.3	25.3
Queyras	88.6	95.0	43.3	30
Thabor	92.3	96.7	28.8	35.7
Ubaye	93.6	97.4	37.6	35.5
Vanoise	91.5	96.6	26.9	33.9
Vercors	NA	NA	70.8	NA

Table 10 : Accuracy rate in number and area for the massifs of French Alps, with the exception of the massifs of Bauges and Vercors where there is no CLPA. For all massifs. For all massifs, the aerial fraction of forests and CLPA extents is also provided.

Diachronic evolution of PRAs

As indicated above, the evolution of PRAs over time is assessed by applying the same PRA detection method with four different forest covers obtained from:

- the IGN *Etat-major* map of 1860;
- aerial photographs obtained in 1952 by the IGN;
- IGN maps from 1952;
- the IGN's “BD foret”, dating from the year 2013 for the Queyras massif, and 2014 for the Haute-Maurienne massif.

Statistical analyses

Different statistical criteria and methods are applied according to the relationships we wish to establish. The relationships between the confusion scores and the topographical characteristics of the PRAs and the massifs are quantified with the Pearson correlation coefficient (Table 11). For each of the variables, if the significance level (p-value) of the associated statistical test is higher than 5%, then the variables can be considered as poorly correlated. Concerning the dichotomous lithology classification, a point-biserial correlation coefficient is computed.

Different descriptive statistics are used to characterise the PRAs at the scale of the French Alps and relate them to the characteristics of the French Alps as a whole (slope, elevation, etc.). Concerning all

the detected PRAs, we assess the distributions of their exposure according to eight aspects (every 45°), and of their area. For the pixels in the PRAs and for all pixels of the French Alps, we also compare the distributions of elevations and slopes. Concerning the characteristics of the PRAs at the scale of the massifs, we compute the average slope, the average elevation, the average curvature and the lithology using the pixels constituting all the PRAs of each massif. Concerning lithology, we assign a value of 0 for the presence of limestone and marl, and a value of 1 for the presence of gneiss and granite (Table 13). We distinguish lithology from the other parameters of the massifs, as it is a binary parameter with only the presence of one or the other rock type.
In addition, categories of massifs are proposed according to the common characteristics of their PRAs, using the *k*-means clustering method. This algorithm consists of classifying different entities using different characteristics that can discriminate them. In each group, the group center corresponds to the average characteristics of the entities belonging to this group, according to their Euclidean distance from the group center. Here, the *k*-means algorithm is applied using the following characteristics: the number of PRAs, the maximum PRA area (km^2), the total PRA area (km^2), the average PRA area (km^2), the average slope (°), the average elevation (m), the maximum elevation (m). Different numbers of clusters are tested in order to select the most sensible one.

4 Results

Evaluation of the PRAs obtained with CLPA extents

For the French Alps as a whole, we obtain an accuracy rate of 90.4% for PRA numbers, and an accuracy rate of 95.3% for PRA areas.

Then, we calculated an accuracy rate in number and area for each of the massifs except for the Bauges and Vercors massifs where there is no data about past avalanches extents in CLPA (Table 10). We obtained accuracy rates in numbers between 81.8% and 95.6% (Grandes Rousses and Embrunais-Parpaillon), and in areas between 86.8% and 98.8% (Grandes Rousses and Embrunais-Parpaillon) (**Table 9**Table 10). In order to explain the variability of these scores between the different massifs, Table 11 gives the correlation coefficients between the accuracy rates and different parameters obtained at the scale of for the massifs.

			Lithology	Total area of massif (km^2)	Studied CLPA area (%)	The surface of forest in relation to massif (%)	Proportion of PRAs in relation to massif (%)	Proportion of number of PRAs per massif in relation to the total number of PRAs (%)	Mean area PRAs (km^2)	The largest area of the PRAs (km^2)	Total area of PRAs (km^2)	Number of PRAs per massif
Accuracy rate (%)	In number	Correlation coefficient	**-0.32**	**0.03**	**-0.37**	**0.35**	**-0.20**	**-0.04**	**-0.15**	**0.21**	**-0.08**	**-0.04**
		(p-value)	0.16	0.89	0.1	0.12	0.38	0.87	0.51	0.37	0.74	0.87
	In area	Correlation coefficient	**-0.27**	**0.11**	**-0.38**	**0.34**	**-0.14**	**-0.04**	**0.07**	**0.29**	**-0.02**	**-0.04**
		(p-value)	0.23	0.63	0.09	0.13	0.53	0.85	0.77	0.20	0.92	0.85

Table 11 : Correlation coefficients between the accuracy rates and different parameters obtained at the scale of the massifs or for the corresponding PRAs. P-values indicate the significance of the correlation.

The most characteristic parameters are those with the highest correlation coefficient. A stronge relationship is obtained with the lithology, the best scores corresponding to massifs with erodible rocks. Strong negative correlations are also obtained between the accuracy rates and the proportion of the massifs covered by the CLPA, better scores being obtained when this percentage is high. Eventually, the highest positive correlations are obtained with the proportion of forest area in the massif, the highest accuracy rates in number and in area being obtained when forested areas in the massif are more dominant. Some of these relationships have clear explanations. As wooded areas are

filtered out of the PRAs, the number of PRAs found is limited in massifs with a forest area covering a large part of the territory. In the case of avalanche-prone areas with well-documented historical avalanches, the number of detected PRAs that do not overlap with the CLPA decreases, which increases the accuracy rates in numbers and areas.

Yet, overall, accuracy rates show that the PRAs detection method performs well over all the massifs. The following section will be dedicated to a statistical assessment of these PRAs for the entire French Alps.

Results for the French Alps

Aspect

Figure 19 shows the exposure of the pixels contained in the PRAs. These exposures are more or less evenly distributed, with percentages per aspect class ranging from 10% (North) to 14% (South).

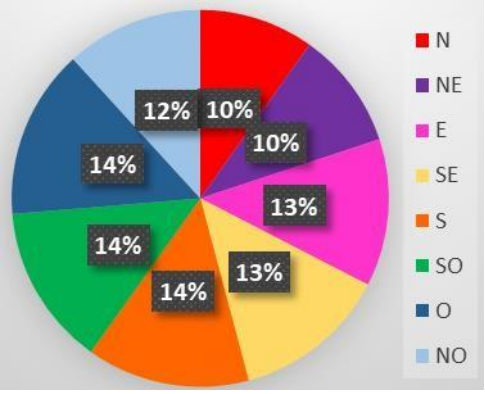

Figure 19 : Distribution of the aspect of the pixels included in the PRAs of the French Alps.

Area of PRAs

By definition, detected PRAs have a minimum area of 0.00625 km2 corresponding to the minimum threshold of 10 pixels at a 25 m resolution. In average, PRAs have an area of 0.036 km2, and a maximum area of 1.625 km2. Figure 20 shows the number of PRAs corresponding to different area intervals, obtained every 5000 m2, for the whole French Alps. We can see that the number of PRAs logically rather quickly decreases with their size but that large PRAs are not completely unlikely.

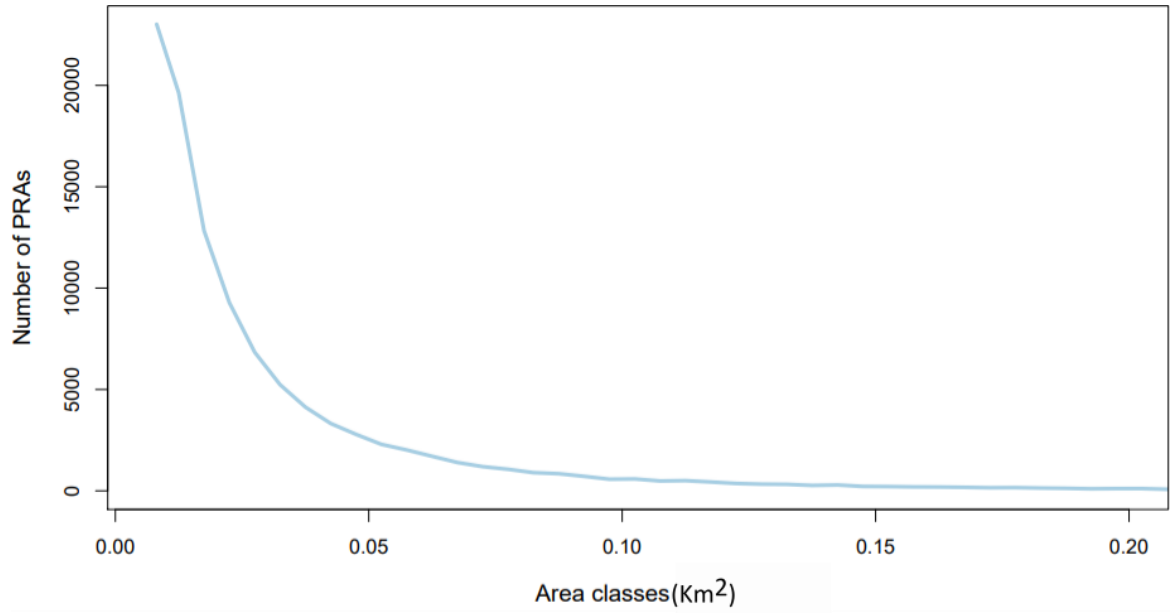

Figure 20 : Distribution of PRAs by class of area (every 5000 m²) for the whole French Alps.

Comparison between topographical characteristics of the PRAs and those of the FrenchAlps

Figure 21 shows the distributions of PRA areas as a function of the elevation, in comparison to the whole French Alps. A minimum elevation of 1400 m being applied in the PRAs detection method, these distributions are shown from 1400 m to 3800 m (as there are few peaks above 4000 m in the French Alps). While the number of pixels decreases as a function of the elevation over the whole French Alps all over the considered elevation range, PRAs are more frequent between 2200 m and 2500 m (Figure 21 a). Hence, the proportion of pixels contained in the PRAs clearly increases as a function of elevation (Figure 21b) and exceeds 50% above 3000 m.

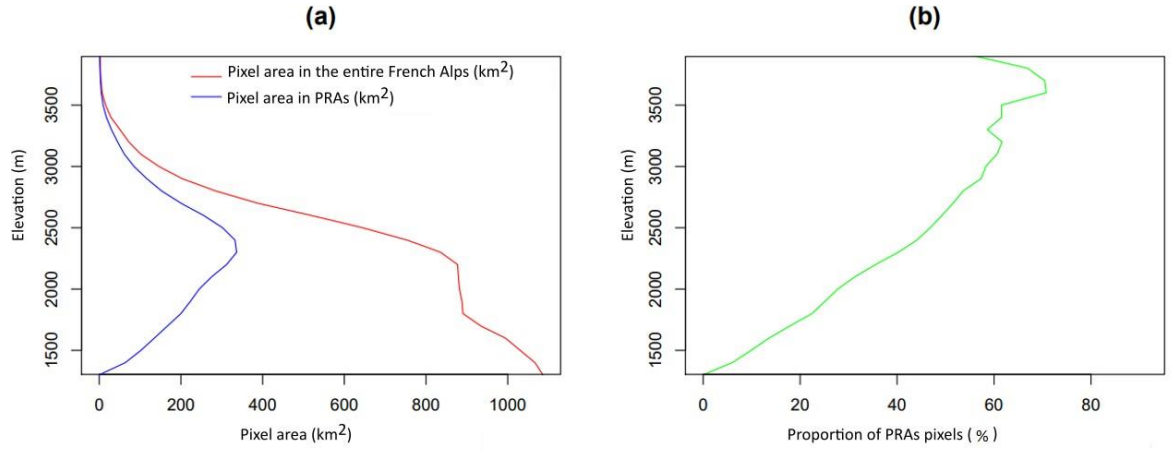

Figure 21 : (a) Distribution of pixels in PRAs in relation to pixels in the French Alps according to elevation. (b) Proportion of PRAs pixels to French Alps pixels by elevation.

Figure 22 presents similar comparisons as a function of slopes. In the French Alps, the most frequent slopes are between 24° and 34° (Figure 22a). Concerning the pixels in the PRAs, which are restricted by construction between 28° and 60°, the most frequent slopes are between 31° and 34°. The

proportion of pixels in the PRAs compared to the pixels in the French Alps exceeds 60% for slopes above 50° (Figure 22b). These steep areas are often located at an elevation above 1400 m and can therefore be retrieved with the PRAs determination method.

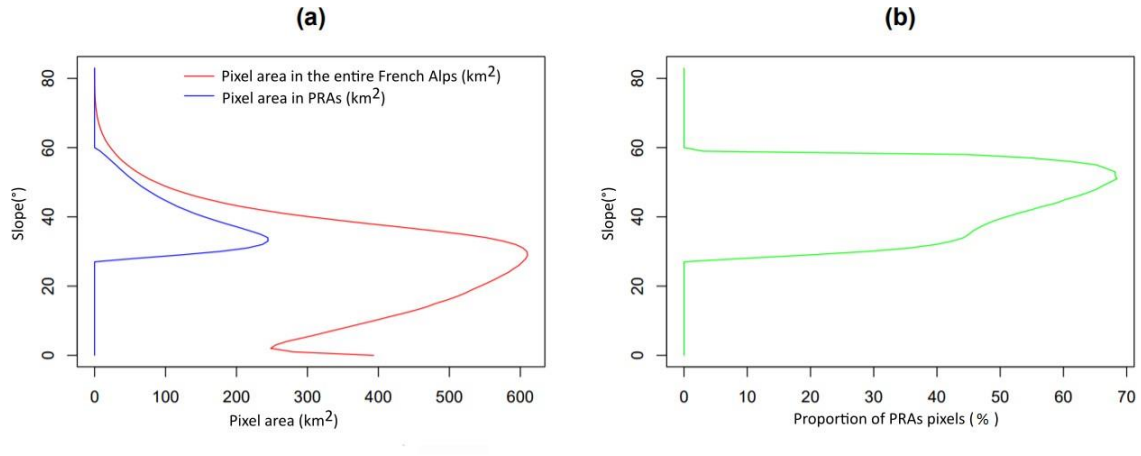

Figure 22 : (a) Distribution of pixels in PRAs in relation to pixels in the French Alps according to slope. (b) Proportion of PRAs pixels to French Alps pixels by slope.

Now that we have studied the PRAs in the French Alps, we study the PRAs at the scale of the massifs, and try to find the characteristics of the PRAs that are specific to them.

Spatial variability at the scale of the massifs

Table 12 shows the correlation coefficients obtained between three characteristics of the PRAs obtained at the scale of the massifs (maximum area of PRAs, total area covered by the PRAs and total number of PRAs) and some characteristics of these massifs (maximum elevation, percentage of forested area, mean slope). The correlation between the total area of PRAs and the proportion of forested area is -0.43, showing that areas covered by the PRAs are smaller in massifs where the forest covers a larger part of the massif. This was expected since the PRA determination method excludes forested areas from the PRAs. The correlations with the maximum elevation and the mean slope of the massif is 0.64 and 0.73, respectively, indicating that the area covered by the PRAs is larger for massifs with high elevations and mean slopes, for which a greater number of pixels can lead to a PRA.

Parameters from PRAs	Parameters from massifs	Correlation coefficient (p-value)
The largest area of the PRAs (km^2)	Maximum Elevation from massif (m)	**0.68 (0.0003)**
	The surface of forest in relation to massif (%)	**-0.34 (0.11)**
	Mean slope (°)	**0.60** (0.002)
	Studied CLPA area (%)	**0.09** (0.70)
Total area of PRAs (km^2)	Maximum elevation from massif (m)	**0.64** (0.001)
	The surface of forest in relation to massif (%)	**-0.43** (0.04)
	Mean slope (°)	**0.73** (6.831e-05)
	Studied CLPA area (%)	**0.45** (0.04)
Total number of PRAs	Maximum elevation (m)	**0.59** (0.003)
	The surface of forest in relation to massif (%)	**0.49** (0.02)
	Mean slope (°)	**0.65** (0.0007)
	Studied CLPA area (%)	**0.47** (0.03)

Table 12 : Correlation coefficients between parameters from PRAs and the massif parameters. Corresponding p-values are provided between brackets.

Table 13 shows similar correlation coefficients for the lithology of the massifs. Strong correlations are found between the indicator of the lithology of the massif (classified as 1 for massifs with erodible rocks and 2 for massifs with hard rocks) and the mean and maximum elevation of the PRAs, and the total number of PRAs per massif.

Lithology	Total number of PRAs	**0.33** (0.12)
	Total area of PRAs (km^2)	**0.44** (0.03)
	The largest area of the PRAs (km^2)	**0.23** (0.29)

Table 13 : Correlation coefficients between lithology of massifs and parameters from PRAs.

Table 14 summarizes the characteristics of the pixels included in the PRAs. They have an average elevation between 1652 m for the Chartreuse massif and 2679 m for the Haute-Maurienne massif, and a maximum elevation varying between 2056 m for the Chartreuse and 4763 m for the Mont-Blanc massif. The average slopes range from 37.3° for the Haut-Var Haut-Verdon massif to 41.2° for the Mont-Blanc massif.

% of pixels included in all PRAs	Mean elevation (m)	Maximal elevation (m)	Mean slope (°)	Total number of PRAs per massif	% of convex pixels per massif	% of concave pixels per massif	% of pixels without curvature per massif
Minimum value	1652 Chartreuse	2056 Chartreuse	37.3 Haut-Var Haut-Verdon	721 Chartreuse	25 Mont-Blanc	10.5 Chartreuse	46.2 Belledonne
Maximum Value	2680 Haute-Maurienne	4763 Mont-Blanc	41.2 Mont-Blanc	9528 Vanoise	35.8 Chartreuse	24.3 Oisans	57.0 Vercors

Table 14 *:* Minimum and maximum values for the characteristics of the pixels included in the PRAs: average and maximum elevation, average slope, total number of PRAs per massif, proportion of convex pixels per massif (%), proportion of concave pixels per massif (%), proportion of flat pixels per massif (%).

The number of PRAs per massif varies between 721 for the Chartreuse massif and 9528 for the Vanoise massif. The lower number of PRAs detected in the Chartreuse massif compared to the other massifs is related to a high forest cover peercentage of 60.9% for this massif and a small maximum elevation (2075 m), which limits the number of PRAs that can be detected with the minimum threshold of 1400 m. In contrast, the Vanoise massif has a forest cover fraction of 26.9%, and a maximum elevation of 3846 m, allowing a greater number of PRAs to be determined (see Table 16 below which provides these characteristics for all the massifs).

Table 15 provides the proportion of concave, convex and flat pixels within PRAs for the different massifs. Convex pixels represent between 25% (for the Mont-Blanc massif) and 35.8% (for the Chartreuse massif) of the pixels included in the PRAs. The concave pixels represent between 10.5% (for the Chartreuse massif) and 24.3% (for the Oisans massif) of the pixels. Flat pixels represent between 46.2% (for the Belledonne massif) and 57.0% (for the Vercors massif) of the pixels.

Massifs	Proportion of concave pixels (%)	Proportion of convex pixels (%)	Proportion of flat pixels (%)
Aravis	19.7	30.5	49.9
Beaufortin	20.0	25.4	54.7
Bauges	16.7	31.3	52.0
Belledonne	20.3	33.4	46.2
Chartreuse	10.5	35.8	52.1
Chablais	20.7	28.0	51.3
Champsaur	23.4	27.5	49.1
Dévoluy	21.1	30.1	48.7
Embrunais	21.2	29.8	49.0
Gandes rousses	18.5	25.6	56,0
Haute maurienne	17.1	27.6	55.4
Haute tarentaise	18.1	25.8	56.0
Haut var verdon	20.9	28.3	50.8
Mercantour	20.3	27.7	52.0
Mont-Blanc	21.7	30.0	48.3
Oisans	22.2	25.0	52.8
Thabor	24.3	27.3	48.6
Pelvoux	18.3	31.1	50,6
Queyras	23.5	26.7	49,8
Ubaye	19.2	28.6	52.1
Vanoise	19.8	27.6	52.6
Vercors	19.8	25.7	54.5

Table 15 : Proportion of concave, convex and flat pixels within detected PRAS, for the different massifs.

Finally, we propose categories of massifs, grouped according to the similarity of the characteristics of their PRAs. The 23 massifs of the French Alps are thus grouped by applying the *k*-means algorithm on the following characteristics: the number of PRAs detected per massif, the average slope of the PRAs, the average and maximum elevation of the PRAs, the average, maximum and total area of the PRAs. Figure 23 shows the groups obtained when the number of different groups is set to 3.

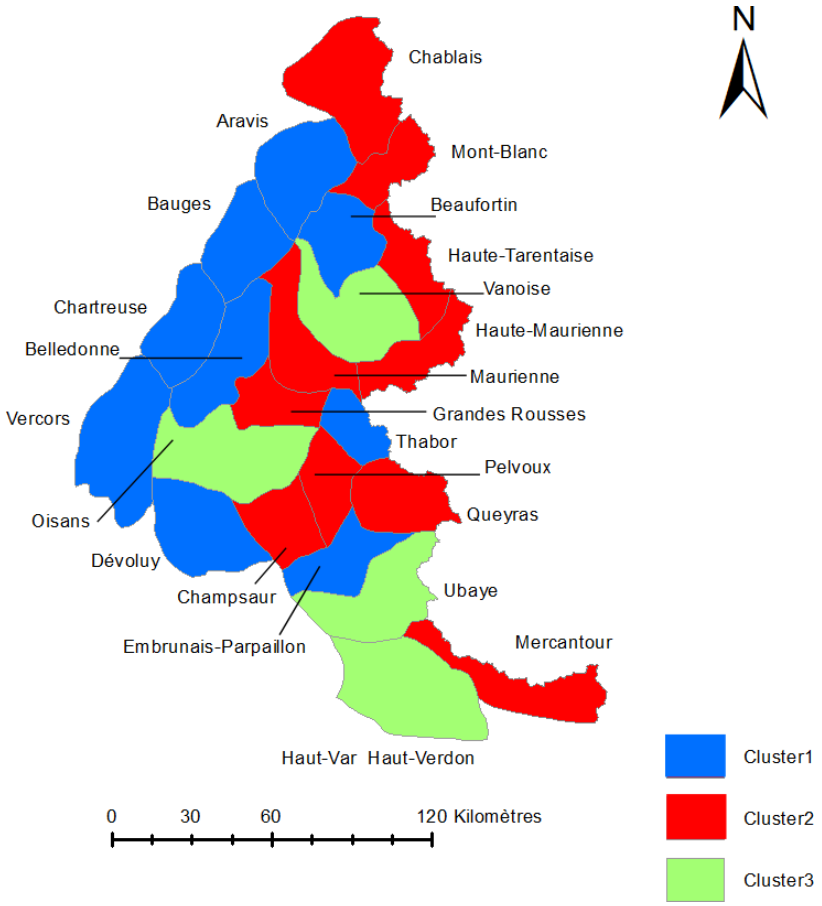

Figure 23 : Massifs of the French Alps: divided using *k*-means algorithm into three classes.

We observe a strong spatial coherence. The characteristics of these clusters can be described as follows:

- Cluster 1: Low-elevation massifs, mostly made of limestones (except the Belledonne, Champsaur and Beaufortin granitic massifs), with a reduced number of PRAs compared to the other massifs. In majority, these massifs are part of the so-called Pre-Alps range (Devoluy, Vercors, Chartreuse, Bauges, Aravis).

- Cluster 2: Massifs with high average elevations, medium number of PRAs (compared to relatively low numbers of PRAs in cluster 1 and to large numbers of PRAs in cluster 3). The proportion of the massifs covered by PRAs is larger than for the two other clusters.

- Cluster 3: This small cluster differs from cluster 2 by its larger number of PRAs obtained for the massifs of Haut-Var Hat-Verdon (8246), Oisans (7630), Ubaye (8193), Vanoise (9528). In these massifs PRAs also cover a larger area (321 km^2 in average versus 189 km^2 for cluster 2 and 74 km^2 for cluster 1).

Massifs	Number of PRAs	Maximum area of PRAs (km^2)	Total area of PRAs (km^2)	Mean area of PRAs (km^2)	Mean slope (°)	Mean elevation (m)	Maximum elevation (m)	Proportion of PRAs to massif (%)	Cluster (2 classes)	Cluster (3 classes)	Cluster (4 classes)	Cluster (5 classes)
Aravis	2804	0.4	96.5	0.03	39.3	1863	2736	9.0	1	2	1	3
Bauges	1258	0.2	37.7	0.03	39.0	1686	2191	4.3	1	2	4	2
Belledonne	3241	0.7	119.4	0.04	39.6	2208	2929	12.0	1	2	1	3
Beaufortin	3356	0.5	93.8	0.03	38.1	2163	2967	12.4	1	2	1	3
Chablais	4650	0.6	140.6	0.03	38.6	1943	3072	10.2	1	3	3	4
Champsaur	4636	1.2	200.5	0.04	40.0	2300	3471	30.5	1	3	3	4
Chartreuse	721	0.2	15.4	0.02	39.3	1652	2056	1.8	1	2	4	2
Dévoluy	2991	0.7	110.9	0.04	38.3	1929	2765	10.1	1	2	1	3
Embrunais-Parpaillon	1984	1.5	68.4	0.03	39.1	2339	3037	9.7	1	2	1	3
Grandes Rousses	5005	0.6	170.7	0.03	37.9	2332	3458	30.7	1	3	3	4
Haute-Maurienne	5655	0.9	208.0	0.03	38.7	2680	3724	30.9	1	3	3	4
Haute-Tarentaise	5701	0.6	185.2	0.03	38.5	2603	3764	29.4	1	3	3	4
Haut-Var Haut-Verdon	8246	0.9	253.1	0.03	37.3	2130	3027	15.8	2	1	2	1
Maurienne	3638	0.5	115.1	0.03	37.5	2185	3160	12.5	1	3	1	3
Mercantour	5353	1.0	323.2	0.03	37.6	2251	3112	35.4	1	3	3	4
Mont-Blanc	3679	1.1	174.2	0.05	41.2	2581	4763	30.1	1	3	3	5
Oisans	7630	1.2	438.9	0.06	41.1	2360	3990	30.4	2	1	2	1
Pelvoux	4730	1.6	217.3	0.05	40.6	2628	4063	37.4	1	3	3	4
Queyras	5034	0.6	154.0	0.03	37.5	2513	3278	18.4	1	3	3	4
Thabor	2862	0.5	84.6	0.03	39.0	2537	3208	18.6	1	2	1	3
Ubaye	8193	0.7	264.0	0.03	38.2	2460	3366	23.1	2	1	2	1
Vanoise	9528	1.0	303.0	0.03	38.6	2469	3835	24.9	2	1	2	1
Vercors	907	0.2	24.9	0.03	40.2	1731	2312	1.8	1	2	4	2

Table 16 : Characteristics of PRAs in the massifs of the French Alps used in the *k*-means algorithm.

Class centres	Number of PRAs	Mean area of PRAs (km²)	Maximum area of PRAs (km²)	Total area of PRAs (km²)	Proportion of PRAs to massif (%)	Mean slope (°)	Mean elevation (m)	Maximum elevation (m)
1	6189.7	0.037	0.92	240.99	26.42	38.70	2389.02	3513.33
2	2494.6	0.029	0.60	85.84	11.13	39.10	2079.55	2920.36
1	2236.0	0.031	0.55	73.64	8.86	39.04	2012.11	2689.0
2	4799.7	0.034	0.93	188.59	26.55	38.80	2401.56	3586.5
3	8399.2	0.038	0.97	321.86	23.55	38.77	2354.66	3554.5
1	2982.23	0.029	0.69	99.09	12.06	38.62	2174.96	2971.71
2	8399.25	0.038	0.97	321.86	23.55	38.77	2354.66	3554.50
3	4928.79	0.0375	0.93	196.76	28.11	38.95	2425.62	3633.89
4	962.0	0.026	0.21	28.06	2.63	39.53	1689.77	2186.33
1	8399.2	0.038	0.97	321.86	23.55	38.77	2354.66	3554.50
2	962.0	0.026	0.21	28.06	2.63	39.53	1689.77	2186.33
3	2982.29	0.029	0.69	99.09	12.06	38.62	2174.96	2971.71
4	5085.0	0.037	0.90	200.55	27.86	38.67	2406.20	3492.75
5	3679.0	0.045	1.12	166.45	30.14	41.15	2581.00	4763.00

Table 17 : Class centers for the characteristics of PRAs, obtained using the *k*-means classification, for 2 to 5 clusters.

Figure 24 shows the sum of the squared distance between each member of a cluster and its cluster centroid. This illustration can help to determine the most appropriate number of classes, as this sum of squared errors is expected to decrease significantly when an additional cluster has a low within-group variance. Figure 24 shows that the sum of squared errors decreases significantly from three clusters which motivates this choice.

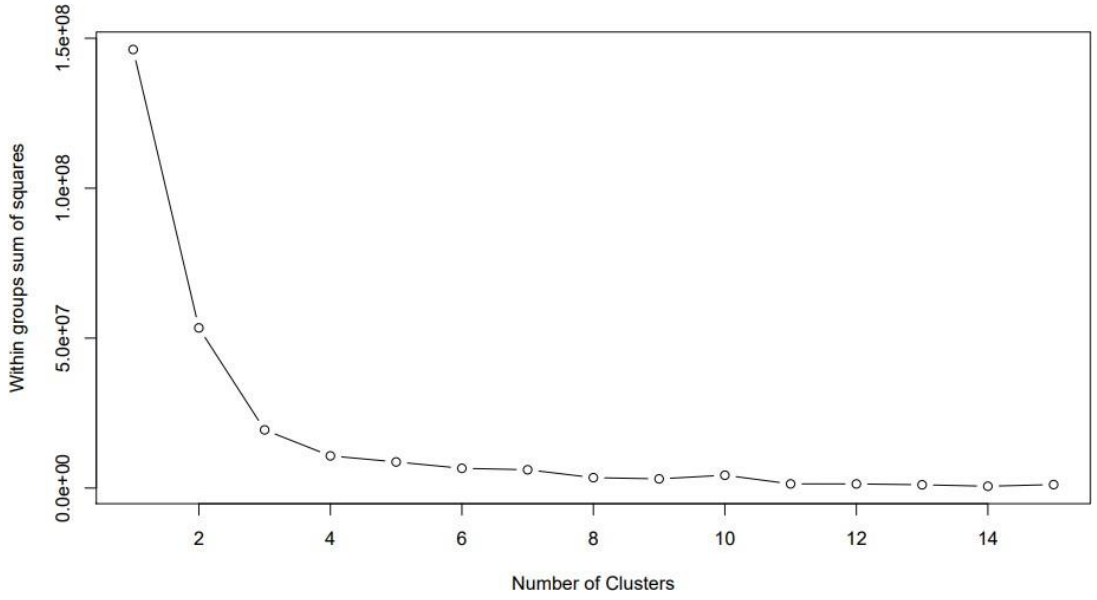

Figure 24 : Sum of the squared distance between each member of a cluster and its cluster centroid, as a function of the number of clusters.

Temporal evolution on the 2 massifs: Queyras and Haute-Maurienne

For the Queyras and Haute-Maurienne massifs, we repeat the PRA extraction exercise for different forest covers corresponding to the years 1860, 1952, 2013 and 2014 in order to describe the influence of this evolution on the PRAs characteristics. For the most recent forest, in the years 2000, we use the same forest area as in the determination method, i.e. DB forest of IGN.

Figure 26 and Figure 28 show the maps of the different forest covers within areas of the massifs of Queyras and Haute-Maurienne, respectively. Both figures show that the two forest areas corresponding to the year 1952 have small differences. Notably, the forest from photographs covers parts of the study area not covered by the forest from maps. However, the difference between the forest from the map and the forest from aerial photographs at the same date is rather small, which allows the analysis of the variation between 1860 and the 2000s (2013 for the Queyras massif and 2014 for the Haute-Maurienne massif) without further correction. Yet, as the forest from aerial photographs is more accurate than that obtained from the map, we use the number of PRAs obtained from the photographs for this date in further analyses.
Table 18 provides different statistics of the PRAs obtained with the different forest covers, for the massifs of Queyras and Haute-Maurienne. In both areas we see that the number of PRAs decreased between 1860 and the 2000s, as the forest cover increased.

	Years	Number of PRAs detected	Proportion of forest to study area (%)	Total area of PRAs (km^2)	Minimum elevation (m)	Mean elevation (m)	Maximum elevation (m)
Massif of Queyras	1860	1793	15.9	61.84	1461	2465	3280
	1952 from map	1792	20.5	60.04	1461	2476	3280
	1952 from photograph	1826	16.9	61.04	1475	2481	3280
	2013	1578	43.1	48.41	1474	2565	3280
Massif of Haute-Maurienne	1860	3043	3.2	118.85	1498	2756	3724
	1952 from map	3038	3.3	118.4	1503	2759	3724
	1952 from photograph	3050	3.6	118.03	1503	2762	3724
	2014	2971	5.7	115.64	1501	2773	3724

Table 18 : Number of PRAs detected, proportion of forest to study area (%), for each date for the study areas (Fig. 1) within the massifs of Queyras massifs of Queyras and Haute-Maurienne.

Queyras

Figure 25a shows the distribution of the total areas covered by the PRAs for different elevation bands, and for the forest covers in 1860, 1952 and 2013. Between 1600 m and 2400 m, the area of the pixels constituting the PRAs corresponding to the year 2013 is smaller than in other years. For example, between 1900 and 1950m, this area is 0.19 km^2 in 2013, 0.66 km^2 or 0.77 km^2 in 1952 depending on the use of aerial photographs or geo-referenced maps, and 0.95 km^2 in 1860. Reforestation until 2013 may explain this decrease in the number of PRAs and the development of the forest. From 2800 m onwards, the divergences between the four curves become less pronounced as there is little forest cover at these higher elevations.

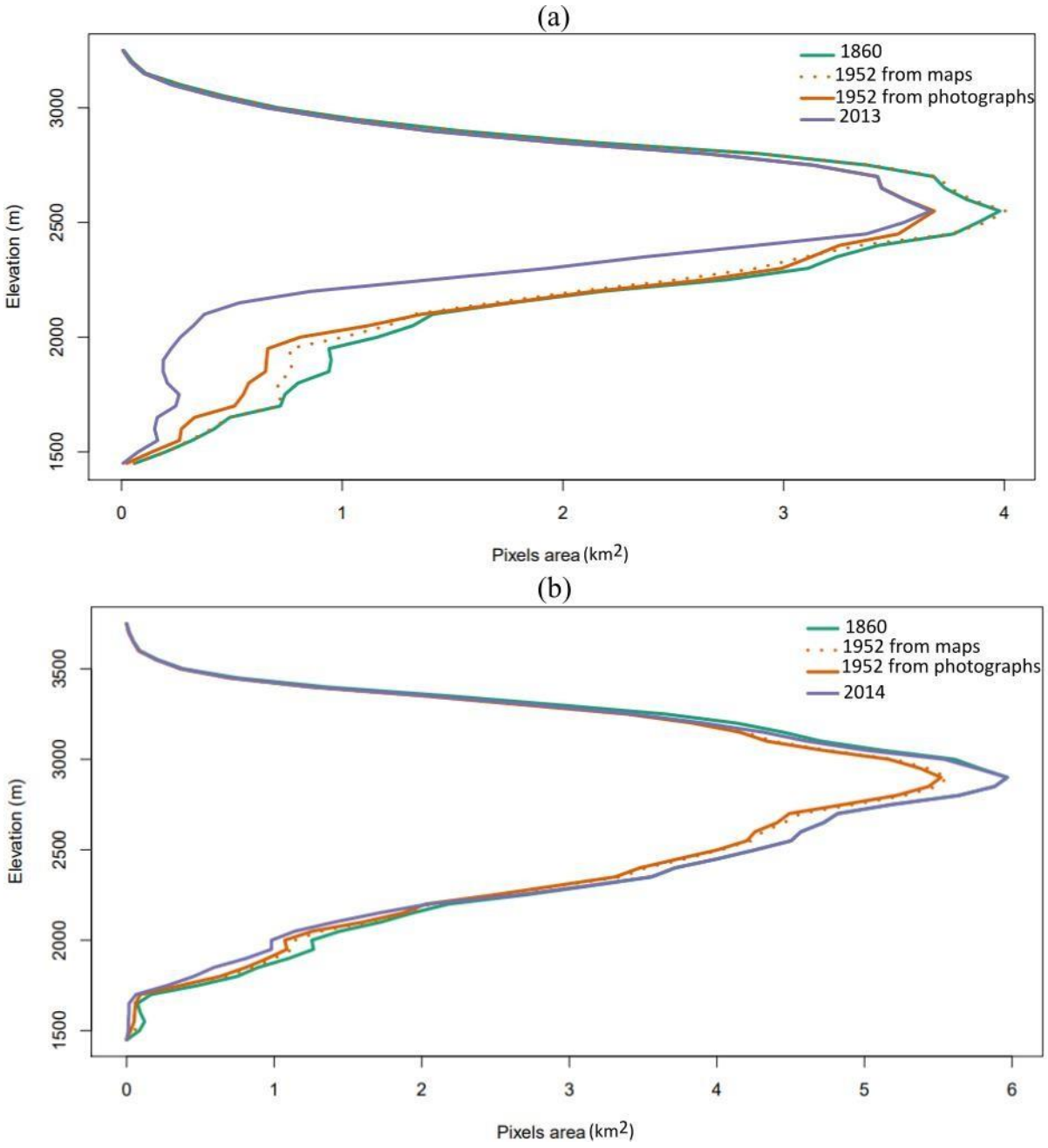

Figure 25 : Distribution of pixel area in PRAs in 1860, 1952 from map and photograph, 2013 and 2014, as a function of elevation for the study areas (Figure 17) within the massifs of Queyras (a), and for the massifs of Haute-Maurienne (b).

Figure 27 shows the PRAs obtained with the different forest covers, for the massif of Queyras. We observe that PRAs areas have decreased over time on lower slopes as a consequence of the extension of the forest covers at low elevations. This is notably the case above the town of Abriès-Ristolas, where a whole side of the mountain has been reforested. Between 1860 and 2013, the minimum elevation of the PRAs increased from 1461 to 1474 m, which means that 13 m of forest was gained on the PRA.

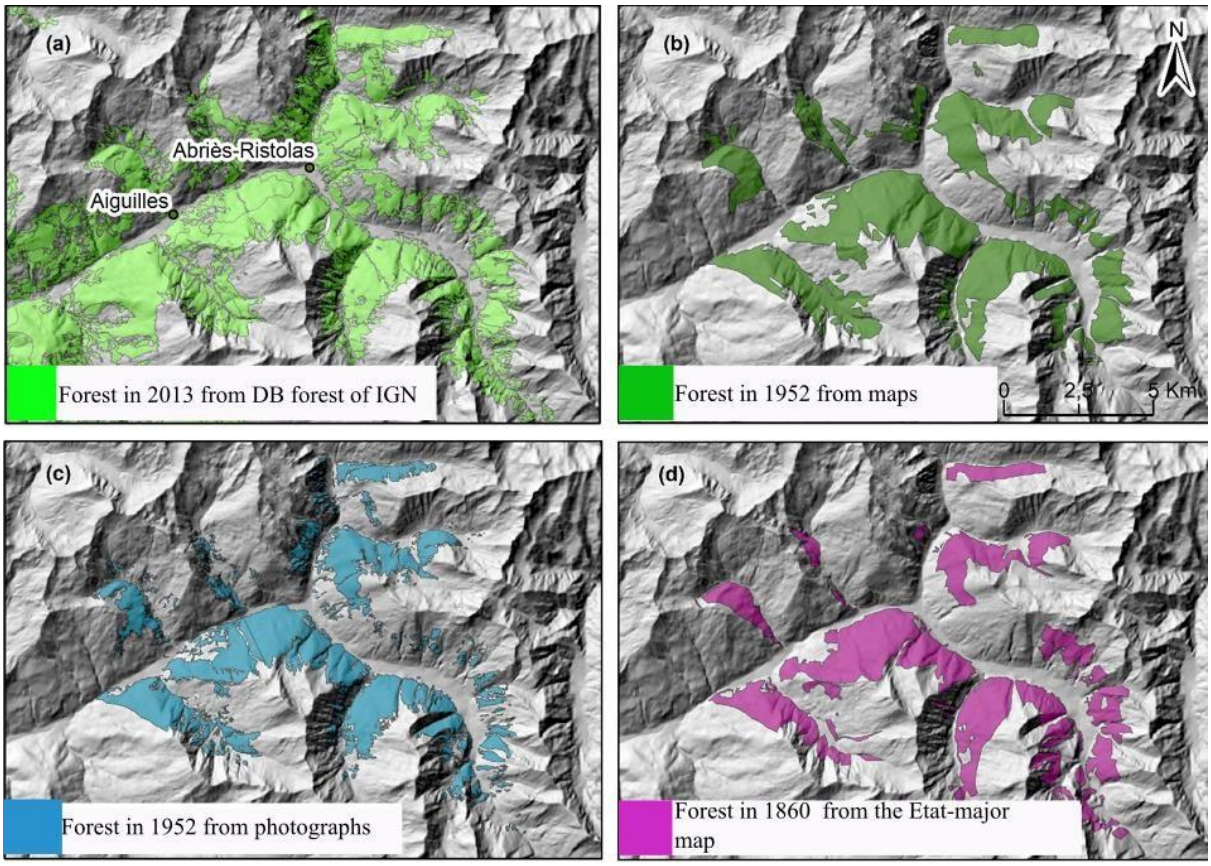

Figure 26 : Forest covers for the Queyras, for different years. (a) in 2013 from DB forest of IGN, (b) 1952 from maps, (c) 1952 from photographs, (d) 1860 from the map of Etat-major, digitalised by Zgheib and al. (2020).

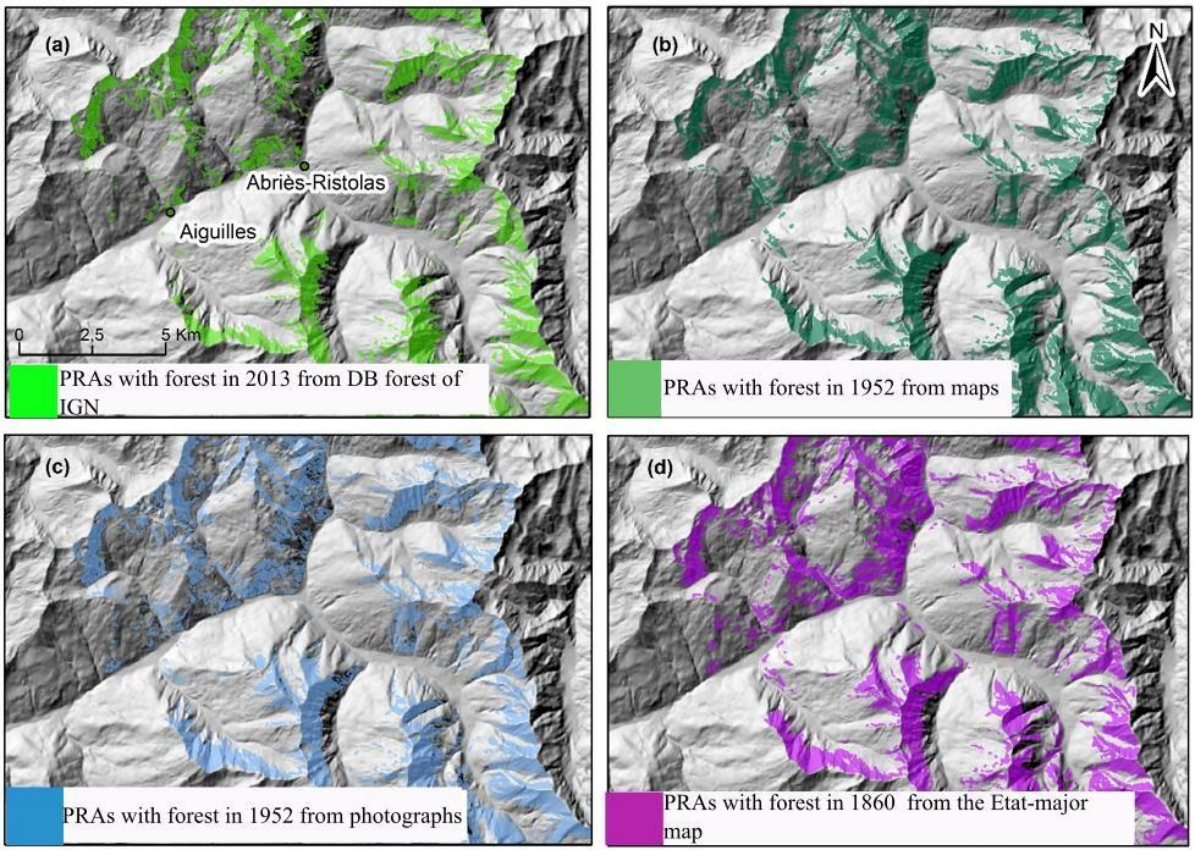

Figure 27 : Map of PRAs for the Queyras, for different years. (a) in 2013 from DB forest of IGN, (b) 1952 from maps, (c) 1952 from photographs, (d) 1860 from the map of Etat-major, digitalised by Zgheib and al. (2020).

Haute-Maurienne

The three towns studied in the massif of Haute-Maurienne are located at the bottom of a deep valley with a minimum elevation of 1673 m. The slopes surrounding the towns are steep, sparsely wooded and therefore particularly avalanche-prone. This is why buildings are located in the centre of the valley, in order to limit the potential damage to the buildings.

Over time, the forest area has increased (3.2% in 1860, 3.6% in 1952, and 5.7% in 2014), leading to a decrease in the number of PRAs detected between 1860 and 2014 (3043 in 1860, 3050 in 1952, 2971 in 2014, see Table 18, Figure 25b and Figure 28). Between 1860 and 2014, the average elevation of PRAs increased by 17 m.

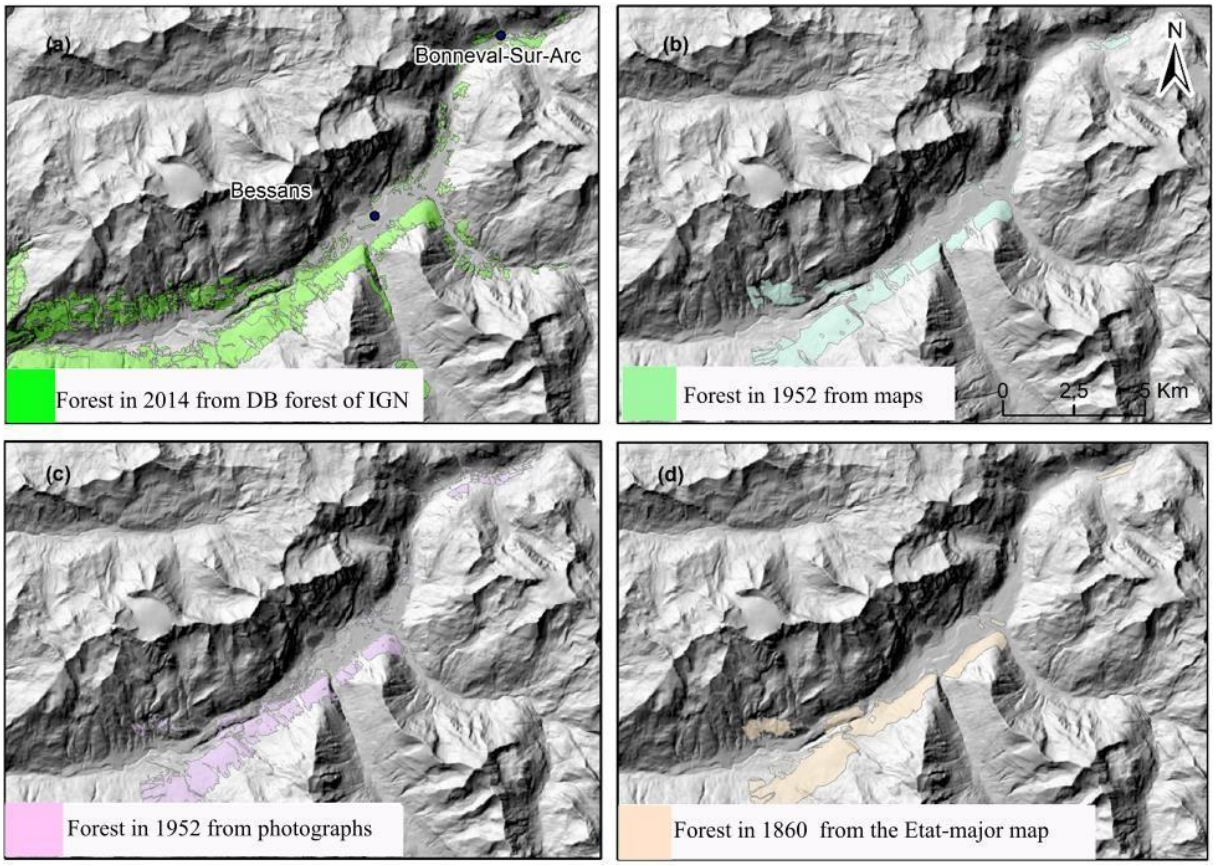

Figure 28 : Forest covers for the Haute-Maurienne, for different years. (a) in 2014 from DB forest of IGN, (b) 1952 from maps, (c) 1952 from photographs, (d) 1860 from the map of Etat-major, digitalised by Zgheib and al. (2020).

Evolutions of the forest cover can mainly be explained by human activities. Zgheib and al. (2020) describe in details the main stages of economic and forestry development in these three towns of the Haute-Maurienne. In particular, this study indicates that in 1860, the Haute-Maurienne was more populated, but between 1860 and 1929, the population decreased due to the abandonment of land, livestock (cattle, sheep), and wars. The decline in livestock farming allowed the forests to recover.
Between 1929 and 1952, the population continued to decrease with the war, and the land, the meadows and the livestock were abandoned. Yet, passing livestock limited the development of the forest. Between 1952 and 1979, the meadows were developed to increase livestock, pastoralism and cheese production. The population increased, accompanied by the growth of tourism linked to the development of ski resorts in the area, leading to an expansion of the urban area. These new buildings are located in the upper part of the three towns, close to the avalanche paths, and are therefore exposed to the risk due to avalanches. Finally, a reforestation of avalanche slopes in order to protect human stakes (buildings) took place recently in the 2000s, which explains the decrease in the number of PRAs at low elevations close to houses shown in this study.

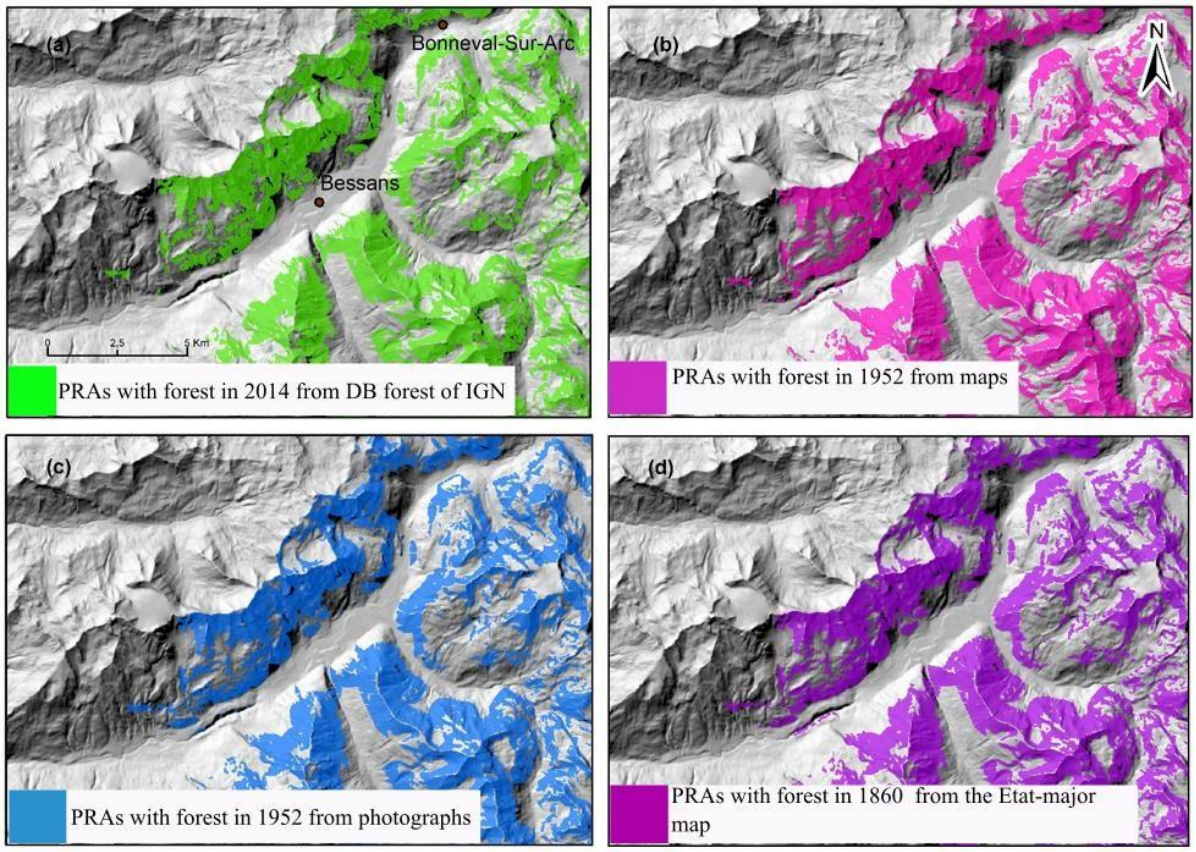

Figure 29 : Map of PRAs for the Haute-Maurienne , for different years. (a) in 2014 from DB forest of IGN, (b) 1952 from maps, (c) 1952 from photographs, (d) 1860 from the map of Etat-major, digitalised by Zgheib and al. (2020).

5 Discussion

The purpose of approach

Before this study was carried out, all studies concerning the characteristics of avalanche starting zones and avalanche terrain were carried out on a small scale in specific locations (none of them in France), and among all these studies, only two concerned the analysis of avalanche starting zones according to topographic parameters. In addition these studies did not take into account the evolution over time of the forest cover and the climate. In this study, we applied the PRA determination method proposed in Duvillier and al. (2023), mostly based on topographic parameters and adapted to the French Alps. This method was applied at a large scale in order to study the statistical properties of the PRAs for the whole French Alps, whereas the few past studies with the same objectives were focusing on small regions. Accuracy scores obtained by comparison to the CLPA taken as ground truth were shown to vary with the massifs' surface area of the detected PRAs in relation to the area of the massif (%), area of the largest detected PRAs, CLPA surface area, and proportion of forest in relation to the massif. Yet probative scores were obtained in all massifs allowing a statistical exploitation of the results to better understand the properties of avalanche terrain. In particular, the characteristics of the PRAs were described at the scale of the different massifs, and different relationships between the characteristics of the PRAs and those of the massifs were inferred to understand and explain the the frequency, size, elevation, slopes of the PRAs. Because the forest cover has a direct influence on the detected PRAs, we also studied the evolution of the PRAs properties according to different forest cover obtained for different years.

PRAs in the French Alps

We detected 101,802 PRAs with a total area of 3799.2 km^2, which represents 17.8% of the total area of the French Alps. The detected PRAs have an average area of 0.036 km^2, and a maximum area of 1.625 km^2. Within all the detected PRAs, we observe that the aspects are equally distributed, with percentages ranging from 10% (North) to 14% (South). PRAs are mainly located at elevations between 2000 m and 2600 m, with slopes between 30° and 45°.

Furthermore, a grouping of the massifs in three classes is proposed according to the characteristics of the PRAs, using the k-means clustering method. A spatial pattern is obtained, with a group of massifs with low elevations and a reduced number of PRAs compared to the other massifs, another group composed of massifs with high elevations, greater numbers of PRAs, and larger areas covered by the PRAs, and a last group but with larger proportions of the massifs covered by PRAs in terms of area but a lower number of PRAs.

Evolution of PRAs with land use

A last part of the study was dedicated to the diachronic evolution of the PRAs in the Queyras and Haute-Maurienne massifs, according to the forest cover obtained for different years (1860, 1952 and 2013-2014. In these two areas, the location of the PRAs at different years depends solely on whether or not the forest portions overlap.

In the Guil valley in the Queyras massif and in the Haute-Maurienne massif, the number of PRAs detected has decreased between 1860 and the 2000s, because the area studied has been reforested, which has the effect of limiting the number of PRAs that can be detected. Yet, the Haute-Maurienne is much less forested than the Queyras, so that variations in forest cover are less marked. All the changes in the forest cover are linked to the rural exodus, the reduction of pastoral practices in particular pastoralism, the evolution of agricultural practices, which have allowed the development of the forest and the colonization of the avalanche PRAs with the growth of trees and shrubs (Zgheib and al. 2020; Favillier and al. 2020; Mainieri and al. 2020).

6 Conclusion and outlooks

In this study, a systematic detection and evaluation of PRAs was performed in the whole French Alps, using the method proposed by Duvillier et al. (2023). We studied the topographic characteristics of the PRAs over the whole French Alps, at the scale of the massifs, and then in two smaller study areas (the Guil valley in the Queyras, three towns in the Haute-Maurienne) according to the evolution of the forest cover. We also proposed three classes of massifs based on the characteristics of their PRAs, using the k-means clustering method. This resulted in a spatial coherence of the three clusters of massifs. Eventually in the Queyras and Haute-Maurienne massifs, we showed that the increase in the forest area between 1860 and the 2000s, due to the reduction in pastoralism and changes in agricultural practices which favored the colonization of PRAs by trees and shrubs, led to a decrease in the number and total area of PRAs detected.

The results shown in this study do not consider the evolution of climate, which obviously impacts the PRAs as many areas experience less significant snow cover as climate is warming. This evolution could be taken into account, for example, by modifying the minimum elevation used in the determination of PRAs. Indeed, this minimum elevation could be easily obtained from past snow observations, by taking, for example, the minimum elevation at which the average snow depth is greater than 20 cm during the snow season.

Eventually, as this study demonstrates the feasibility and usefulness of the large-scale application of our PRA detection method and of the analysis of their topographical characteristics, such an approach could be applied to other mountains such as the French Pyrenees, the Massif Central, the Vosges, or the Himalayas, by adapting the thresholds used in the method (slope, minimum elevation, etc.), to improve our knowledge of local avalanche activity.

Conclusion

1 Rappel du contexte et de la problématique de la thèse

Dans les régions de montagne, l'évaluation du risque d'avalanche est un problème important à traiter pour la réduction des pertes humaines et des dommages matériels. L'estimation de ce risque dépend notamment des études existantes et des données concernant les avalanches historiques disponibles dans la région concernée. Un complément utile à la caractérisation de l'aléa est la détermination des zones de départ potentielles (PRAs) sur la base de critères topographiques. Une fois les PRAs obtenues, et à condition d'estimer en complément le volume initial des avalanches potentielles, il est possible d'obtenir les emprises maximales des écoulements en utilisant un logiciel de simulation d'avalanche, puis une évaluation du risque par combinaison avec la vulnérabilité d'enjeux réels ou hypothétiques. Les méthodes de détermination des PRAs existantes à ce jour utilisent des paramètres topographiques comme la pente, la distance à la crête, et sont souvent appliquées (ou tout au moins développées et évaluées) à des échelles spatiales réduites. En outre, les méthodes d'évaluation proposées dans la littérature varient d'un pays à l'autre en fonction des avalanches passées enregistrées, et sont généralement assez peu détaillées.

Plus précisément, pour ce qui est d'évaluer la méthode de détermination des PRAs, dans la plupart des cas, les extensions d'avalanches enregistrées comprennent la zone de départ, la zone d'écoulement, la zone de dépôt, et pas seulement la zone de départ qui nous intéresse. Il est donc important d'extraire uniquement les zones de départs dans les avalanches enregistrées, dans le but de les confronter avec les PRAs détectées. De plus, il n'y a pas encore de méthode de détermination des PRAs, et d'évaluation à partir des avalanches historiques enregistrées en France, qui soient adaptées aux Alpes françaises. D'où la nécessité de faire ce travail fastidieux.

Par ailleurs, les caractéristiques des PRAs n'ont pas fait l'objet d'analyses statistiques en France jusqu'ici. Et même plus largement, les rares études réalisées se déroulent à une petite échelle, dans des localisations précises. Pour l'instant, Il n'y a pas d'étude des caractéristiques des PRAs réalisées à grande échelle, permettant de décrire statistiquement les caractéristiques des zones de départ potentielles des avalanches. Enfin, dans les études passées sur la détermination des PRAs, la surface forestière utilisée est considérée comme stationnaire, alors qu'elle évolue dans le temps. Ainsi, aucune étude n'a quantifié jusqu'ici l'évolution des PRAs (nombre, superficie, distribution altitudinale, etc.) en fonction de l'occupation du sol, en particulier de la présence de forêt, que ce soit en France ou ailleurs dans le monde entier, alors que le couvert forestier est paramètre déterminant dans l'obtention des PRAs.

2 Avancées proposées par la thèse

Détermination des PRAs et confrontation avec la CLPA

Dans un premier temps, nous avons mis au point une méthode de détermination des PRAs à partir de paramètres topographiques, applicable à grande échelle c'est-à-dire pour les Alpes françaises dans leur ensemble, en utilisant des paramètres et seuils topographiques adaptés, ainsi qu'une méthode d'évaluation permettant de confronter ces PRAs aux données de la CLPA qui contient les limites maximales atteintes des avalanches observées dans le passé, sur une vaste zone des Alpes française. Dans la méthode de détermination créée, nous proposons de filtrer les pixels avec une altitude inférieure à 1400 m et avec une pente non comprise entre 28° et 60°. Ensuite, les parties en forêts sont enlevées, puis une distance maximale à la crête la plus proche de 600m est appliquée. Pour finir, un

algorithme de détermination des bassins versants est utilisé pour individualiser chaque zone de départ potentielle.

Dans cette thèse, nous avons mis au point une méthode d'évaluation des PRAs. Pour cela, nous comparons les PRAs obtenues avec la CLPA. Pour comparer ces deux types de données, nous appliquons les mêmes filtres que pour les PRAs aux emprises de la CLPA. Au final, nous obtenons des PRAs individualisées dans les emprises CLPA. A partir des PRAs et des PRAs détectées dans les emprises de la CLPA, nous pouvons calculer une matrice de confusion en nombre et en aire, puis des scores de précision. Nous avons obtenu des scores de précision satisfaisants en nombre et en aire, pour chacun des 23 massifs à l'exception des Bauges et du Vercors car ce sont les seuls massifs où il n'y a pas de données dans la CLPA.

Ensuite, nous avons réalisé des études de sensibilité et obtenu des scores de confusion en nombre et en aire, sur différentes zones (Massifs de la Chartreuse, du Mont Blanc, et de la Maurienne) et à différentes résolutions (5m, 10m, 25m). Nous avons montré la robustesse globale de la méthode de détermination des PRAs, et mis en évidence les paramètres les plus influents comme l'individualisation des PRAs par les bassins versants pour déterminer le bon nombre de PRAs. La méthode d'évaluation reste toutefois améliorable car l'on évalue que les vrais positifs de la matrice de confusion seulement, mais notre approche constitue déjà une avancée méthodologique par rapport à l'état de l'art.

Enfin, une fois les scores de matrice de confusion obtenus pour chacun des massifs, nous avons analysé certaines différences de performances en fonction des paramètres topographiques des massifs et des PRAs. Il en résulte que, globalement, le taux de précision en nombre augmente avec la proportion de surface forestière par rapport au massif (%), et diminue avec le nombre de PRAs par massif, la surface des PRAs détectées par rapport à l'aire du massif (%), l'aire totale des PRAs (km^2), la proportion de PRAs par rapport au nombre total de PRAs (%) et la surface CLPA étudiée par rapport au massif (%).

Etude statistique des caractéristiques des PRAs dans les Alpes Françaises

Cette thèse a proposé une description des caractéristiques des PRAs que nous avons détectées à grande échelle, c'est-à-dire à l'échelle des Alpes françaises entières. L'objectif était de mieux comprendre la localisation des PRAs en fonction des paramètres topographiques et leur évolution dans le temps, dans le but de mieux comprendre les caractéristiques des zones de départ d'avalanches dans les Alpes Françaises.

Nous avons détecté en tout 107 122 PRAs ayant une aire totale 3895,5 km^2, ce qui représente 18,3% de l'ensemble de la surface des Alpes françaises. Les PRAs détectées ont une aire moyenne de 0,036 km^2, et une aire maximale de 1,625 km^2. Sur l'ensemble des PRAs détectées, nous avons établi que les expositions sont réparties de façon équitable, avec des pourcentages compris entre 10 % (Nord) et 14% (Sud). Concernant les pixels compris dans l'ensemble des PRAs, les classes d'altitude les plus représentatives des Alpes françaises sont comprises entre 1400 et 3000m, et les classes de pente 30-45°.

Pour l'ensemble des 23 massifs des Alpes Françaises, nous avons montré que le nombre et les aires totales et maximales des PRAs détectées dépendent principalement de la superficie du massif étudié, de la pente moyenne, des atitudes maximale et moyenne, de la superficie de la couverture foretière par rapport au massif. En effet, plus un massif est vaste, plus il pourra y avoir de PRAs à detecter. C'est d'autant plus vrai lorsque l'altitude moyenne du massif est élevée, qui permet la prise en compte d'un plus grand nombre de pixels avec la méthode de détermination des PRAs. Par ailleurs, la forêt limite les départs d'avalanche, de ce fait plus le massif est boisé moins il y aura de PRAs à détecter, et de

pentes sucpetibles d'etre avalancheuses. De plus, les coéfficients de corrélation entre la lithologie et les paramètres propres aux PRAs montrent que la lithologie est un facteur très important pour les altitudes minimales et maximales des PRAs, le nombre de PRAs par massif, mais qui a un impact négligeable sur la pente moyenne.
Pour finir, nous avons proposé de regrouper les 23 massifs des Alpes françaises ayant les caractéristiques de PRAs les plus proches à l'aide de l'algorithme K-means en faisant 3 classes de massifs. La somme des erreurs au carré indique que le nombre de classe le plus adapté est 3. Par ailleurs, nous observons une certaine cohérence géographique avec les 3 classes de massifs. En effet, nous distinguons un groupe de massif comprenant la majorité des Prés-Alpes calcaires, avec un nombre de PRAs réduit lié à leur basse altitude (cluster1). Le second groupe comprend des massifs de haute altitude, avec un nombre de PRAs plus élevé (cluster2). Par ailleurs, le nombre de PRAs obtenues y est le plus important par rapport aux autres groupes. Le dernier groupe comprend le moins de massifs mais les surfaces des PRAs y sont les plus élevées (cluster3).

Evolution diachronique des PRAs dans des secteurs choisis des Alpes Françaises

L'étude de l'évolution des PRAs dans le temps, en fonction de la couverture forestière au cours du temps, a été menée dans deux zones d'étude qui sont la vallée du Guil dans le Queyras, et 3 communes de la Haute-Maurienne. L'étude a été réalisée de 1860 jusqu'en 2013 pour le Queyras et 2014 pour la Haute-Maurienne, dans des zones où les évolutions des surfaces forestières sont bien documentées.
Dans la vallée du Guil et dans la Haute-Maurienne, le nombre de PRAs détectées a globalement diminué entre 1860 et les années 2013-2014. Dans le Queyras, le nombre de PRAs obtenus passe de 1793 en 1860 pour une surface forestière de 15,9%, à 1578 en 2013 avec une couverture forestière de 43,1%. En Haute-Maurienne, le nombre de PRAs obtenus passe de 3043 en 1860 pour une surface forestière de 3,2%, à 2971 en 2014 avec une couverture forestière de 5,7%.

Ces résultats montrent que le développement de la surface forestière dans les couloirs d'avalanche a entrainé une diminution du nombre de PRAs au cours du temps. Plus précisément dans la vallée du Guil en 1860 et 1952, des PRAs ont été détectées dans l'emprise de la forêt des années 2000, là où aucune PRA n'a été trouvée avec la BD forêt, car la forêt était inexistante en 1860 et 1952. En 1952, la différence entre les deux couvertures forestières issues de cartes et de photographies aériennes sont minimes même si les photographies sont plus précises que la carte, de ce fait nous pouvons garder les forêts de 1952 et 1860 en l'état sans rectification à faire. Par ailleurs, le massif du Queyras a une surface forestière plus dense que le massif de la Haute-Maurienne, d'où un nombre moins important de PRAs trouvés.

3 Perspectives pour des travaux futurs

Différentes pistes pour des développements additionnels ont déjà été proposés dans chacun des deux chapitres/articles, en lien avec des points de discussion spécifiques : amélioration de la méthode de détermination par apprentissage, approfondissement des techniques d'évaluation des PRAs, etc. Nous tenons ici à rappeler quelques perspectives qui nous semblent prioritaires au terme de ce travail.
Dans notre méthode de détermination, la forêt est utilisée sans prise en compte de sa densité (nombre d'arbres, diamètre des troncs, etc.). Une idée serait de prendre en compte la densité du couvert forestier pour gagner en précision dans la méthode de détermination des PRAs, car à certains endroits quelques arbres éparpillés déterminent le classement en zone « forêt » alors que la densité est quand même assez faible, ne rendant pas le déclenchement d'une avalanche impossible en pratique. De plus, il y a des différences entre les couches forêt utilisées, qui ont une influence non négligeable sur les

contours des PRAs. D'où l'utilité d'avoir une couche forêt mieux représentative de la densité forestière réelle, et une méthode de détermination des PRAs suffisamment fine pour prendre en compte la densité forestière, voire l'incertitude liée à la délimitation des zones forestières.

La méthode de détermination a été créée et appliquée uniquement dans les Alpes françaises, alors que sur d'autres massifs en France cette méthode pourrait être testée et adaptée. C'est le cas des Pyrénées françaises, du massif central, des Vosges où les seuils d'altitude doivent être ajustés car l'altitude est globalement moins élevée. Par ailleurs, la méthode pourrait être adaptée et appliquée à l'Himalaya, ou à la Cordelière des Andes avec un ajustement des seuils d'altitude et de pente. En effet, dans certaines zones de la Cordelière des Andes, à une altitude de 2000 m, la pluie et le brouillard permettent le développement de la forêt et des cultures, qui limitent donc les départs d'avalanche (Dollfus, 1968), contrairement aux Alpes. A contrario, dans la région de Lahaul, dans l'Ouest de l'Himalaya, la majorité des départs d'avalanches se produisent sur des pentes comprises entre 28° et 45° (Kumar et al., 2019), au lieu de 28° à 60° dans les Alpes. Une telle application généralisée de la méthode développée est largement possible du fait de son faible coût de calcul et de ses besoins modestes en matière de données d'entrées : un MNT à 25 m et une couche d'occupation forestière.

Dans nos études, l'impact des activités humaines, en particulier le pastoralisme est pris en compte, dans l'évolution des PRAs mais pas le climat, alors que ce dernier fait varier significativement l'activité avalancheuse (Giacona et al., 2021). En effet, l'enneigement et donc l'activité avalancheuse dépendent des conditions de température et de précipitations. Avec le réchauffement climatique, l'enneigement diminue et les températures augmentent. Les évolutions en cours sont déjà très marquées dans les Alpes françaises et vont se poursuivre au cours des prochaines décennies (Durand et al., 2009); (Castebrunet et al., 2014); (Verfaillie et al., 2018) ; (Beaumet et al., 2021). Par conséquent, ces modifications de l'enneigement sont à prendre en compte dans la méthode de détermination des PRAs. Une idée serait de faire varier l'altitude minimale de détermination des PRAs en fonction de la variation de l'enneigement au cours du temps. En complément, une étude de sensibilité en fonction de différents seuils d'altitude minimale pourra être réalisée, en comparant avec les PRAs obtenues à partir d'une altitude minimale de 1400m. Enfin, il serait possible d'évaluer la part respective de l'évolution de l'enneigement et du couvert forestier dans l'évolution des PRAs via une technique de partition de variance.

En France, les informations relatives au risque d'avalanche pour les pratiquants de la montagne, sont disponibles au sein du Bulletin d'Estimation du Risque d'Avalanche (BRA), à l'échelle d'un massif. L'idée serait d'affiner l'estimation du BRA qui est adapté à l'ensemble du massif mais non à de plus petites zones, avec les caractéristiques des PRAs et les groupes issus du clustering. En utilisant les altitudes minimales et maximale pour les différents groupes de massifs, l'estimation du BRA pourra être mieux adaptée aux pratiquants de la montagne en particulier les skieurs hors-piste, en ciblant plus précisément les zones à risque.

Enfin, les résultats de cette thèse ont un intérêt pour différents publics en terme de connaissance de l'aléa dans les différents massifs des Alpes françaises. En complément des modalités habituelles (dépôt en ligne des thèses sur les archives ouvertes), nous pensons faciliter sa diffusion dans les clubs de montagne.

Table des figures

Annexes

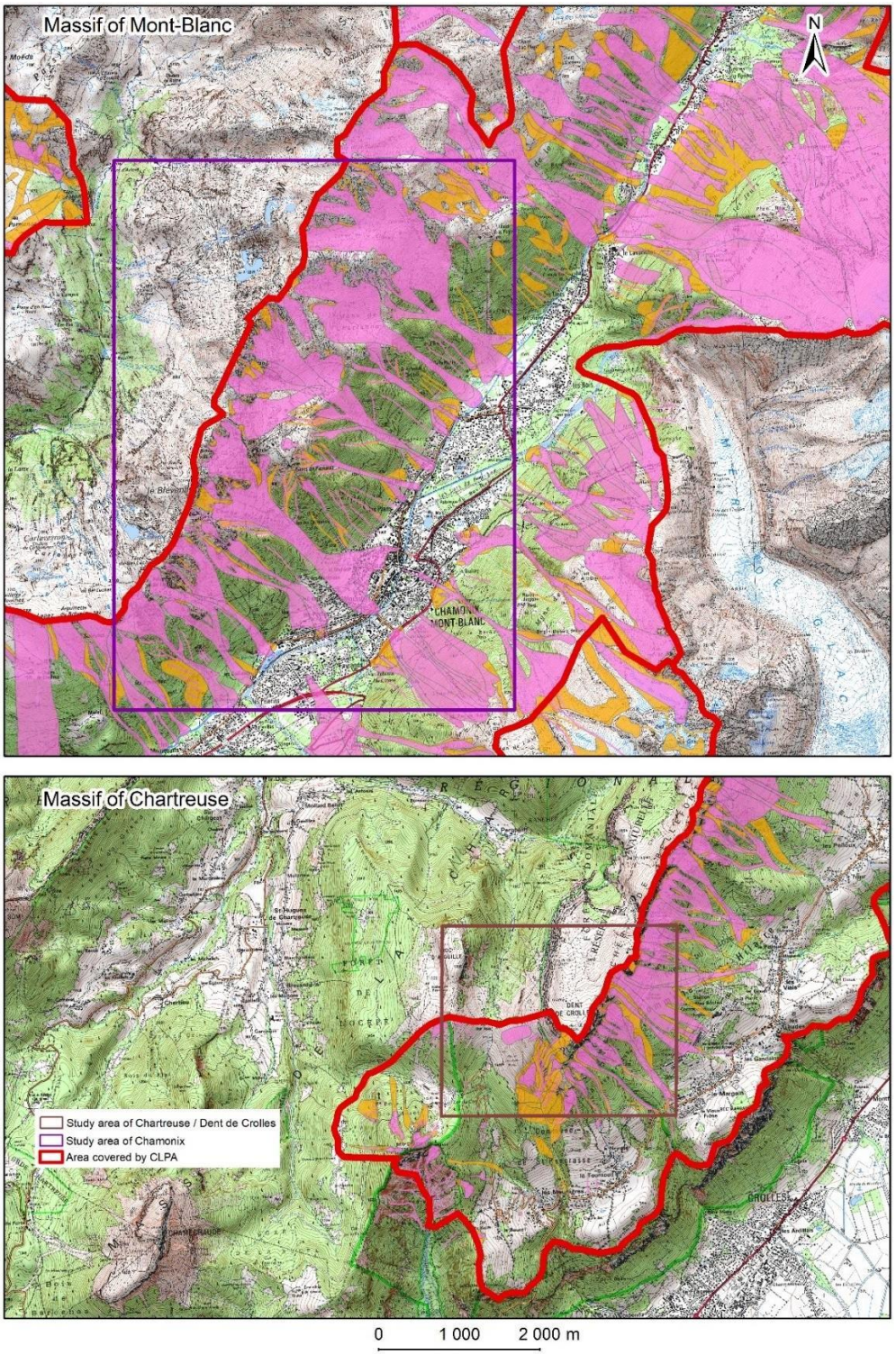

Figure S1: Extracts of the Official French avalanche cadastre "CLPA" (March 2022 edition). Magenta and orange polygons correspond to the extent of past avalanches from i) testimonies and documentary sources and ii) photo-interpretation of landscape footprints, respectively. Full legend at: https://www.avalanches.fr/static/1public/epaclpa/CLPA_feuilles_carte/CLPA_legende_carte.pdf. Study areas of Chamonix and Chartreuse/Dent de Crolles are located, as well as the limits of the areas covered by CLPA in both the Mont Blanc (top) and Chartreuse (bottom) massifs

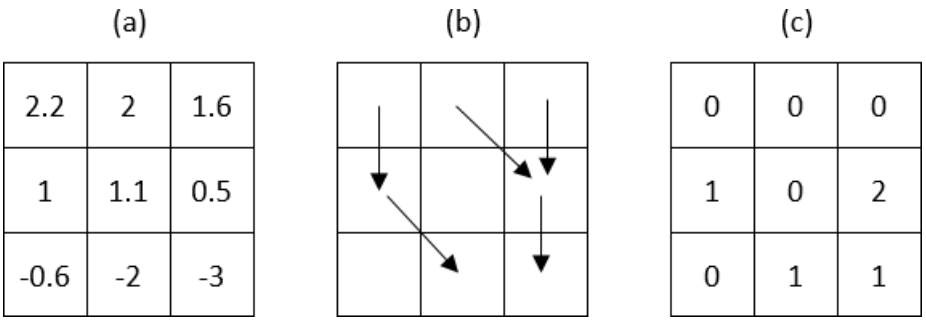

Figure S2: Principle of watershed delineation using flow direction: (a) Local slope for a central pixel and its eight neighbours (adapted from Kinner, 2003) (b) Calculation of flow direction (adapted from Stojkovic et al., 2012) (c) Result: flow accumulation.

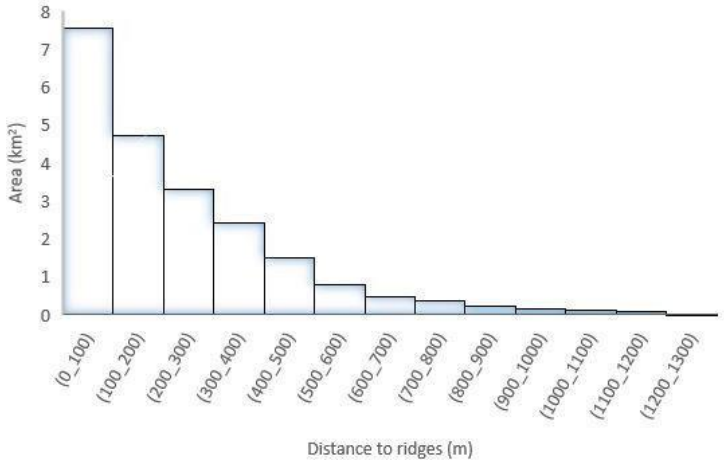

Figure S3: Histogram of the distance to the closest ridge for the pixels of the study area of Chamonix (Figure 5).

			With default values	Without minimal elevation filter	Without slope filter	Without distance to ridge filter	Without minimal area filter	Without watershed delineation	Without forest filter	With Corine Land Cover forest	With Theia forest
Validation sample	Total area of PRAs within CLPA (validation sample) [km²]		1.55	1.55	1.55	1.55	1.55	1.55	1.55	1.55	1.55
	Total number of PRAs within CLPA extents (validation sample)		85	85	85	85	85	85	85	85	85
Detected PRAs	Total area of detected PRAs [km²]		2.35	2.29	2.29	2.35	3.08	2.43	6.16	2.63	4.12
	Difference in area with regards to default values [km²]		/	-0.06	-0.06	0.00	0.73	0.08	3.81	0.28	1.77
	Difference in area with regards to default values (%)		/	-2.5%	-2.5%	-0.2%	31.1%	3.6%	162.3%	12.0%	75.4%
	Total number of detected PRAs		108	107	107	108	364	23	200	110	137
	Difference in numbers with regards to default values		/	-1	-1	0	256	-85	92	2	29
	Difference in numbers with regards to default values (%)		/	-0.9%	-0.9%	0.0%	237.0%	-78.7%	85.2%	1.9%	26.9%
	Total area of detected PRAs within CLPA extents [km²]		2.17	2.10	2.10	2.17	2.29	2.27	4.54	2.35	3.29
	Total number of detected PRAs within CLPA extents		94	93	93	94	128	19	108	92	92
Evaluation	True positive rate (recall), Eq. 3	In numbers (%)	87	86.8	87	87	35.2	82.6	54	82.4	67.2
		In areas (%)	92.4	91.8	91.8	92.4	74.2	87.2	73.6	88.6	80
	Difference in recall with regards to default values	In numbers (%)	/	-0.2	0	0	-51.8	-4.4	-33	-4.6	-19.8
		In areas (%)	/	-0.6	-0.6	0	-18.2	-5.2	-18.8	-3.8	-12.4

Table S1: Same as Table 5, but for the Chartreuse massif.

			With default values	Without minimal elevation filter	Without slope filter	Without distance to ridge filter	Without minimal area filter	Without watershed delineation	Without forest filter	With Corine Land Cover forest	With Theia forest
Validation sample	**Total area of PRAs within CLPA (validation sample) [km²]**		55.72	55.7	55.7	55.7	55.7	55.7	55.7	55.7	55.7
	Total number of PRAs within CLPA extents (validation sample)		1884	1884	1884	1884	1884	1884	1884	1884	1884
Detected PRAs	**Total area of detected PRAs [km²]**		71.6	75.3	203.2	118.5	75.6	97.7	113.8	71.6	86.5
	Difference in area with regards to default values [km²]		/	3.7	131.6	46.9	4.0	26.1	42.2	0.0	14.9
	Difference in area with regards to default values (%)		/	5.2%	183.8%	65.5%	5.6%	36.5%	58.9%	-0.1%	20.8%
	Total number of detected PRAs		2413	2575	1520	3430	5667	526	3276	2664	2794
	Difference in numbers with regards to default values		/	162	-893	1017	3254	-1887	863	251	381
	Difference in numbers with regards to default values (%)		/	6.7%	-37.0%	42.1%	134.9%	-78.2%	35.8%	10.4%	15.8%
	Total area of detected PRAs within CLPA extents [km²]		67.4	69.3	170.4	85.6	67.3	94.7	84.5	67.4	67.4
	Total number of detected PRAs within CLPA extents		2000	2024	701	2045	2606	285	2039	1992	2034
Evaluation	**True positive rate (recall), Eq. 3**	**In numbers (%)**	82.8	78.0	46.0	59.4	46.0	54.2	62.0	74.7	72.2
		In areas (%)	94.0	91.8	83.8	72.2	89.0	96.8	74.2	94.2	77.8
	Difference in recall with regards to default values	**In numbers (%)**	/	-4.8	-36.8	-23.4	-36.8	-28.6	-20.8	-8.1	-10.6
		In areas (%)	/	-2.2	-10.2	-21.8	-5.0	2.8	-19.8	0.2	-16.2

Table S2: Same as Table 5, but for the Maurienne massif

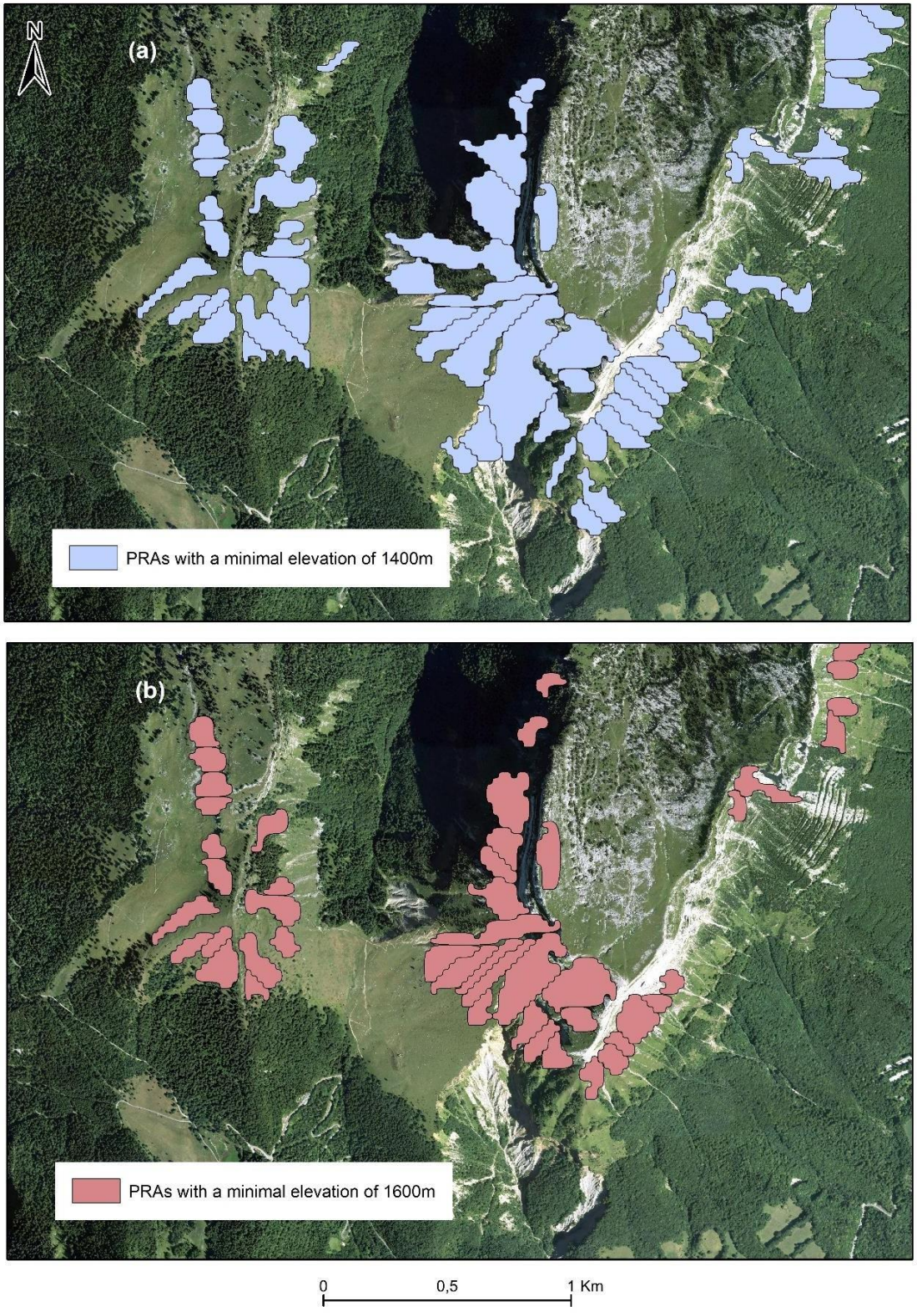

Figure S4: Effect on PRA detection of the minimal elevation threshold, Chartreuse/Dent de Crolles study area. For the PRA detection, the minimal elevation threshold varies, all other factors and the DEM resolution are set to their default values (Figure 7), and forest cover data is from DB forest IGN. Aerial photograph ©IGN 2012. For the determination of the validation sample, all factors and the DEM resolution are set to their default values (Figure 8) and forest cover data is from DB forest IGN.

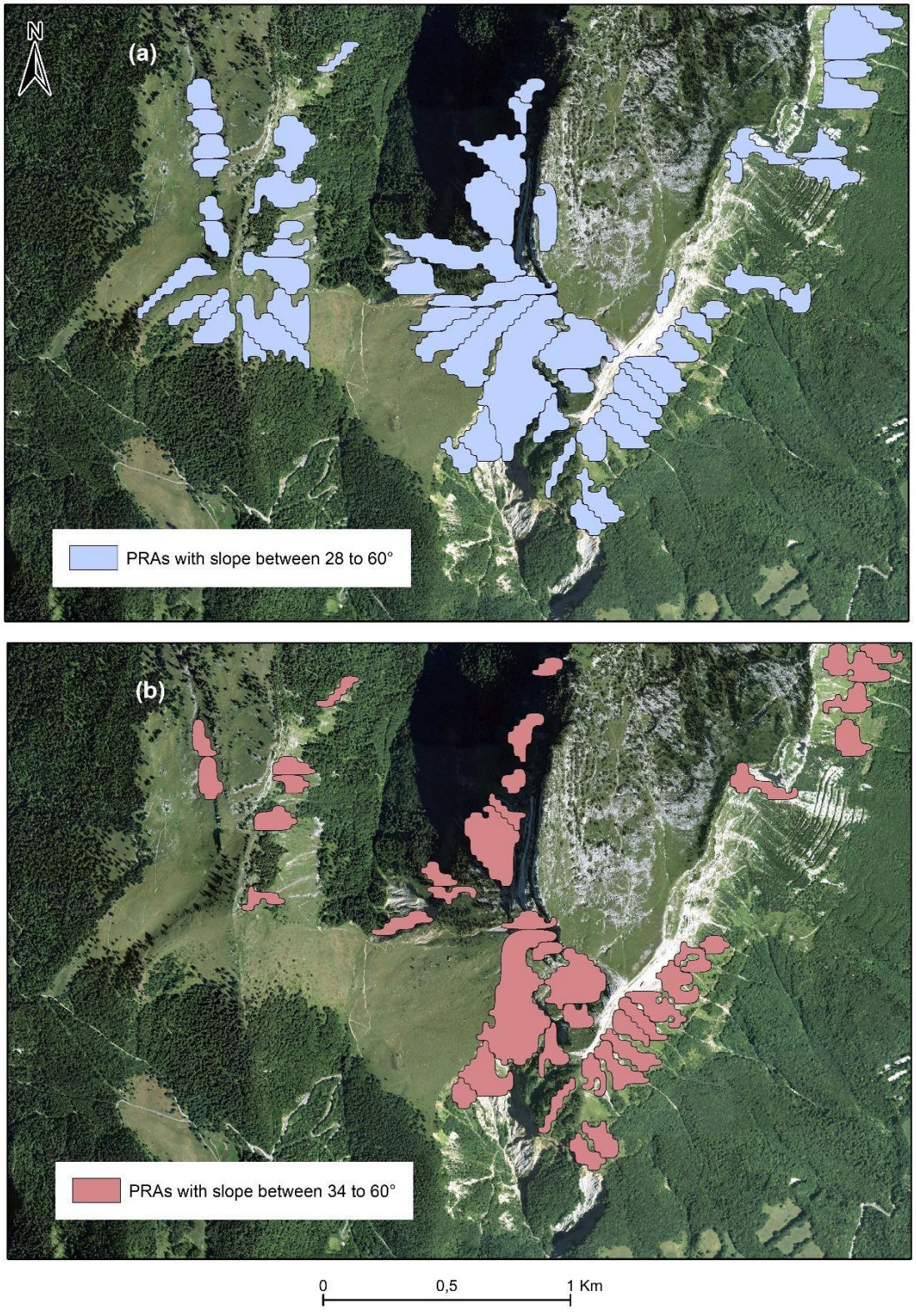

Figure S5: Effect on PRA detection of the slope range, Chartreuse/Dent de Crolles study area. For the PRA detection, the retained slope range varies, all other factors and the DEM resolution are set to their default values (Figure 11), and forest cover data is from DB forest IGN. Aerial photograph ©IGN 2012. For the determination of the validation sample, all factors and the DEM resolution are set to their default values (Figure 12) and forest cover data is from DB forest IGN.

Bibliographie

ADEME, IGN. (2019). Contribution de l'IGN à l'établissement des bilans carbone des forêts des territoires (PCAET),122-4.

Ammann, W., Bebi, P. (2000). WSL Institute for Snow and Avalanche Research SLF, Der Lawinenwinter 1999, Ereignisanalyse, SLF Davos, 588 p.

Ancey, C. (1996). Guide Neige et avalanches Connaissances, pratiques, sécurité. Editions Quae.

Ancey, C., Rapin, F., Taillandier, J. M. (1999). Stratégie de protection des établissements hospitaliers de Saint-Hilairedu-Touvet contre le risque d'avalanches. irstea. 108 p. ⟨hal-02578607⟩.

Ancey, C., Rapin, F., Martin, E., Coleou, C., Naaim, M., Brunot, G. (2000). L'avalanche de Péclerey du 9 février 1999. La Houille Blanche, (5), 45-53.

Armstrong, B. R. (1976). Century of Struggle Against Snow: A History of Avalanche Hazard in San Juan County, Colorado. A Contribution to the United States UNESCO Man et the Biosphere (MAB) Program Project 6, Study of the Impact of Human Activities on Mountain and Tundra Ecosystems (Vol. 18).

Arnalds, P., Jonasson, K., Sigurdson, S. T. (2004). Avalanche hazard zoning in Iceland based on individual risk. Annals of Glaciology. 38. pp 285-290.

Aydin, A., and Eker, R. (2017). GIS-based snow avalanche hazard mapping: Bayburt-Aşağı Dere catchment case. Journal of Environmental Biology, 38(5 (Special Issue)), 937-943.

Baghdadi, N., Selle, A., Biagiotti, I. (2021). Le Pôle Thématique National des Surfaces Continentales Theia. In La télédétection et les données aériennes au service de l'eau.

Barbolini, M., Pagliardi, M., Ferro, F., Corradeghini, P. (2011). Avalanche hazard mapping over large undocumented areas. Natural hazards, 56(2), 451-464.

Bartelt, P., Bühler, Y., Buser, O., Christen, M., Meier, L. (2012). Modeling mass-dependent flow regime transitions to predict the stopping and depositional behavior of snow avalanches. Journal of Geophysical Research : EarthSurface, 117(F1).

Bebi, P., Kulakowski, D., Rixen, C. (2009). Snow avalanche disturbances in forest ecosystems State of research and implications for management. Forest ecology and Management, 257(9), 1883-1892.

Beaumet, J., Ménégoz, M., Morin, S., Gallée, H., Fettweis, X., Six, D., Anquetin, S. (2021). Twentieth century temperature and snow cover changes in the French Alps. Regional Environmental Change, 21(4), 1-13.

Berger, F. (1995). SIG et zonage des fonctions des forêts: l'exemple des forêts à rôle de protection dominant. Arborescences, (55), 5.

Bertrand, M., Liébault, F., Piégay, H. (2017). Regional Scale Mapping of Debris-Flow Susceptibility in the Southern French Alps. Journal of Alpine Research|, (105-4).

Bonnefoy, M., Borrel, G., Richard, D., Bélanger, L., Naaim, M. (2010). La carte de localisation des phénomènes d'avalanche (CLPA): enjeux et perspectives. Sciences Eaux Territoires, 620 (2), 6-14.

Bornard, A., Cozic, P. (1998). Milieux pâturés d'altitude. Intérêts multiples de ces milieux gérés par le pâturage domestique. Fourrages, (153), 13.

Bourova, E., Maldonado, E., Leroy, J. B., Alouani, R., Eckert, N., Bonnefoy-Demongeot, M., Deschatres, M. (2016). A new web-based system to improve the monitoring of snow avalanche hazard in France. Natural Hazards and Earth System Sciences, 16(5), 1205-1216.

Braun, T., Frigo, B., Chiaia, B., Bartelt, P., Famiani, D., Wassermann, J. (2020). Seismic signature of the deadly snow avalanche of January 18, 2017, at Rigopiano (Italy). Scientific reports, 10(1), 1-10.

Bun-Cosme, B., Freydier, B. (2013). Gresse-en-Vercors un siècle de sports d'hiver.

Bühler, Y., Kumar, S., Veitinger, J., Christen, M., Stoffel, A., Snehmani, S. (2013). Automated identification of potential snow avalanche release areas based on digital elevation models. Natural Hazards and Earth System Sciences, 13(5), 1321-1335.

Bühler, Y., Hafner, E. D., Zweifel, B., Zesiger, M., Heisig, H. (2019). Where are the avalanches? Rapid mapping of a large snow avalanche period with optical satellites. Cryosph. Discuss, 119.

Bühler, Y., von Rickenbach, D., Stoffel, A., Margreth, S., Stoffel, L., Christen, M. (2018). Automated snow avalanche release area delineation–validation of existing algorithms and proposition of a new object-based approach for large-scale hazard indication mapping. Natural Hazards and Earth System Sciences, 18(12), 3235-3251.

Bühler, Y. Bebi, P., Christen, M., Margreth, S., Stoffel, L., Stoffel, A., Marty, C., Schmucki, G., Caviezel, A., Kühne, R., Wohlwend, S., Bartelt, P. (2002). Automated avalanche hazard indication mapping on a statewide scale, Nat. Hazards Earth Syst. Sci., 22, 1825-1843.

Butler, D. R., Walsh, S. J. (1990). Lithologic, structural, and topographic influences on snow-avalanche path location, Eastern Glacier National Park, Montana. Annals of the Association of American Geographers, 80(3), 362-378.

Caetano, M., V., Nunes, A., Nunes.(2009). CORINE Land Cover 2006 for Continental Portugal, Technical Report, Instituto Geográfico Português.

Castebrunet, H., Eckert, N., Giraud, G., Durand, Y., Morin, S. (2014). Projected changes of snow conditions and avalanche activity in a warming climate: the French Alps over the 2020–2050 and 2070–2100 periods. The Cryosphere, 8(5), 1673-1697.

ChuecaCía, J., Andrés, A. J., Montanes Magallon, A. (2014). A proposal for avalanche susceptibility mapping in the Pyrenees using GIS: the Formigal-Peyreget area (Sheet 145-I; scale 1: 25.000). Journal of Maps, 10(2), pp.203-210.

Dollfus, O. (1968). Le Pérou : introduction géographique à l'étude du développement. Éditions de l'IHEAL.

Durand, Y., G. Giraud, M. Laternser, P. Etchevers, L. Mérindol, and B. Lesaffre. (2009). "Reanalysis of 47 Years of Climate in the French Alps (1958–2005): Climatology and Trends for Snow Cover." Journal of Applied Meteorology and Climatology 48 (12), 2487–2512.

Duvillier, C., Eckert, N., Evin, G., Deschâtres, M.(2022). Development and validation using ground truth of a method to identify potential release areas of snow avalanches based on watershed delineation, Nat. Hazards Earth Syst. Sci. Discuss. [preprint], https://doi.org/10.5194/nhess-2022-177, in review, 2022.

Eckert, N., Keylock, C. J., Bertrand, D., Parent, E., Faug, T., Favier, P., Naaim, M. (2012). Quantitative risk and optimal design approaches in the snow avalanche field: Review and extensions. Cold Regions Science and Technology, 79, 1-19.

Eckert, N., Naaim, M., Parent, É. (2010). Long-term avalanche hazard assessment with a Bayesian depth-averaged propagation model. Journal of Glaciology, 56(198), 563-586.

Eckert, N., Naaim, M., Giacona, F., Favier, P., Lavigne, A., Richard, D., Parent, E. (2018). Repenser les fondements du zonage règlementaire des risques en montagne «récurrents». La Houille Blanche, (2), 38-67.

Etchevers, P., et Martin, E. (2002). Impact d'un changement climatique sur le manteau neigeux et l'hydrologie des bassins versants de montagne. L'eau en montagne, 8.

Evans, S. (1972). General Geomorphometry, derivatives of altitude and descriptive statistics in: Chorley, R.J., Ed., Spatial Analysis in Geomorphology, Methuen and Co. Ltd., London, 17-90.

Evin, G., Sielenou, P. D., Eckert, N., Naveau, P., Hagenmuller, P., Morin, S. (2021). Extreme avalanche cycles: Return levels and probability distributions depending on snow and meteorological conditions. Weather and Climate Extremes, 33, 100344.

Faug, T., Naaim-Bouvet, F., Bonnefoy-Demongeot, M., Thibert, E., Eckert, N. (2018). L'avalanche du Bourgeat survenue le 9 janvier 2018. Risques infos.

Favillier, A., Mainieri, R., Lopez-Saez, J., Saulnier, M., Eckert, N., Peiry, J.-L., Stoffel, M., and Corona, C. (2020). Impacts of land-cover changes on dendrogeomorphic reconstructions of snow avalanches: Insights from the Queyras massif (French Alps). Anthropocene, *30*, 100244.

Fischer, J. T., Kofler, A., Fellin, W., Granig, M., Kleemayr, K. (2015). Multivariate parameter optimization for computational snow avalanche simulation. Journal of Glaciology, 61(229), 875-888.

Fourchy, P., Huin, F. (1957). Un exemple récent de travaux de protection contre les avalanches.
tes traverses d'Ornon (Isère). Revue forestière française, 3, pp.169-172.

Gaucher, R., Pasquier, X., Bonnefoy, M., Escande, S., Eckert, N., Deschâtres, M. (2009). Quelques exemples d'avalanches exceptionnelles. Neige et avalanches, 126, pp. 8-12.

Gaume, J., Eckert, N., Chambon, G., Naaim, M., Bel, L. (2013). Mapping extreme snowfalls in the French Alps using max-stable processes. Water Resources Research, 49(2), 1079-1098.

Giacona, F., Eckert, N., Corona, C., Mainieri, R., Morin, S., Stoffel, M., Naaim, M. (2021). Upslope migration of snow avalanches in a warming climate. Proceedings of the National Academy of Sciences, 118(44), e2107306118.

Giacona, F., Eckert, N., Martin, B. (2017). A 240-year history of avalanche risk in the Vosges Mountains based on non-conventional (re) sources. Natural Hazards and Earth System Sciences, 17(6), 887-904.

Giacona, F., Eckert, N., Mainieri, R., Martin, B., Corona, C., Lopez-Saez, J., Stoffel, M. (2018). Avalanche activity and socio-environmental changes leave strong footprints in forested landscapes: a case study in the Vosges medium-high mountain range. Annals of Glaciology, 59(77), 111-133.

Glass, B., Huet, P., Rat, M., Tordjeman, R. (2000). Retour d'expérience sur l'avalanche du 9 février 1999 à Montroc, commune de Chamonix. Inspection Générale de l'Environnement. Rapport d'expertise.

Gleason, J. A. (1996). Terrain parameters of avalanche starting zones and their effect on avalanche frequency (Doctoral dissertation, Montana State University-Bozeman, College of Letters & Science).

Gruber, U., Bartelt, P. (2007). Snow avalanche hazard modelling of large areas using shallow water numerical methods and GIS. Environmental Modelling and Software, 22(10), 1472-1481.

Gubler, H., Rychetnik, J. (1991). Effects of forests near timberune on avalanche formation.

Harman, P. E., Rule, A. C. (2006). High school students' mnemonic devices for Mohs hardness scale. Journal of geoscience education, 54(1), 69-73.

IRASMOS Consortium. (2009). Best practice of integral risk management of snow avalanches, rock avalanches and debris flows in Europe. Delivrable 5.4. Sixth Framework Programme (2002-2006). 138 p. available at: http://irasmos.slf.ch/results_wp5.htm.

Jasiewicz, J., Stepinski, T. F. (2013). Geomorphons a pattern recognition approach to classification and mapping of landforms. Geomorphology, 182, pp.147-156.

Karas, A., Karbou, F., Giffard-Roisin, S., Durand, P., Eckert, N. (2021). Automatic color detection-based method applied to sentinel-1 sar images for snow avalanche debris monitoring. IEEE Transactions on Geoscience and Remote Sensing, 2021.

Keylock, C. J., McClung, D. M., Magnússon, M. M. (1999). Avalanche risk mapping by simulation.: Journal of Glaciology, 45(150), 303-314.

Kern, H., Jomelli, V., Eckert, N., Grancher, D., Deschâtres, M. (2020). Variabilité des volumes des dépôts d'avalanche et relations avec la morphologie des couloirs d'écoulement (Bessans, Savoie, France). Géomorphologie: relief, processus, environnement, 26(2).

Kinner, D. A. (2003). Delineation and characterization of the Boulder Creek. Comprehensive Water Quality of the Boulder Creek Watershed, Colorado, During High-flow and Low-flow Conditions, 2000, 3(4054), 27.

Kumar, S., Srivastava, P. K., Bhatiya, S. (2019). Geospatial probabilistic modelling for release area mapping of snow avalanches. Cold Regions Science and Technology, 165, 102813.

Lavigne, A., Bel, L., Parent, E., Eckert, N. (2012). A model for spatio-temporal clustering using multinomial probit regression: application to avalanche counts. Environmetrics, 23(6), 522-534.

Lavigne, A., Eckert, N., Bel, L., Deschâtres, M., Parent, E. (2017). Modelling the spatio-temporal repartition of right-truncated data: an application to avalanche runout altitudes in Hautes-Savoie. Stochastic Environmental Researchand Risk Assessment, 31(3), 629-644.

Lavigne, A., Eckert, N., Bel, L., Parent, E. (2015). Adding expert contributions to the spatiotemporal modelling of avalanche activity under different climatic influences. Journal of the Royal Statistical Society: Series C (Applied Statistics), 64(4), 651-671.

Lehning, M., Doorschot, J., Bartelt, P. (2000). A snowdrift index based on SNOWPACK model calculations. Annals of Glaciology, 31, 382-386.

Lenoir, J., Gégout, J. C. (2010). La remontée de la distribution altitudinale des espèces végétales forestières tempérées en lien avec le réchauffement climatique récent. Revue forestière française, 62(3-4), 465-476.

Le Roux, E., Evin, G., Eckert, N., Blanchet, J., Morin, S. (2021). Elevation-dependent trends in extreme snowfall in the French Alps from 1959 to 2019. The Cryosphere, 15(9), 4335-4356.

Lied, K., S. Bakkehoi. (1980). Empirical calculations of snow avalanche runout distances based on topographic parameters, J. of Glaciology, 26(94), 165-177.

Mainieri, R., Favillier, A., Lopez-Saez, J., Eckert, N., Zgheib, T., Morel, P., Corona, C. (2020). Impacts of land-cover changes on snow avalanche activity in the French Alps. Anthropocene, 30, pp.13.

Maggioni, M., Gruber, U., Stoffel, A. (2002). Definition and characterisation of potential avalanche release areas. In Proceedings of the ESRI Conference, San Diego.

Maggioni, M., Gruber, U. (2003). The influence of topographic parameters on avalanche release dimension and frequency. Cold Regions Science and Technology, 37(3), pp.407-419.

Margreth, S. (2004): Die Wirkung des WaldesbeiLawinen. - Schutzwald und Naturgefahren. Forum fürWissen 2004: 21-26. « L'effet de la forêt sur les avalanches ». Waldwissen.

Naaim-Bouvet, F., and Richard, D. (2015). Les risques naturels en montagne. Editions Quae.

Naaim, M., Naaim-Bouvet, F., Faug, T., Bouchet, A. (2004). Dense snow avalanche modeling: flow, erosion, deposition and obstacle effects. Cold regions science and technology, 39(2-3), 193-204.

Naaim, M., Durand, Y., Eckert, N., Chambon, G. (2013). Dense avalanche friction coefficients: influence of physical properties of snow. Journal of Glaciology, 59(216), 771-782.

Nolting, S., Marin, C., Steger, S., Schneiderbauer, S., Notarnicola, C., Zebisch, M. (2018). Regional scale statistical mapping of snow avalanche likelihood and its combination with an optical remote sensing based avalanche detection approach–first attempts for the province of South Tyrol (Italy), International snow science workshop 2018 (ISSW), Innsbruck.

Oller, P., Baeza, C., Furdada, G. (2021) Empirical α–β runout modelling of snow avalanches in the Catalan Pyrenees. Journal of Glaciology, 67(266), 1043-1054.

Ortner, G., Bründl, M., Kropf, C. M., Röösli, T., Bühler, Y., Bresch, D. N.(2022). Large-scale risk assessment on snow avalanche hazard in alpine regions. Natural Hazards and Earth System Sciences Discussions, 1-31.

Rapin, F., Ancey, C. (2000). Occurrence conditions of two catastrophic avalanches at Chamonix, France.

Schnyder, D., Frey, W. (2005). Reboiser les pentes avalancheuses-oui mais comment?.

Schweizer, J., Bruce Jamieson, J., Schneebeli, M. (2003). Snow avalanche formation. Reviews of Geophysics, 41(4), 2003.

Sielenou, P. D., Viallon-Galinier, L., Hagenmuller, P., Naveau, P., Morin, S., Dumont, M., Eckert, N. (2021). Combining random forests and class-balancing to discriminate between three classes of avalanche activity in the French Alps. Cold Regions Science and Technology, 187, 103276.

Silleos, N. G., Alexandridis, T. K., Gitas, I. Z., Perakis, K. (2006). Vegetation indices: advances made in biomass estimation and vegetation monitoring in the last 30 years. Geocarto International, 21(4), pp.21-28.

Stojkovic, M., Milivojevic, N., and Stojanovic, Z. (2012). Use of information technology in hydrological analysis. Esociety Journal, 105.

Sykes, J., Haegeli, P., Bühler, Y. (2021). Automated snow avalanche release area delineation in data sparse, remote, and forested regions. Natural Hazards and Earth System Sciences Discussions, 1-39.

Veitinger, J., Purves, R. S., Sovilla, B. (2016). Potential slab avalanche release area identification from estimated winter terrain: a multi-scale, fuzzy logic approach. Natural Hazards and Earth System Sciences, 16(10), 2211.

Verfaillie, D., Lafaysse, M., Déqué, M., Eckert, N., Lejeune, Y., Morin, S. (2018). Multi-component ensembles of future meteorological and natural snow conditions for 1500 m altitude in the Chartreuse mountain range, Northern French Alps. The Cryosphere, 12(4), 1249-1271.

Vontobel, I., Harvey, S., Purves, R. (2013). Analyse des caractéristiques des zones de départ d'avalanches déclenchées par des skieurs. Neige et avalanche,145, 20.

Yariyan, P., Avand, M., Abbaspour, R. A., Karami, M., Tiefenbacher, J. P. (2020). GIS-based spatial modeling of snow avalanches using four novel ensemble models. Science of the Total Environment, 745, 141008.

Zevenbergen, L. W., Thorne, C. R. (1987). Quantitative analysis of land surface topography. Earth surface processes and landforms, 12(1), pp.47-56.

Zgheib, T., Giacona, F., Granet-Abisset, A. M., Morin, S., Eckert, N. (2020). One and a half century of avalanche risk to settlements in the upper Maurienne valley inferred from land cover and socio-environmental changes. Global Environmental Change, 65, 102149.

Zgheib, T., Giacona, F., Granet-Abisset, A. M., Morin, S., Lavigne, A., Eckert, N. (2022). Spatio-temporal variability of avalanche risk in the French Alps. Regional Environmental Change, 22(1), 1-18.